

# Dynamical quantum ergodicity from energy level statistics

Amit Vikram<sup>1</sup> and Victor Galitski<sup>1</sup>

<sup>1</sup>Joint Quantum Institute and Department of Physics, University of Maryland, College Park, MD 20742, USA

## Abstract

Ergodic theory provides a rigorous mathematical description of classical dynamical systems and in particular includes a formal definition of the ergodic hierarchy consisting of merely ergodic, weakly-, strongly-, and K-mixing systems. Closely related to this hierarchy is a less-known notion of cyclic approximate periodic transformations [see, *e.g.*, I. Cornfield, S. Fomin, and Y. Sinai, *Ergodic theory* (Springer-Verlag New York, 1982)], which maps any “ergodic” dynamical system to a cyclic permutation on a circle and arguably represents the most elementary notion of ergodicity. This paper shows that cyclic ergodicity generalizes to quantum dynamical systems, and this generalization is proposed here as the basic rigorous definition of quantum ergodicity. It implies the ability to construct an orthonormal basis, where quantum dynamics transports an initial basis vector to all other basis vectors one by one, while minimizing the error in the overlap between the time-evolved initial state and a given basis state with a certain precision. It is proven that the basis, optimizing the error over all cyclic permutations, is obtained via the discrete Fourier transform of the energy eigenstates (for Hamiltonian systems) and quasienergy eigenstates (for Floquet systems). This relates quantum cyclic ergodicity to level statistics. We then show that Wigner-Dyson level statistics implies quantum cyclic ergodicity, but that the reverse is not necessarily true. For the former, we study CUE, COE, and CSE ensembles and quantitatively demonstrate the relation between spectral rigidity and ergodicity. For the latter, we study an irrational flow on a 2D torus and argue that both classical and quantum flows are cyclic ergodic. However, the corresponding level statistics is neither Wigner-Dyson nor Poisson. Finally, we use the cyclic construction to motivate a quantum ergodic hierarchy of operators and argue that under the additional assumption of Poincaré recurrences, cyclic ergodicity is a necessary condition for such operators to satisfy the eigenstate thermalization hypothesis. This work provides a general framework for transplanting some rigorous results of ergodic theory to quantum dynamical systems.

# Contents

<b>1</b>	<b>Introduction</b>	<b>3</b>
<b>2</b>	<b>A short review of classical ergodic theory</b>	<b>5</b>
2.1	The classical ergodic hierarchy . . . . .	5
2.2	Discretizing ergodicity with cyclic permutations . . . . .	6
<b>3</b>	<b>Dynamical quantum ergodicity and cyclic permutations</b>	<b>8</b>
3.1	Pure state cyclic permutations for quantum dynamics . . . . .	8
3.2	Quantum error bounds on cyclic ergodicity and aperiodicity . . . . .	10
3.3	Optimizing cyclic permutations with energy level statistics . . . . .	11
<b>4</b>	<b>Cyclic permutations for systems with typical rigid spectra</b>	<b>15</b>
4.1	Periodic and random parts of time evolution . . . . .	15
4.2	Gaussian estimate for persistence amplitudes . . . . .	16
4.3	Spectral rigidity for Gaussian persistence amplitudes . . . . .	17
4.4	Cyclic ergodicity and aperiodicity for Wigner-Dyson random matrices . . . . .	18
<b>5</b>	<b>Mixed states and the classical limit</b>	<b>19</b>
5.1	Summary of classical limit heuristics . . . . .	21
5.2	Mixed state cyclic permutations for quantum dynamics . . . . .	22
5.3	Spectral rigidity of an ergodic flow on a KAM torus . . . . .	23
<b>6</b>	<b>Discussion</b>	<b>25</b>
6.1	Thermalization time scales, and a late-time ergodic hierarchy . . . . .	27
6.2	Poincaré recurrences and eigenstate thermalization . . . . .	29
<b>7</b>	<b>Conclusions</b>	<b>30</b>
	<b>Appendix A Classical cyclic permutations (review)</b>	<b>38</b>
	<b>Appendix B Quantum cyclic permutations</b>	<b>38</b>
B.1	Fastest decay of persistence . . . . .	38
B.2	Optimal errors for cyclic permutations . . . . .	39
B.3	Decrease of persistence for small permutations of sorted energy levels . . . . .	43
	<b>Appendix C Time dependence of persistence amplitudes</b>	<b>45</b>
C.1	Error coefficient pairing in discrete sum over paths . . . . .	45
C.2	Gaussian estimate . . . . .	46
C.3	Minimum error constraints from the SFF . . . . .	47
C.4	Numerical evidence for error coefficient pairing . . . . .	47
	<b>Appendix D The classical limit</b>	<b>48</b>
D.1	Wigner quasiprobabilities and mixed states . . . . .	48
D.2	Cyclic permutations for a harmonic oscillator . . . . .	49
	<b>Appendix E Mixed state cyclic permutations</b>	<b>49</b>
	<b>Appendix F Cyclic permutations for linear flows on a 2D torus</b>	<b>52</b>
F.1	Classical cyclic permutations for the 2D torus . . . . .	52
F.2	Additional data and discussion for quantized torus . . . . .	52

# 1 Introduction

Ergodic theory [1–3] concerns itself with a study of the statistical properties of classical dynamical systems, centered around a mathematically precise classification of dynamics into different levels of randomness called the ergodic hierarchy [4, 5] (see Fig. 1). These levels, such as ergodic, mixing, K-mixing and others [1–5] (in order of increasing randomness, discussed in more detail in Sec. 2.1), can be used to motivate different elements of classical statistical mechanics [4, 5]: ergodicity justifies the use of the microcanonical ensemble, and mixing the approach to thermal equilibrium, while K-mixing is responsible for chaotic dynamics.



Figure 1: The Ergodic Hierarchy (according to e.g. Ref. [4]).  $\lambda$  indicates the maximal Lyapunov exponent, whose nonzero value is a defining signature of chaos [4, 5]. The Bernoulli level has more randomness than the K-mixing level, but isn’t directly relevant for this work. (Reused from Ref. [6])

In contrast, our present understanding of quantum statistical mechanics is founded on a much less precise, but empirically successful, connection to the statistical properties of random matrices [7, 8]. Direct contact with the thermalization of observables is made through a comparison of the energy eigenstates (or eigenvectors) of a system with random eigenvectors, via the Eigenstate Thermalization Hypothesis (ETH) [9–15] and related approaches [16–21]. While ETH has some basic mathematical backing from canonical typicality [16, 17], and shows some resemblance to ergodicity and mixing for local observables [13], much remains unclear about the physical mechanism through which ETH arises in individual systems, for precisely which observables in which kinds of systems, and whether it is the only mode of quantum thermalization [13, 14].

Such observable-dependent ambiguities are avoided in the comparison of the statistics of energy eigenvalues (i.e. level statistics) of a system with those of random matrices, at the apparent cost of direct dynamical relevance to thermalization. This approach is based on the observation that on quantization, typical classically non-ergodic systems show highly fluctuating energy spectra with Poisson (locally uncorrelated) level statistics [22], while classically chaotic systems show rigid spectra with the local level statistics of Wigner-Dyson random matrices (after appropriately accounting for symmetries) [23–26]. A semiclassical “periodic orbit” argument for Wigner-Dyson level statistics soon followed [27, 28] (with further developments in e.g. Refs. [29–32]), assuming the dominance of isolated periodic orbits in semiclassical contributions to level statistics, a certain uniform distribution of these periodic orbits, and a K-mixing classical system [7]. However, extremely recent numerical studies of systems without K-mixing show that Wigner-Dyson level

statistics can emerge even on quantization of merely mixing [33] or merely ergodic [34] classical systems. At minimum, this merits a theoretical explanation of spectral rigidity that connects to the classical limit but does not rely on K-mixing.

Similar trends of spectral rigidity have been observed analytically and numerically in fully quantum many-body systems [13, 35–44] (along with a number of intermediate cases [45–47]) which do not necessarily have a classical limit, where in the absence of a precise classification, judgements of the chaoticity of a system have been largely based on intuition. At the same time, correlation functions of *local* observables have been rigorously characterized, in a manner similar to the ergodic hierarchy, in the specific case of dual-unitary quantum circuits [48, 49] — but without any apparent link to level statistics. In all these cases, it remains unclear if there are direct observable consequences of level statistics in time evolution, with the exception of a small correction (the “ramp” [35]) to some correlation functions at late times [41, 50], as well as protocols designed specifically to measure spectral rigidity [51, 52].

In this work, we show that level statistics does have a precise role in determining a quantum version of ergodicity in the time domain, if one considers not local observables, but dynamical structures — cyclic permutations — in the Hilbert space of an individual system. This quantum notion is a natural “quantization” of a discrete version of classical ergodicity i.e. cyclic ergodicity, that can be rigorously defined in terms of cyclic permutations in classical ergodic theory, but does not rely on a classical limit. Conversely, our results strongly suggest that cyclic ergodicity underlies ergodicity in any classical dynamical system that can be quantized. We provide analytical and numerical evidence for the applicability of this picture to Wigner-Dyson level statistics which has been near-universally seen in quantum “chaotic” systems, as well as the spectral rigidity of Kolmogorov-Arnold-Moser (KAM) tori — classically ergodic systems (depending on parameters) that possess neither periodic orbits nor K-mixing and do not show Wigner-Dyson level statistics on quantization.

The rest of this paper is organized as follows. Sec. 2 reviews some necessary aspects of classical ergodic theory, including the use of cyclic permutations to “discretize” a dynamical system [1, 2, 53, 54], and defines cyclic ergodicity and cyclic aperiodicity as discrete, primitive forms of ergodicity and mixing that can be extended to quantum mechanics. Sec. 3 defines their analogues in quantum mechanics, and proves that cyclic ergodicity and aperiodicity are directly determined by a specific measure of level statistics and spectral rigidity (namely, mode fluctuations [33, 55, 56]).

While our derivations up to this point are rigorous, the subsequent sections discuss the application of these results to physical systems using a combination of analytical and numerical arguments. Sec. 4 considers the typical time evolution of cyclic permutations, and provides detailed evidence that quantum systems with Wigner-Dyson spectra are ergodic and aperiodic by this definition, while those with Poisson spectra are not. Sec. 5 argues that quantum cyclic permutations may be identified with classical cyclic permutations in phase space for systems with a classical limit, and provides primarily numerical evidence that the spectra of quantized KAM tori satisfy cyclic ergodicity, suggesting that the latter is a genuine quantum version of classical ergodicity even where random matrix theory is not applicable. Finally, Sec. 6 discusses some insights about thermalization in quantum systems that may be gained from cyclic permutations, in a largely semi-qualitative manner that may motivate future rigorous work.



## 2 A short review of classical ergodic theory

In classical ergodic theory [1–4], one is concerned with dynamics on a phase space (or a smaller region of interest)  $\mathcal{P}$ , with an operator  $\mathcal{T}^t : \mathcal{P} \rightarrow \mathcal{P}$  that evolves points in the space by time  $t$  (which may be a continuous or discrete variable, corresponding to flows or maps). The main questions of interest are which regions of phase space are explored over time by an initial point, and how rapidly a typical point explores these regions.

These questions are conveniently posed when there is a measure  $\mu(A) \geq 0$  defined for subsets  $A \subseteq \mathcal{P}$  that is preserved by time evolution,  $\mu(\mathcal{T}^t A) = \mu(A)$  (in Hamiltonian dynamics, this measure is given by the phase space volume  $\int_A d^n q d^n p$ ). An important feature of such systems is guaranteed by the *Poincaré recurrence theorem* [1–3]: for any  $A \subseteq \mathcal{P}$  such that  $\mu(A) > 0$ , almost every point in  $A$  eventually returns to  $A$ , each within some (long) finite time (i.e. with the exceptions forming a set of measure zero).

Given such a measure, how well an initial point explores the phase space is generally expressed through correlation functions of various sets, the behavior of which is classified into the ergodic hierarchy [4, 5]. In what follows, we normalize the measure so that  $\mu(\mathcal{P}) = 1$ .

### 2.1 The classical ergodic hierarchy

We first ask whether almost all initial points explore every region of nonzero measure in  $\mathcal{P}$ . If so, the dynamics is said to be *ergodic* in  $\mathcal{P}$ . If not,  $\mathcal{P}$  can be decomposed into (say)  $M$  subsets that are invariant under  $\mathcal{T}$ , i.e.  $\mathcal{P} = \bigcup_{j=1}^M \mathcal{P}_j$  (each with a measure induced by  $\mu$ ), such that the dynamics is ergodic within each  $\mathcal{P}_j$ . In terms of correlation functions, ergodicity in  $\mathcal{P}$  is expressed [1–5] as the following condition:

$$\lim_{T \rightarrow \infty} \frac{1}{2T} \int_{-T}^T dt \mu \left[ (\mathcal{T}^t A) \cap B \right] = \mu(A)\mu(B), \quad \forall A, B \subseteq \mathcal{P}. \quad (1)$$

Here, we use  $dt$  either as a continuous integration measure or that corresponding to a discrete sum, depending on the domain of  $t$ .

*Mixing* is a property of time evolution eventually becoming uncorrelated with initial conditions, and represents how rapidly typical points explore a phase space region  $\mathcal{P}$  on which time evolution is ergodic. The simplest such criterion is expressed in terms of two element correlation functions [1–5],

$$\lim_{t \rightarrow \infty} \mu \left[ (\mathcal{T}^t A) \cap B \right] = \mu(A)\mu(B), \quad \forall A, B \subseteq \mathcal{P}, \quad (2)$$

and is conventionally merely called mixing (with two variants, weakly mixing and strongly mixing, depending on whether the limit converges with measure zero exceptions in  $t$ , or exactly [3–5]). This can be extended to higher order correlation functions [57], and the dynamics is said to be *K-mixing* when all higher order correlation functions become uncorrelated in the above sense. These criteria form a hierarchy in the sense that *K-mixing* implies mixing, which implies ergodicity [4, 5]. Additional levels of randomness may also be considered [4, 5]; see Fig. 1 for a depiction of the hierarchy of Ref. [4].

It is interesting to note that if one defines a unitary operator  $U_{\mathcal{T}}$  induced by  $\mathcal{T}$  on the space of functions  $L_2(\mathcal{P})$  on the phase space (Koopman and von Neumann’s Hilbert space representation of classical mechanics [1–3, 54, 58, 59]), some of these properties can be translated to those of the eigenvalues and eigenfunctions of  $U_{\mathcal{T}}$ , whose direct extensions to quantum mechanics have been previously considered [60]. For instance, ergodicity translates to non-degenerate eigenvalues with eigenfunctions of uniform magnitude, and weak mixing to a continuous spectrum with no

non-constant eigenfunction, of  $\mathcal{U}_{\mathcal{T}}$  [3]. For a discrete quantum spectrum corresponding to phase spaces or energy shells of finite measure by Weyl's law [7], the eigenvalues are almost always non-degenerate (i.e. are non-degenerate or can be made so by infinitesimal perturbations) and the spectrum is necessarily discrete, prompting us to seek alternate avenues in which the above properties are at best emergent in the classical limit.

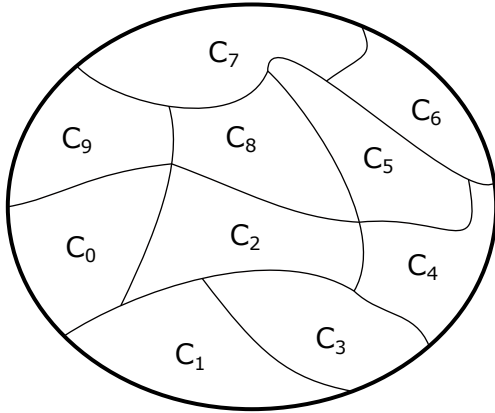
## 2.2 Discretizing ergodicity with cyclic permutations

We eventually want to understand how quantum mechanics with its discrete set of energy levels can lead to ergodic and mixing behaviors, defined classically for continuous systems. A useful bridge between continuum and discrete descriptions is offered by the technique of discretizing an arbitrary dynamical system with cyclic permutations, which have been studied in Refs. [53, 54] (see also Refs. [1, 2, 58, 59] for reviews and related results). Here, we discuss and adapt the elements of this framework that are most relevant for our purposes, following Ref. [54].

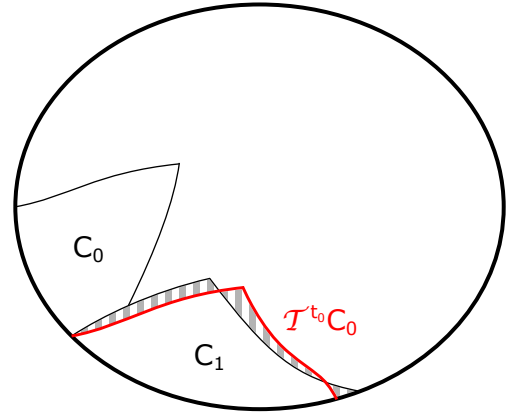
Let  $\mathcal{C} = \{C_k\}_{k=0}^{n-1}$  be a decomposition of the phase space  $\mathcal{P}$  into a large number of  $\mu$ -disjoint (i.e. with measure zero intersection) closed sets of identical measure,  $\mu(C_k) = 1/n$ , with a well-defined  $n \rightarrow \infty$  limiting procedure. Introduce a time evolution operator  $\mathcal{T}_{\mathcal{C}}$  on  $\mathcal{P}$ , which cycles the elements of the decomposition,  $\mathcal{T}_{\mathcal{C}} C_k = C_{k+1}$  (with  $(n-1)+1 \equiv 0$  i.e. the addition is modulo  $n$ ). As a measure of how well  $\mathcal{T}_{\mathcal{C}}$  approximates  $\mathcal{T}^{t_0}$  for some  $t_0$ , define the error of the permutation (differing from that in Ref. [54] by the factor of  $1/2$ ):

$$\bar{\epsilon}_{\mathcal{C}}(t_0) = \frac{1}{2} \sum_{k=0}^{n-1} \mu \left[ (\mathcal{T}^{t_0} C_k) \triangle C_{k+1} \right], \quad (3)$$

where  $A \triangle B = (A \cup B) - (A \cap B)$ . We will often drop  $\mathcal{T}_{\mathcal{C}}$  and directly call  $\mathcal{C}$  the cyclic permutation for brevity, as any  $\mathcal{T}_{\mathcal{C}}$  that cyclically permutes the elements of  $\mathcal{C}$  has the same error. We also note that  $t_0$  could implicitly depend on  $n$ , in particular for a flow with continuous time. A schematic is depicted in Fig. 2



(a) Partitioning of phase space into  $\{C_k\}_{k=0}^{10-1}$ .



(b) Contribution to error from  $(\mathcal{T}^{t_0} C_0) \triangle C_1$  (shaded region).

Figure 2: Schematic depiction of an  $(n = 10)$ -element cyclic permutation for some phase space  $\mathcal{P}$  (interior of ellipse).

The error  $\bar{\epsilon}_{\mathcal{C}}(t_0)$  can serve as a probe of ergodicity. In particular, Ref. [54] shows that with an additional assumption, the error provides a bound on the number  $M$  of subsets  $\mathcal{P}_j \subseteq \mathcal{P}$  that

are ergodic with respect to  $\mathcal{T}$ , in the  $n \rightarrow \infty$  limit. In Appendix A, we recount a version of this argument without the additional assumption, where the bound is on the number  $M_C$  of the  $\mathcal{P}_j$  that completely contain at least one of the  $C_k$ . The essence of the argument is that  $\mathcal{T}_C$  is ergodic on  $\mathcal{C}$ , which is a coarse graining of  $\mathcal{P}$ ; the only way  $\mathcal{T}$  can avoid being ergodic on this coarse graining is if it is sufficiently different from  $\mathcal{T}_C$ . In fact, one obtains the precise bound  $\bar{\epsilon}_C(t_0) \geq M_C/n$  for  $M_C \geq 2$ .

The bound is to be interpreted as follows: the existence of any  $n$ -element cyclic permutation  $\mathcal{C}$  that approximates  $\mathcal{T}^{t_0}$  with  $\bar{\epsilon}_C(t_0) < 2/n$ , implies that none of the  $C_k$  are contained inside any invariant subset of  $\mathcal{P}$  (other than  $\mathcal{P}$  itself). Motivated by this property, we define the property of “cyclic ergodicity” of a cyclic permutation.

**Definition 2.1 (Classical cyclic ergodicity).** *A cyclic permutation  $\mathcal{C}$  shows cyclic ergodicity iff any element  $C_j \in \mathcal{C}$  sequentially intersects a non-vanishing fraction of every other  $C_k \in \mathcal{C}$  at least once under (future and past) time evolution:*

$$n\mu \left[ (\mathcal{T}^{p t_0} C_j) \cap C_{j+p} \right] > 0 \text{ as } n \rightarrow \infty, \text{ for all } j \text{ and } |p| \leq \frac{n}{2}, \quad (4)$$

where  $p$  represents the number of integer steps of time evolution in units of  $t_0$ .

Cyclic ergodicity implies ergodicity in the sense of Eq. (1) if we further require that all invariant subsets of  $\mathcal{P}$  must contain at least one  $C_k$ , which is the additional assumption imposed in Ref. [54]. In such cases, the index  $k$  of  $C_k$  can be loosely thought of as an approximate time coordinate in  $\mathcal{P}$  (when  $n \rightarrow \infty$ ). Cyclic ergodicity and non-ergodicity are depicted in Fig. 3

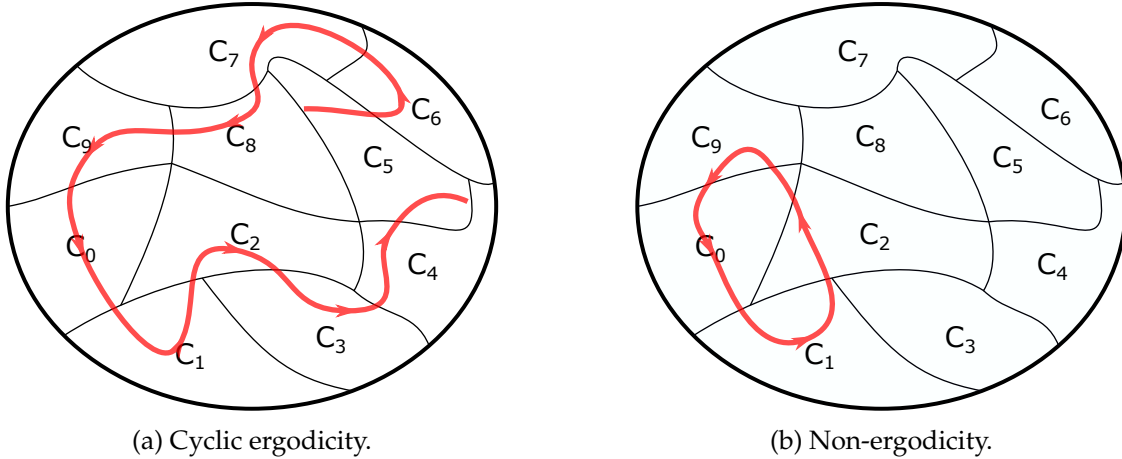


Figure 3: Schematic depiction of cyclic ergodicity and non-ergodicity for the cyclic permutation of Fig. 2. The trajectory may be thought of as the future and past history of the center of  $C_0$ , for 5 steps of  $t_0$  each (arrows indicate the forward flow of time).

It is also useful to define the “cyclic aperiodicity” of a cyclic permutation.

**Definition 2.2 (Classical cyclic aperiodicity).** *A cyclic permutation  $\mathcal{C}$  shows cyclic aperiodicity iff  $\mathcal{T}^t C_k$  never returns to intersect a non-vanishing fraction of  $C_k$  for any  $t$  satisfying  $t_0 \ll t \lesssim O(nt_0)$ :*

$$n\mu \left[ (\mathcal{T}^t C_j) \cap C_j \right] = 0 \text{ as } n \rightarrow \infty, \text{ for all } j \text{ and } t_0 \ll t \lesssim O(t_0 n). \quad (5)$$

This can be shown along similar lines [54] (see Appendix A for a review) to imply  $\bar{\epsilon}_C(t_0) \geq 1/n$ . Cyclic aperiodicity is a necessary condition for mixing in the  $n \rightarrow \infty$  limit [54] (albeit with

a subtlety in the order of limits, requiring  $n \rightarrow \infty$  faster than  $t \rightarrow \infty$  in Eq. (2)). More generally, the existence of an  $n$ -element cyclic permutation with  $\bar{\epsilon}_C < 1/n$  rules out mixing in the sense of Eq. (2) at least until times  $t > nt_0$ .

The above statements connect properties of discretized classical dynamics to levels of the ergodic hierarchy. The next section aims to find parallels to these properties in quantum mechanics.

### 3 Dynamical quantum ergodicity and cyclic permutations

Let  $\hat{U}_H(t)$  be the unitary time evolution operator, with  $D$  (possibly nonunique) eigenstates  $(|E_n\rangle)_{n=0}^{D-1}$  and  $D$  (correspondingly, possibly degenerate) eigenvalues  $e^{-iE_n t}$ :

$$\hat{U}_H(t)|E_n\rangle = e^{-iE_n t}|E_n\rangle. \quad (6)$$

The time variable  $t$  can be chosen to be continuous or discrete, with  $E_n$  respectively corresponding to the eigenvalues of a Hamiltonian or eigenphases of a Floquet map. Without loss of generality, we will use terminology associated with Hamiltonians in what follows.

The time evolution of an arbitrary (normalized) state  $|\psi(t)\rangle$  preserves the overlaps  $|\langle E_n|\psi(t)\rangle|^2$ . Thus, if the Hilbert space  $\mathcal{H}$  of states is interpreted as a phase space in the sense of classical ergodic theory, it always decomposes [13, 14] into a continuum of ergodic sectors, which are subsets of the invariant regions  $\mathcal{H}(r)$  in  $\mathcal{H}$  with definite values of the tuple  $(r_n) = \left(|\langle E_n|\psi\rangle|^2\right)_{n=1}^D$ . However, none of the  $\mathcal{H}(r)$  themselves form subspaces, and consequently, they do not offer sufficient structure to consider superpositions and projective measurements.

#### 3.1 Pure state cyclic permutations for quantum dynamics

More useful notions of ergodicity can be defined if one attempts to construct a primitive version of a classical dynamical system with suitable primitive properties within the Hilbert space. We will see that the construction of pure state cyclic permutations, in analogy with classical cyclic permutations, provides one way to achieve this goal; in particular, quantum versions of cyclic ergodicity and cyclic aperiodicity (Eqs. (4) and (5)) can then be defined naturally.

We work in an invariant subspace  $\Sigma_d \subseteq \mathcal{H}$  (an ‘energy subspace’) spanned by any subset of suitably relabeled eigenstates  $(|E_n\rangle)_{n=0}^{d-1}$ . This subspace contains several of the invariant regions  $\mathcal{H}(r) = \Sigma_d(r) \subset \Sigma_d$ , which we will call subshells. Among these, the unbiased subshell  $\Sigma_d(\bar{r})$  with  $\bar{r}_n = 1/d$  is unique in containing entire orthonormal bases for  $\Sigma_d$ , while no other subshell contains even a single orthonormal basis.

We seek cyclic permutations that approximate  $\hat{U}_H(t)$  within this energy subspace. To this end, let  $\mathcal{C} = \{|C_k\rangle\}_{k=0}^{d-1}$  be an orthonormal basis spanning  $\Sigma_d$  with cycling operator  $\hat{U}_C|C_k\rangle = |C_{k+1}\rangle$ . The eigenvalues of  $\hat{U}_C$  are necessarily distinct  $d$ -th roots of unity,  $\{\exp(-2\pi i n/d)\}_{n=0}^{d-1}$ . It is convenient to introduce the  $p$ -step persistence amplitudes (relative to the action of  $\hat{U}_C^p$ ),

$$z_k(p; t_0) = |\langle C_{k+p}|\hat{U}_H(pt_0)|C_k\rangle|, \quad (7)$$

for some choice of  $t_0$ ; these satisfy  $z_k(p; t_0) \in [0, 1]$ . Then, we say that  $\hat{U}_C$  approximates  $\hat{U}_H(t_0)$  with  $p$ -step error

$$\varepsilon_C(p; t_0) = 1 - \left( \min_{k \in \mathbb{Z}_d} z_k(p; t_0) \right)^2. \quad (8)$$

A pure state approximation scheme for unitaries has been constructed in Ref. [59], in analogy to certain classical non-cyclic transformations (which are indirectly related to classical cyclic permutations [61]), to formalize results on e.g. the degeneracy of  $U_T$  in classical ergodic theory [1, 3, 54, 61] (cf. Sec. 2.1). As we will see in Sec. 3.3, the construction of pure state cyclic permutations as above allows us to go much further, and tackle non-trivial measures of the level statistics of  $\hat{U}_H(t)$  that can e.g. meaningfully distinguish between Wigner-Dyson and Poisson statistics.

In analogy with the definitions for classical cyclic permutations (Eqs. (4) and (5)), we can define cyclic ergodicity and cyclic aperiodicity for these pure state quantum cyclic permutations (see Fig. 4 for a schematic depiction, and Fig. 5 in Sec. 3.3.2 for examples with exact numerical data).

**Definition 3.1 (Quantum cyclic ergodicity).** *A pure state quantum cyclic permutation  $\mathcal{C}$  shows cyclic ergodicity iff*

$$|\langle C_{k+p} | \hat{U}_H(p t_0) | C_k \rangle|^2 \gg O(d^{-1}) \text{ for all } k \text{ and } |p| \leq d/2, \quad (9)$$

*ensuring that any initial state  $|C_k\rangle \in \mathcal{C}$  “visits” all the other elements of  $\mathcal{C}$  sequentially with greater-than-random overlap at least once (including its future and past evolution).*

Cyclic ergodicity can be expressed concisely in terms of the  $p$ -step error,

$$1 - \varepsilon_C(p; t_0) \gg O(d^{-1}) \text{ for all } |p| \leq d/2. \quad (10)$$

**Definition 3.2 (Quantum cyclic aperiodicity).** *A pure state quantum cyclic permutation  $\mathcal{C}$  shows cyclic aperiodicity iff*

$$|\langle C_k | \hat{U}_H(t) | C_k \rangle|^2 \lesssim O(d^{-1}), \text{ for all } k \text{ and } t_0 \ll |t| \lesssim O(t_0 d), \quad (11)$$

The restriction  $t \lesssim O(t_0 d)$  is particularly important here. The quantum recurrence theorem (Poincaré recurrence for the flow of phases of vectors in the energy eigenbasis [62]) on the subshell containing  $|C_k\rangle$ , guarantees that aperiodicity will eventually be violated after some time (but possibly only at times exponentially large in  $d$ ; see e.g. [63] for a related discussion of recurrences). This requires the errors at nonzero integer multiples of  $d$  to be large,

$$1 - \varepsilon_C(n d; t_0) \lesssim O(d^{-1}), \text{ for all } |n| \in \mathbb{N}, \text{ with } n \sim O(1). \quad (12)$$

These definitions involve an explicit cutoff scale  $O(d^{-1})$  for the overlaps of states, which is the order of magnitude of the overlap of a typical random state with any given state [16, 17, 64]. This choice of the cutoff will prove most convenient for our approach, especially in the context of random matrix theory. Additionally, we will often drop the “cyclic” qualifier for ergodicity and aperiodicity in the remainder of this paper, when there is no ambiguity. It is also convenient to talk of quantum systems being ergodic or aperiodic in an energy subspace, according to the following definition. We note that this definition pertains to a dynamical (i.e. time-domain) version of ergodicity, and is distinct from the use of “quantum ergodicity” in the mathematical literature to refer to the delocalization of energy eigenstates [65, 66].

**Definition 3.3 (Ergodicity and aperiodicity of a quantum system).** *We call a quantum system (dynamically) **ergodic** in the energy subspace  $\Sigma_d$  within a time  $T > 0$ , if it admits at least one cyclic permutation in the subspace satisfying cyclic ergodicity for some  $t_0$  with  $t_0 d < T$ . Similarly, the system is **aperiodic** in  $\Sigma_d$  within  $T$  if no ergodic cyclic permutation in  $\Sigma_d$  violates aperiodicity for any choice of  $t_0$  with  $t_0 d < T$  (and quasiperiodic otherwise).*

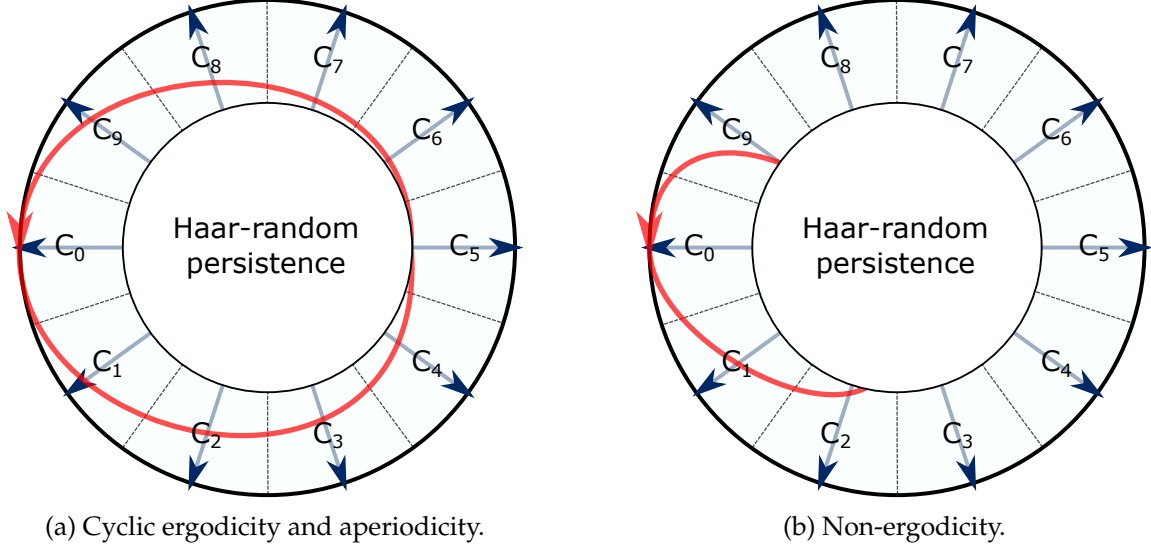


Figure 4: Schematic depiction of cyclic ergodicity and non-ergodicity for a ( $d = 10$ )-element quantum cyclic permutation, in a polar representation  $(r, \theta) \in [0, 1] \times [0, 2\pi)$  of the corresponding ( $d = 10$ )-dimensional Hilbert space  $\Sigma_d$ ; the angular direction is parametrized as  $\theta = 2\pi p/d$ , and the radial coordinate is  $r = f\left(\left|\langle C_0 | (\hat{U}_C^\dagger)^p | \psi \rangle\right|\right)$  for any vector  $|\psi\rangle \in \Sigma_d$ , where  $f : [0, 1] \rightarrow [0, 1]$  is some monotonic function and  $\hat{U}_C^p$  is extrapolated to non-integer  $p$  in some convenient manner (e.g. connecting the  $|C_k\rangle$  along some smooth path). The basis vectors  $|C_k\rangle$  are depicted by arrows representing the corresponding axes. Each of (4a) and (4b) may be loosely regarded as a “quantization” of the respective classical versions in Fig. 3. The trajectory indicates the persistence amplitude  $z_0(p, t_0)$  of the initial state  $|C_0\rangle$  (1 at the outermost boundary, 0 at the center) in the radial direction up to  $|p| = 5$  (visible trajectory) and beyond (“Haar-random persistence”). The region of “Haar-random persistence” refers to  $z_0(p, t_0) = O(d^{-1/2})$ , which includes all Haar random states by canonical typicality [16, 17]. Consequently, this region has by far the largest (Haar) volume in the (unbiased subshell of the) Hilbert space  $\Sigma_d$ , while the depicted outer regions of non-random overlap with the  $|C_k\rangle$  together form a relatively tiny fraction of the space.

For example, every system is always ergodic and not aperiodic in any subspace  $\Sigma_1$  consisting of a single energy level. For typical quantum systems, we will implicitly assume a choice of  $T$  that is as large as possible while being much less than the quantum recurrence time scale. In general, identifying which energy subspaces of the system satisfy these properties provides an observable-independent characterization of the ergodicity of a quantum system.

### 3.2 Quantum error bounds on cyclic ergodicity and aperiodicity

Now, we ask how the 1-step error  $\varepsilon_C(1; t_0)$  can be used to determine the overall ergodicity and aperiodicity of a cyclic permutation. For this, we need to determine the fastest possible decay of the persistence  $z_k(p; t_0)$  with time  $p$ , taking into account the possibility of superposition of errors from successive times. As shown in Appendix B.1, the fastest decay of the persistence occurs when the action of the error unitary  $\hat{U}_\Delta = \hat{U}_C^\dagger \hat{U}_H(t_0)$  corresponds to a rotation in a (complex) 2D plane.

This is quantified by the nonlinear relation:

$$\begin{aligned} & \text{sgn}(p_2) \min \left\{ \arccos z_k(p_2; t_0), \frac{\pi}{2} \right\} - \text{sgn}(p_1) \min \left\{ \arccos z_k(p_1; t_0), \frac{\pi}{2} \right\} \\ & \leq (\text{sgn}(p_2) - \text{sgn}(p_1)) \sum_{p=p_1}^{p_2} \arccos z_{k+p}(1; t_0). \end{aligned} \quad (13)$$

For  $\varepsilon_C(1; t_0) \ll 1$ , as would be the case for any but the poorest possible approximation of  $\hat{U}_H(t_0)$  by cyclic permutations, Eq. (13) further implies

$$\begin{aligned} & \text{sgn}(p_2) \arccos z_k(p_2; t_0) - \text{sgn}(p_1) \arccos z_k(p_1; t_0) \\ & \leq (p_2 - p_1) \varepsilon_C^{1/2}(1; t_0) + O[(p_2 - p_1) \varepsilon_C^{3/2}(1; t_0)], \end{aligned} \quad (14)$$

when either term on the left hand side does not exceed  $\pi/2$  in magnitude. Setting  $p_2 = \pm d/2$ ,  $p_1 = 0$  and imposing Eq. (10) at  $p = p_2$  gives

$$\left[ \varepsilon_C(1; t_0) \leq \frac{\pi^2}{d^2} + O(d^{-5/2}) \right] \implies \text{Cyclic ergodicity of } \mathcal{C}. \quad (15)$$

Similarly, setting  $p_2 = \pm d$ ,  $p_1 = 0$  and imposing Eq. (12) at  $n = \pm 1$  (respectively) gives

$$\text{Cyclic aperiodicity of } \mathcal{C} \implies \left[ \varepsilon_C(1; t_0) \geq \frac{\pi^2}{4d^2} + O(d^{-5/2}) \right]. \quad (16)$$

The 1-step persistence amplitudes  $z_k(1; t_0)$  and error  $\varepsilon_C(1; t_0)$  are quantities that are accessible at the significantly early time  $t_0$ , much smaller than the period  $t_0 d$  of a cyclic permutation. In contrast, the higher  $p$ -step persistence amplitudes of the cyclic permutation — and consequently, ergodicity and aperiodicity — are sensitive to the detailed structure (such as the precise energy levels and eigenstates) of  $\hat{U}_H(t_0)$ , particularly at late times  $p \sim O(d)$ . The existence of bounds such as Eqs. (15) and (16) (or more generally, Eq. (13)) allows one to prove ergodicity and disprove aperiodicity for a system based entirely on information available at time  $t = t_0$ , bypassing a refined knowledge of  $\hat{U}_H(t_0)$ .

### 3.3 Optimizing cyclic permutations with energy level statistics

The best possible determination of ergodicity and aperiodicity using the inequalities Eq. (15) and Eq. (16) is when  $\varepsilon_C(1; t_0)$  attains its minimum value over all possible choices of cyclic permutations  $\mathcal{C}$ . More generally, it is reasonable to expect the cyclic permutation with minimum  $\varepsilon_C(1; t_0)$  to have the largest  $p$ -step persistence amplitudes for a range of  $p$ . The optimal (minimum)  $p$ -step errors (including for  $p = 1$ ) can be identified with the help of the following statement, proved in Appendix B.2.

**Theorem 3.4 (Optimal cyclic permutations).** *If the system (in some energy subspace  $\Sigma_d$ ) admits some cyclic permutation  $\mathcal{C}'$  with  $p$ -step error  $\varepsilon_{\mathcal{C}'}(p; t_0) \leq (2/d)$  for a given  $p$  and  $t_0$ , then  $\varepsilon_C(p; t_0)$  attains its minimum value among all cyclic permutations for a cyclic permutation  $\mathcal{C}$  whose cycling operator  $\hat{U}_C$  satisfies*

$$\lim_{\delta \rightarrow 0} \left[ \hat{U}_H(t_0) e^{i\delta \hat{Y}}, \hat{U}_C \right] = 0. \quad (17)$$

Here,  $\hat{Y}$  is any fixed Hermitian operator (which effectively selects a unique eigenbasis of  $\hat{U}_H(t_0)$  if the latter is degenerate). In particular, the global minimum of the error is achieved by one such  $\hat{U}_C$  for every choice of  $\hat{Y}$ .

The rest of this paper discusses how the above statement can be utilized to reveal connections between ergodicity and energy level statistics. For now, we note a curious coincidence — the cutoff value  $(2/d)$  for the  $p$ -step quantum error, below which Eq. (17) is satisfied by an optimal pure state cyclic permutation, is precisely the cutoff value of the error of a *classical*  $d$ -element cyclic permutation that would guarantee ergodicity for  $p = 1$  [54] (cf. Sec. 2.2).

### 3.3.1 Discrete Fourier Transforms of energy eigenstates

Given a complete orthonormal set of eigenvectors  $\{|E_n\rangle\}_{n=0}^{d-1}$  of  $\hat{U}_H(t_0)$ , it follows from Eq. (17) that a sufficiently complete set of  $\hat{U}_C$  that extremize the errors is given by

$$\hat{U}_C = \sum_{n=0}^{d-1} e^{-2\pi i n/d} |E_{q(n)}\rangle \langle E_{q(n)}|, \quad (18)$$

where  $q(n)$  represents an arbitrary permutation acting on  $n \in \{0, \dots, d-1\}$ . The corresponding cyclic basis  $\mathcal{C}$  is completely contained in the unbiased subshell; parametrizing the basis by  $q$ , as well as arbitrary phases  $\varphi_n$  that don't influence  $\hat{U}_C$ , the elements of  $\mathcal{C}(q, \varphi_n)$  can be written as a discrete Fourier transform (DFT) of the energy eigenstates

$$|C_k(q, \varphi_n)\rangle = \frac{1}{\sqrt{d}} \sum_{n=0}^{d-1} e^{-2\pi i n k/d} e^{-i\varphi_n} |E_{q(n)}\rangle. \quad (19)$$

It is immediately seen that all the  $p$ -step persistence amplitudes that are relevant for ergodicity (Eq. (9)) are equal,  $z_k(p; t_0) = z(p; t_0)$  in such a basis, and can be concisely expressed as

$$z(p; t_0) = \left| \frac{1}{d} \text{Tr} [\hat{U}_H(p t_0) \hat{U}_C^{-p}] \right| = \left| \frac{1}{d} \sum_{n=0}^{d-1} \exp \left[ i p \left( \frac{2\pi n}{d} - E_{q(n)} t_0 \right) \right] \right|. \quad (20)$$

The statement of aperiodicity (Eq. (11)) in such a basis can be expressed in terms of the spectral form factor (SFF) [7],

$$K(t) \equiv \left| \frac{1}{d} \text{Tr} [\hat{U}_H(t)] \right|^2 \lesssim O(d^{-1}), \text{ for } t_0 \ll |t| \lesssim O(t_0 d). \quad (21)$$

From Eq. (20), we obtain a discrete set of  $d!$  possible minima (corresponding to the number of possible permutations) of each  $p$ -step error,

$$\varepsilon_C(p, t_0, q) = 1 - \left| \frac{1}{d} \sum_{n=0}^{d-1} \exp \left[ i p \left( \frac{2\pi n}{d} - E_{q(n)} t_0 \right) \right] \right|^2, \quad (22)$$

among which some  $\varepsilon_C(p, t_0, q_{\min}(p))$  is a global minimum for each  $p$  (if the error is less than  $(2/d)$ ). The minimum of the error also corresponds to a maximum of the mean  $p$ -step persistence amplitude. Thus, the minimum  $p$ -step error (or maximum  $p$ -step mean persistence) among cyclic permutations is an *invariant feature of the energy levels*, and can itself be considered a measure of energy level statistics. In such a DFT basis, the persistence probabilities  $z^2(p; t_0)$  are given by the spectral form factor of the *error* unitary  $\hat{U}_\Delta$ , satisfying the simple 1-step error bound (from Eq. (14))

$$z^2(p, t_0) \geq \begin{cases} \cos^2 \left( p \sqrt{\varepsilon_C(1, t_0, q)} \right), & \text{for } |p| < \pi / \sqrt{4\varepsilon_C(1, t_0, q)}, \\ 0, & \text{for } |p| \geq \pi / \sqrt{4\varepsilon_C(1, t_0, q)}, \end{cases} \quad (23)$$

neglecting  $O[p\varepsilon_C^{3/2}(1, t_0, q)]$  contributions.



### 3.3.2 Persistence amplitudes and spectral mode fluctuations

The main measure of level statistics appearing in the errors  $\varepsilon_C(p, t_0, q)$  (cf. Eq. (22)), as well as the persistence of cyclic permutations, is the deviation of energy levels from a regularly spaced spectrum. Namely, let

$$\Delta_n(t_0, q) = \left( \frac{t_0 d}{2\pi} E_{q(n)} \right) - n, \quad (24)$$

representing the deviation of the  $q(n)$ -th level in a rescaled spectrum from the integer  $n$ . The persistence as a function of time as given by

$$z^2(p, t_0) = \left| \frac{1}{d} \sum_n e^{-i(2\pi p/d) \Delta_n(t_0, q)} \right|^2 \xrightarrow{d \rightarrow \infty} \left| \int d\Delta f(\Delta; t_0, q) e^{-i(2\pi p/d) \Delta} \right|^2, \quad (25)$$

where  $f(\Delta; t_0, q)$  is the probability density function of the  $\Delta_n(t_0, q)$ .

Intuitively, the persistence at any time  $p$  would be maximized when the  $\Delta_n$  are minimized. A practically reasonable choice of  $t_0$  and  $q$  to estimate the global minimum of the 1-step error, for uniform density of states  $\Omega(\Sigma_d) = (d-1)/(E_{\max} - E_{\min})$  (uniform over large energy windows), is one in which the rescaled levels  $t_0 d E_{q(n)}/2\pi$  are each close to the  $n$ -th integer. In other words,  $t_0 \approx 2\pi\Omega(\Sigma_d)/d$ , with  $q$  being the permutation that sorts the energy levels in ascending order ( $E_n > E_m \implies n > m$ ). For a given  $t_0$ , it is shown in Appendix B.3 that Eq. (25) is indeed maximized at  $p = 1$  when  $q(n)$  is the sorting permutation, among a certain class of “small” permutations when  $\Delta_n \ll d$ . In other words, the sorting permutation is a (discrete version of a) local minimum for the error.

In this case, the  $\Delta_n$  are essentially what have been called mode fluctuations in the spectrum<sup>1</sup> [33, 55, 56]; the Gaussianity of their distribution has been conjectured to be a signature of chaos [55, 56]. A minor, but important, technical distinction between  $\Delta_n$  and conventional mode fluctuations, is that there is no unfolding [7, 8] of the energy levels to make  $\Omega(\Sigma_d)$  appear uniform prior to calculating the  $\Delta_n$ . Such a procedure, while indispensable in the numerical comparison of level statistics with random matrix predictions, would not preserve the dynamics of the system in the time domain. Given this qualifier, we find in Eq. (25) that the Fourier components of mode fluctuation distributions, *without unfolding*, directly determine the optimal persistence of cyclic permutations.

By the reciprocal relation of Fourier variables, a slow decay of the persistence corresponds to a narrow distribution  $f(\Delta; t_0, q)$ ; when  $q$  is a sorting permutation, this essentially implies a high rigidity of the spectrum e.g. as measured by the variance  $\sigma_\Delta^2$  of the distribution. While the precise connection between ergodicity and spectral rigidity depends on the functional form of this distribution, the following proposition acquires special importance for Wigner-Dyson level statistics:

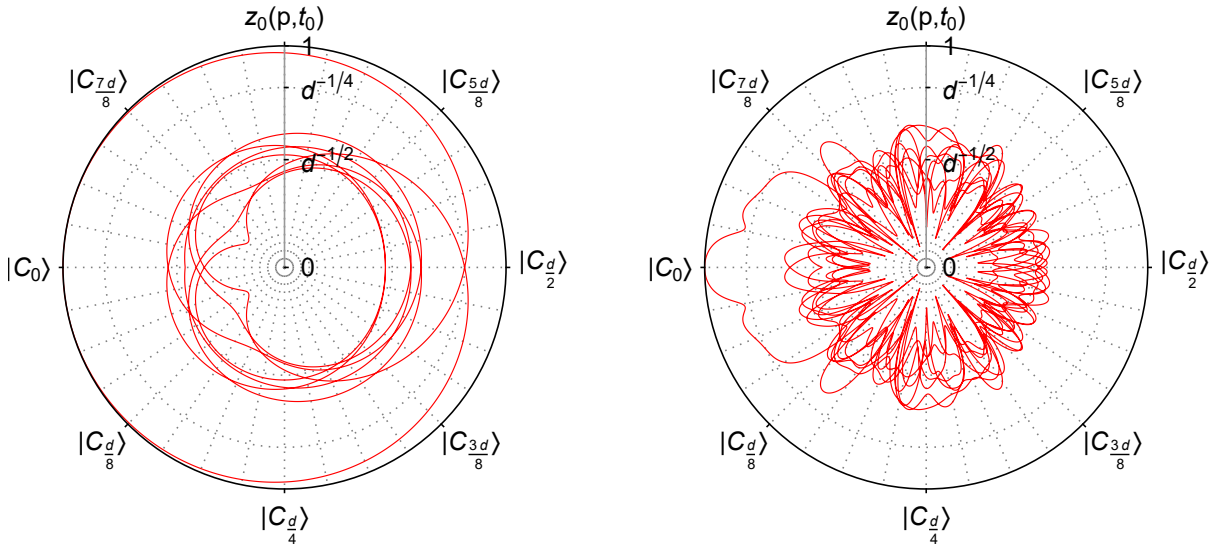
**Proposition 3.5 (Ergodicity, aperiodicity and Wigner-Dyson spectral rigidity).** *If  $z(p, t_0) = e^{-\gamma p^2} +$*

<sup>1</sup>The term “mode fluctuations” has been used with at least two different meanings in the literature [33, 55, 56]. In Refs. [55, 56] and related works cited there, it refers to the fluctuations of the *spectral staircase* around a straight line. Our usage is in the sense of Ref. [33], referring to deviations of the levels themselves from a straight line. The two are different in general, but show close agreement in their statistical properties for Wigner-Dyson random matrix ensembles [67, 68] (see also Sec. 4.4).

$O(d^{-1/2})$  with  $\gamma > 0$  when  $|p| \lesssim O(t_0 d)$  for some DFT cyclic permutation  $\mathcal{C}$ , then

$$\text{Cyclic ergodicity and aperiodicity of } \mathcal{C} \iff \left[ \sigma_\Delta^2 = \frac{\alpha^2}{4\pi^2} \ln d \text{ with } \alpha \in [1, 2], \text{ as } d \rightarrow \infty \right]. \quad (26)$$

This form of  $\sigma_\Delta^2$  is precisely that of the Wigner-Dyson circular random matrix ensembles [7, 8, 67, 68] for  $\alpha = 1, \sqrt{2}, 2$ , while the near-Gaussianity of  $z^2(p, t_0)$  for these ensembles is supported by the observed Gaussianity of  $f(\Delta; t_0, q)$  for mode fluctuations. We will consider the applicability of this proposition to Wigner-Dyson random matrices in greater detail in the next section, using analytical arguments and numerical results. Overall, this proposition suggests that (circular) Wigner-Dyson random matrices are ergodic and aperiodic, which is anticipated by the numerical data in Fig. 5.



(a) Cyclic ergodicity and aperiodicity (staying closer to the boundary than  $O(d^{-1/2})$  for more than one and less than two full rotations); data for a single Circular Unitary Ensemble (CUE [7, 8]) random matrix.

(b) Non-ergodicity (staying closer to the boundary than  $O(d^{-1/2})$  for less than one full rotation); data for a single realization of Poisson/uncorrelated energy levels.

Figure 5: Exact numerical data for polar representation of cyclic ergodicity and aperiodicity, as well as non-ergodicity, via the trajectory of  $|C_0\rangle$  in a Hilbert space  $\Sigma_d$  with  $d = 2048$ . Essentially, the cyclic permutation basis elements  $|C_k\rangle$  are points on the boundary (with  $p = k$ ) of the polar representation, and the permutation is ergodic if the actual trajectory of any such point remains close to the boundary for a full rotation of the angular coordinate (including future and past evolution). The angular coordinate is  $\theta = 2\pi p/d$  (depicted here for  $p \in \mathbb{Z}$ ), and the radial coordinate represents  $z_0(p, t_0)$  via the map  $r = g(z_0(p, t_0))/g(1)$  with  $g(x) = \{1 + \tanh[\log(x^2 d/2)/6]\}$ . The trajectories extend up to  $|p| = 4d$ . The chosen cyclic permutation in both cases is the sorted DFT cyclic permutation. This figure anticipates the ergodicity of Wigner-Dyson level statistics and non-ergodicity of Poisson level statistics (Sec. 4). The central region  $z_0(p, t_0) = O(d^{-1/2})$  of Haar-random persistence again corresponds to nearly all of the Haar volume of  $\Sigma_d$  by canonical typicality [16, 17], and is where the trajectory typically remains for long times with the exception of occasional recurrences near the boundary. See Fig. 6 for a different depiction of similar data.

## 4 Cyclic permutations for systems with typical rigid spectra

Sec. 3.3.2 identified a connection between a Gaussian time-dependence of the persistence of DFT cyclic permutations, and the spectral rigidity of Wigner-Dyson ensembles. In this section, we expand on this connection by considering the development of states in the  $\mathcal{C}$ -basis over time, motivating a Gaussian estimate for the typical time dependence of persistence amplitudes. This Gaussian estimate is used to derive direct constraints on the error from level statistics, based on the SFF of the system. We also show in detail that ergodic and aperiodic systems with a nearly exact Gaussian persistence amplitude must have a spectral rigidity equal to any weighted average of the three circular ensembles: COE, CUE and CSE. This conclusion is supported with numerical results for individual realizations of these ensembles.

### 4.1 Periodic and random parts of time evolution

For a cyclic permutation  $\mathcal{C}$  with cycling operator  $\hat{U}_C$  that commutes with  $\hat{U}_H$  (i.e. a cyclic permutation of a DFT basis), the  $p$ -step persistence probability is given by the normalized SFF of the error unitary  $\hat{U}_\Delta = \hat{U}_C^{-1} \hat{U}_H(t_0)$  (as noted before Eq. (23)):

$$|z(p; t_0)|^2 = \left| \frac{1}{d} \text{Tr} [\hat{U}_\Delta^p] \right|^2. \quad (27)$$

To study the development of the persistence over time, it is convenient to write a general expression for  $\hat{U}_\Delta^p$  in terms of the  $p$ -step errors  $\varepsilon_C(p; t_0)$ . On account of  $[\hat{U}_\Delta, \hat{U}_C] = 0$ , we have

$$\hat{U}_\Delta^p = \left[ \left( \sqrt{1 - \varepsilon_C(p; t_0)} \right) \hat{1} + \left( \sqrt{\varepsilon_C(p; t_0)} \right) \sum_{m=1}^{d-1} v_m(p) \hat{U}_C^m \right] e^{i\phi_\Delta(p)}, \quad (28)$$

for some phases  $\phi_\Delta(p)$  and complex error coefficients  $v_m(p)$ . Unitarity  $\hat{U}_\Delta^\dagger \hat{U}_\Delta = \hat{1}$  translates to nonlinear constraints on the  $v_m(p)$ :

$$\sum_{m=1}^{d-1} |v_m(p)|^2 = 1, \quad (29)$$

$$v_m(p) + v_{-m}^*(p) = -g_p \sum_{k=1}^{d-1} v_k^*(p) v_{k+m}(p), \text{ for } m \neq 0, \quad (30)$$

where  $v_0(p) \equiv 0$ , and  $g_p \equiv \sqrt{\varepsilon_C(p, t_0) / [1 - \varepsilon_C(p, t_0)]}$ .

As a matter of nomenclature, we call the first term proportional to  $\hat{1}$  in Eq. (28) the “periodic part”, and the remaining terms involving  $\hat{U}_C^m$  (orthogonal to the periodic part) the “random part”, of time evolution. This is because the former becomes a term proportional to  $\hat{U}_C^p$  in  $\hat{U}_H(pt_0)$ , while we expect the  $v_m(p)$  to generally (but not necessarily) look “random”. In fact, (a subset of) the  $v_m(p)$  are directly related to the SFF of  $\hat{U}_H(pt_0)$  within the subspace  $\Sigma_d$ , via:

$$K(pt_0) = \left| \frac{1}{d} \text{Tr} [\hat{U}_H(pt_0)] \right|^2 = \varepsilon_C(p; t_0) |v_{-p}(p)|^2, \quad (31)$$

and the expectation of randomness in the  $v_m(p)$  reflects the randomness in the SFF [37, 41, 69] (more precisely, particularly in the phases of  $\text{Tr}[\hat{U}_H(t)]$ ). Additionally,  $K(pt_0)$  serves as a (rather

weak) lower bound for the  $p$  step errors. In particular,  $\varepsilon_C(p; t_0) = O(1)$  if  $K(pt_0) = O(1)$ , establishing the impossibility of finding cyclic permutations that are reasonably close to  $\hat{U}_H(t_0)$ , when  $t_0$  is in the early time slope regime of the SFF. To refine this bound, we will need a generic expression for the time dependence of  $\varepsilon_C(p; t_0)$ , derived in the following subsection.

## 4.2 Gaussian estimate for persistence amplitudes

Using Eq. (28), one can readily express the persistence at arbitrary time  $p$  in terms of the 1-step parameters  $\varepsilon_C(1; t_0)$  and  $v_m(1)$ . The resulting expression involves a complicated multinomial expansion in the  $v_m(1)$  (with  $\binom{p}{s}$  representing binomial coefficients),

$$\hat{U}_\Delta^p e^{-ip\phi_\Delta(1)} = (1 - \varepsilon_C(1, t_0))^{p/2} \sum_{s=0}^p \binom{p}{s} g_1^s \sum_{m_1, \dots, m_s} v_{m_1}(1) \dots v_{m_s}(1) \hat{U}_C^{m_1 + \dots + m_s}, \quad (32)$$

which is hard to extract general predictions out of. To simplify the expression, we invoke a heuristic argument relying on the expected randomness of the  $v_m$ .

Specifically, we assume that the  $v_m(1)$  are well described by an ensemble of complex numbers with fixed magnitudes and random phases, subject to the constraints Eq. (29) and Eq. (30). Further, if one neglects  $O(\sqrt{\varepsilon_C(p; t_0)})$  corrections to the  $v_m$ , Eq. (30) essentially becomes

$$v_m(p) \approx -v_{-m}^*(p). \quad (33)$$

Thus, pairings of  $v_m(1)$  and  $v_{-m}(1)$  in Eq. (32) have a definite phase and generate contributions that potentially interfere constructively, while the remaining random terms add out of phase. This suggests following a strategy similar to methods based on the pairing of closed Feynman paths in studies of generic semiclassical [7, 28, 30, 31, 70] and quantum [37, 71] chaotic systems: we evaluate the contribution from terms dominated by pairings of  $v_m(1)$  and  $v_{-m}(1)$  with at most one free  $v_{m_k}(1)$ , assuming (with no proof beyond the above argument) that the remaining terms are negligible. As is common with these methods, other contributions would eventually dominate at large enough times, when  $\varepsilon_C(p; t_0)$  is sufficiently large and  $v_m(p)$  is sufficiently random, invalidating Eq. (33) for such  $p$ .

The assumed dominance of paired error coefficients can be used to derive a general form of  $\hat{U}_\Delta^p$  for small  $p$ , and from there an estimate for  $z(p; t_0)$  using a recurrence relation; this is detailed in Appendix C, with numerical evidence for error coefficient pairing. For  $\varepsilon_C(1, t_0) \ll 1$  and  $p \ll 1/\sqrt{\varepsilon_C(1, t_0)}$ , the general form is

$$\hat{U}_\Delta^p e^{-ip\phi_\Delta(1)} \approx \frac{z(p, t_0)}{\sqrt{1 - \varepsilon_C(1, t_0)}} \left[ \sqrt{1 - \varepsilon_C(1, t_0)} \hat{1} + p \sqrt{\varepsilon_C(1, t_0)} \sum_{r=1}^{d-1} v_r(1) \hat{U}_C^r \right]. \quad (34)$$

In other words, time evolution for small  $p$  simply manifests as a relative growth of the random part in comparison to the periodic part, up to an overall phase. This gives a simple Gaussian expression for the persistence amplitude (in the same regime of small error and time):

$$z(p, t_0) \approx \exp \left[ -\frac{1}{2} \frac{\varepsilon_C(1, t_0)}{1 - \varepsilon_C(1, t_0)} p^2 - \frac{1}{2} \varepsilon_C(1, t_0) |p| \right]. \quad (35)$$

The second (linear) term in the exponent is negligible until  $|p| \sim 1/\varepsilon_C(1, t_0)$ , and we will simply drop it in further calculations. The Gaussian follows the sinusoidal lower bound in Eq. (23) rather closely, suggesting that typical cyclic permutations are surprisingly close to saturating the lower bound. In other words,  $\hat{U}_\Delta^p$  remains close to a 2D rotation in Hilbert space, until a time  $p \sim 1/\sqrt{\varepsilon_C(1, t_0)}$  when the cyclic permutation develops a large ( $\sim 1$ ) error.

### 4.3 Spectral rigidity for Gaussian persistence amplitudes

#### 4.3.1 The spectral form factor determines the minimum error for a system

Now we are in a position to quantitatively analyze the connection between familiar measures of spectral rigidity and the persistence of cyclic permutations. The 1-step error coefficients  $v_m(1)$  can be related to the SFF  $K(pt_0)$  in the  $p \ll 1/\sqrt{\varepsilon_C(1, t_0)}$  regime, using Eqs. (28), (31) and (34):

$$|v_{-p}(1)|^2 \approx \frac{1 - \varepsilon_C(1, t_0)}{z^2(p, t_0) \varepsilon_C(1, t_0)} \frac{K(pt_0)}{p^2}. \quad (36)$$

Summing over  $p = -\bar{p}$  to  $\bar{p}$  excluding 0, the left hand side can be at most 1 on account of the normalization constraint, Eq. (29). Expanding  $z^2(p, t_0) = 1 - O(\varepsilon_C(1, t_0)p^2)$  and using  $K(t) = K(-t)$ , we get

$$\sum_{p=1}^{\bar{p}} K(pt_0) \left\{ \frac{1}{p^2} + O[\varepsilon_C(1, t_0)] \right\} \lesssim \frac{\varepsilon_C(1, t_0)}{2(1 - \varepsilon_C(1, t_0))}. \quad (37)$$

Every term on the left hand side is positive. Considering only the first term and choosing the largest possible  $\bar{p}$  for which the second term is negligible, then, gives a reasonably restrictive lower bound on  $\varepsilon_C(1, t_0)$ . Correspondingly, we take  $\bar{p} = 1/(M\sqrt{\varepsilon_C(1, t_0)})$  where  $M$  is some large number satisfying  $M = O(1) \geq 1$ .

We can derive more explicit bounds from Eq. (37) for specific cases. As sums of the SFF over time are self-averaging [37], we replace  $K(pt_0)$  with a smooth power law expression  $K(t) = \lambda t^\gamma$  for  $t_0 \leq t \ll t_0 d$ ,  $\gamma \geq 0$ , and with  $\lambda \ll 1$ , which accounts for the behavior of a wide variety of systems<sup>2</sup>. Evaluating the sum in Eq. (37) for this power law (Appendix C.3) gives the following constraints on the error:

$$\varepsilon_C(1, t_0) \gtrsim \begin{cases} 2\lambda t_0^\gamma \zeta(2 - \gamma), & \text{for } 0 \leq \gamma < 1, \\ \lambda t_0^\gamma \ln \frac{1}{\lambda}, & \text{for } \gamma = 1, \\ \left[ 2\lambda t_0^\gamma \frac{\gamma - 1}{M^{\gamma-1}} \right]^{\frac{2}{\gamma+1}}, & \text{for } \gamma > 1, \end{cases} \quad (38)$$

where  $\zeta(z)$  is the Riemann zeta function.

Now we consider the most important (i.e. typical) cases of practical interest. Poisson statistics [7] corresponds to  $\lambda = d^{-1}$  and  $\gamma = 0$ , for which we obtain

$$\varepsilon_C(1, t_0)|_{\text{Poisson}} \gtrsim \frac{\pi^2}{3d}. \quad (39)$$

Together with the conditions for Eq. (17), this implies that every (DFT and non-DFT) cyclic permutation for a system with Poisson level statistics has  $\varepsilon_C(1, t_0) > (2/d)$ . On the other hand, the circular Wigner-Dyson ensembles [7, 8] have  $\gamma = 1$  and  $\lambda = 2/(\beta d^2)$  with  $\beta = 1, 2, 4$  for COE, CUE, CSE respectively. With  $t_0 = 1$  ( $= 2\pi\Omega/d$ ), the error satisfies

$$\varepsilon_C(1, 1)|_{\text{Wigner-Dyson}} \gtrsim \frac{4}{\beta d^2} \ln d, \text{ with } \beta \in \{1, 2, 4\}. \quad (40)$$

<sup>2</sup>In the following sense:  $\gamma = 0$  and  $\lambda = d^{-1}$  corresponds to generic integrable systems with Poisson statistics [7, 22];  $\gamma = 1$  and  $\lambda \geq O(d^{-2})$  corresponds to generic chaotic systems when  $\lambda = O(d^{-2})$  [7, 8], and those with macroscopic conserved quantities for larger magnitudes of  $\lambda$  [72, 73]; integer  $\gamma > 1$  with  $\lambda = O(d^{-2})$  corresponds to tensor products of  $\gamma$  independent chaotic systems, as well as the  $\gamma$ -particle sectors of single-particle chaotic systems with  $\lambda = O(\gamma! d^{-2})$  (for large  $d$ ), in which the many-particle SFF shows an exponential ramp [42, 45, 46].

These relations encode the following property: any system admits cyclic permutations with large error, but only sufficiently rigid spectra can admit cyclic permutations with small error, quantifying the discussion in Sec. 3.3.2. For instance, if a system is known to have a cyclic permutation with error smaller than  $(2/d)$ , we can rule out Poisson statistics for that system.

#### 4.3.2 Spectral rigidity for ergodic, aperiodic systems with exact Gaussianity

From the viewpoint of the Gaussian estimate, an idealized situation is when the persistence amplitude  $z(p; t_0)$  remains exactly Gaussian as it decays all the way through to the random state (order of magnitude) value  $z(p; t_0) \sim O(d^{-1/2})$ . Writing  $g_1^2 = \varepsilon_C(1, t_0)/[1 - \varepsilon_C(1, t_0)]$ , we can solve for  $g_1$  corresponding to ergodic or quasiperiodic evolution by imposing:

$$\exp \left[ -\frac{1}{2\alpha^2} g_1^2 d^2 \right] \geq c d^{-1/2}, \quad (41)$$

where  $\alpha = 2$  for ergodicity and  $\alpha = 1$  for quasiperiodicity (from Eqs. (9), (11)), while  $c$  is some  $O(1)$  positive constant. From Eq. (25), we also obtain a Gaussian distribution for mode fluctuations given some  $g_1$  (assuming that the DFT cyclic permutation under discussion corresponds to a level permutation function  $q$ ),

$$f(\Delta; t_0, q) = \frac{1}{\sqrt{2\pi\sigma_\Delta^2}} \exp \left[ -\frac{1}{2\sigma_\Delta^2} \Delta^2 \right], \quad (42)$$

with variance  $\sigma_\Delta^2 = g_1^2 d^2 / (4\pi^2)$ . Requiring ergodicity and aperiodicity therefore gives:

$$\sigma_\Delta^2 = \frac{\alpha^2}{4\pi^2} \ln d + O(1), \text{ with } \alpha \in [1, 2]. \quad (43)$$

This amounts to a derivation of Eq. (26).

The logarithmic growth of the variance of mode fluctuations with the dimension  $d$  of the energy subspace is a direct consequence of the Gaussianity of the persistence. In less idealized situations, it is possible to have a non-Gaussian tail in Eq. (35), for  $p \gtrsim 1/\sqrt{\varepsilon_C(1, t_0)}$ , even if the Gaussian estimate holds for smaller times. It is worth noting that non-Gaussian tails at long times would show up as non-Gaussianities near  $\Delta \approx 0$  in the mode fluctuation distribution; such deviations from Gaussianity are largely determined by the complicated correlations between the errors  $v_m$ , partly encoded in the fluctuations of the SFF  $K(pt_0)$ . The main takeaway here is instead the extremely specific numerical range  $\alpha \in [1, 2]$ , of the coefficient multiplying the logarithm, demanded by ergodicity and aperiodicity. For non-Gaussian tails, one would have a similarly specific range of some other parameter.

#### 4.4 Cyclic ergodicity and aperiodicity for Wigner-Dyson random matrices

For Wigner-Dyson random matrix ensembles as well as individual systems with Wigner-Dyson (local) level statistics, it is convenient to choose  $\Sigma_d$  to be an energy shell spanned by  $d$  consecutive energy levels. There is numerical evidence that the mode fluctuation distribution is Gaussian [33, 55, 56] (as well as analytical evidence for a related measure, number fluctuations [74]) especially near  $\Delta \approx 0$ , suggestive of an idealized Gaussian persistence. In Refs. [67, 68], the leading behavior of the variance  $\sigma_\Delta^2$  (there called  $\Delta^*$ ) for these ensembles has been shown to be equal to that of the (spectrum or ensemble averaged) spectral rigidity parameter  $\Delta_3(d)$  [8, 28, 75] — measuring the variance of the “spectral staircase” around a best fit straight line — when  $t_0$  is chosen to be

the slope of the straight line and  $q$  the sorting permutation. Moreover,  $\Delta_3(d)$  can be calculated exactly [8, 28, 70] from the ensemble-averaged SFF  $\overline{K(t)}$  within the energy subspace.

In fact, the leading contribution for large  $d$  comes only from the early time linear ramp region, given by  $\overline{K(t)} \approx t/(\beta\pi\Omega d)$  with  $\beta = 1, 2, 4$  respectively for COE, CUE and CSE (much like in the derivation of Eq. (40)). The result is a logarithmic dependence of  $\sigma_\Delta^2$  on  $d$  to leading order (for  $t_0 = 1$  and  $q$  being the sorting permutation),

$$\sigma_\Delta^2 \Big|_{\text{Wigner-Dyson}} = \frac{1}{\beta\pi^2} \ln d + O(1), \text{ with } \beta \in \{1, 2, 4\}. \quad (44)$$

This precisely corresponds (via  $\sigma_\Delta^2 = g_1^2 d^2 / (4\pi^2)$ ) to an error that saturates the lower bound in Eq. (40), providing an important sanity check. Comparing this with Eq. (43) (cf. Eq. (26)), we see that the Wigner-Dyson ensembles span exactly the range of allowed coefficients for ergodic, aperiodic systems with a Gaussian persistence. CUE is well within this range, whereas COE is at the upper bound and barely ergodic while CSE is at the lower bound and barely aperiodic (here, it is worth noting that the CSE variance is for one non-degenerate half of the spectrum [7, 8]).

In generic quantized classically chaotic systems, Eq. (44) only holds for an energy shell with  $d$  small enough to avoid longer range nonuniversal correlations between far apart energies [28, 70], such as a varying density of states (with no unfolding). In particular, the ergodicity and aperiodicity of systems that show Wigner-Dyson level statistics only applies in a regime that avoids non-universal spectral rigidity saturation effects [28, 33, 56, 70]. From a dynamical standpoint, this is to be expected — such systems are typically ergodic only in infinitely thin energy shells (in the classical limit) and not over phase space volumes covering a wide range of energies.

It remains to be verified that the mode fluctuation distribution in random matrix ensembles is indeed well approximated by a Gaussian all the way until the persistence decays to  $O(d^{-1/2})$ , so that the identification between Eq. (44) and Eq. (43) can be made with some confidence. We provide numerical support for this statement in Fig. 6 for  $d = 2048$ . While we do not treat small deviations from Gaussianity here, it seems reasonable to conclude that a similar identification would hold even for a range of such deviations that do not significantly affect the time when the persistence reaches  $O(d^{-1/2})$ .

## 5 Mixed states and the classical limit

Cyclic ergodicity and aperiodicity have been defined in Eqs. (9) and (11) for a general quantum system, irrespective of the existence of a reasonable classical limit. While these definitions are already very similar-looking to the corresponding classical ones (Eqs. (4) and (5)), it is desirable to establish the connection at a somewhat more concrete level. This is the aim of the present section.

Without a clearly defined general procedure for the classical limit, some parts of our argument are necessarily heuristic (but can be motivated e.g. using Wigner quasiprobabilities [10, 70, 76]). We state the heuristic parts in Sec. 5.1 as a direct correspondence between phase space regions and mixed states. In addition, we motivate the existence of orthonormal bases that resemble coordinates in a phase space region, mixed states in which can presumably be identified with classical cyclic permutations.

Independent of such heuristic assumptions, we attempt to mathematically connect mixed state cyclic permutations to spectral rigidity by constructing a corresponding pure state cyclic permutation. We find that there is an unavoidable ambiguity in this procedure at the level considered here, that may require further information to resolve. Ignoring this ambiguity, for the time

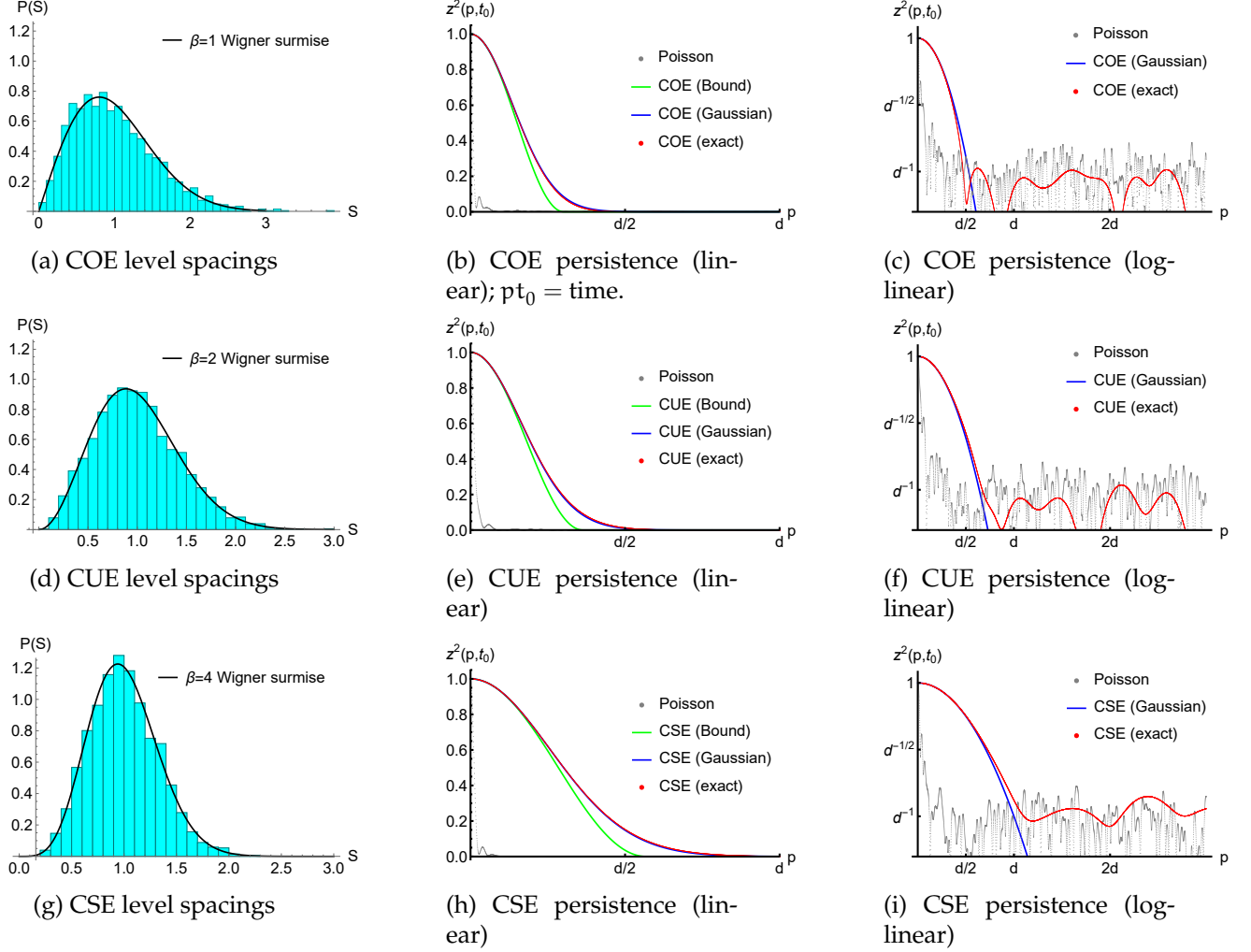


Figure 6: Numerical support for ergodicity and aperiodicity of realizations of Wigner-Dyson random matrix ensembles, for  $d = 2048$ ,  $t_0 = 1$  and  $q$  being the sorting permutation. Level spacing [7] data depicts the closeness of the realization to an ideal Wigner-Dyson distribution. Persistence is plotted (in red) in terms of persistence probabilities  $z^2(p, t_0)$ . The lower bound (“Bound”, green) of Eq. (23) is satisfied, and good agreement is seen with the Gaussian estimate (“Gaussian”, blue) of Eq. (35) including the tail at long times; both are calculated based on the numerical value of  $\varepsilon_C(1, t_0)$  for the realization. The Poisson persistence probability fluctuations (for a sorted distribution of an uncorrelated distribution of points in the same range of energies/eigenphases; in gray) are included to provide a visual reference for the range of persistence probabilities that should be considered  $O(d^{-1})$  for random states, while simultaneously confirming the non-ergodicity of Poisson statistics. The time scales when the random matrix persistence amplitudes reach  $O(d^{-1})$  are consistent with  $p = d/2$  for COE,  $p = d/\sqrt{2}$  for CUE and  $p = d$  for CSE as predicted by Eqs. (41), (43) and (44).

being, allows us to (again, heuristically) construct a pure state cyclic permutation corresponding to a classical cyclic permutation in phase space.

Finally, we consider the level statistics of a (quantized) irrational flow on a 2D Kolmogorov-Arnold-Moser (KAM) torus, a classically ergodic dynamical system that possesses no periodic orbits. We find numerically that it shows level repulsion inconsistent with random matrix predictions (echoing previous numerical results by Berry and Tabor [22] for the closely related 2D



harmonic oscillator); at the same time, it admits an ergodic pure state cyclic permutation. The error of this permutation is consistent with restrictions obtained from the arguments involving mixed states. This result, together with those of Sec. 4.4, suggests a wider applicability of cyclic permutations than random matrix theory in the study of quantum ergodicity.

## 5.1 Summary of classical limit heuristics

The assumed correspondence between mixed states and the classical limit is as follows:

1. Every classical phase space region  $A$  of measure  $\mu(A) \gg 1/d$  can be represented by a mixed state  $\hat{\rho}_A$  with equal eigenvalues, with

$$\mu(A) \approx \frac{1}{d \text{Tr}(\hat{\rho}_A^2)}. \quad (45)$$

2. Given two regions  $A$  and  $B$ , the measure of their intersection is proportional to the overlap of the corresponding mixed states:

$$\frac{\mu(A \cap B)}{\mu(A)\mu(B)} \approx d \text{Tr}(\hat{\rho}_A \hat{\rho}_B). \quad (46)$$

We emphasize that there is no reason to assume the converse - not every mixed state looks like a simple phase space region in the classical limit. The use of approximate equalities here represents the unavoidable ambiguity in quantizing a classical system (where any corrections that vanish as  $d \rightarrow \infty$  are allowed). Loosely speaking, Eqs. (45) and (46) follow from considering each mixed state to be an (equal) ensemble of a subset of orthogonal pure states, where each pure state has a fixed phase space volume (in accordance with Weyl's law for the density of states [7]). In Appendix D.1, we discuss an alternate argument based on Wigner quasiprobability functions.

One can then identify the pure state cyclic permutations of Sec. 3.1 as a limiting case of classical cyclic permutations, when  $n = d$ . The error  $\varepsilon_C(t_0)$  (Eq. (22)), however, corresponds to the maximum of  $n\mu(C_k \triangle C_{k+1})$  rather than the average as for  $\bar{\varepsilon}_C(t_0)$  (Eq. (3)). Assuming the two are approximately equal (as for a DFT basis), it follows that any classical system with  $\bar{\varepsilon}_C(t_0) < (2/n)$  (a sufficient condition for cyclic ergodicity), if quantized to make the naïve  $n \rightarrow d$  limit admissible, has a more rigid spectrum than Poisson statistics by Eq. (39).

An additional link to the classical limit that is useful to consider is a *phase space basis*, which can be loosely thought of as orthogonal minimum uncertainty (i.e. low eccentricity) wavepackets on a thin classical energy shell. More precisely, let  $\mathcal{B}(n) = \{B_k(n)\}_{k=0}^{n-1}$  be a partitioning of the classical phase space  $\mathcal{P}$  into  $\mu$ -disjoint closed sets of nonzero measure. Define an  $n \rightarrow \infty$  limiting procedure such that any  $B_k(n+1)$  is completely contained in some  $B_j(n)$ , and  $\mu(B_k(n \rightarrow \infty)) = 0$  (e.g. nested cyclic permutations). One can formally define “phase space observables”  $A[B_k(n)]$  that take distinct values on each  $B_k(n)$  and have a well defined  $n \rightarrow \infty$  limit, such as a coarse graining of the set of coordinates on  $\mathcal{P}$ . The standard procedure of quantization (e.g. the postulates in Ref. [77]) associates an orthonormal basis of eigenstates  $\mathcal{C}_B = \{|B_k\rangle\}_{k=0}^{d-1}$  (i.e. a phase space basis) spanning some  $\mathcal{H}_B \subseteq \mathcal{H}$  with projective measurements of such an observable.

The importance of such observables is that their classical evolution is first order in time, given by Liouville's equation [78, 79] with the initial phase space distribution being a delta function. Correspondingly, one would expect the quantum time evolution in such a basis to be relatively non-dispersive, and one mixed state in this basis would evolve into another in the same basis (at

least over short times [80, 81]; see also Sec. 6.1). This allows a potential mapping of classical cyclic permutations to mixed states (only) in such a basis; see Appendix D.2 for a simple example<sup>3</sup>.

For a purely quantum system without a known classical limit, the main content of these assumptions is that the purity and overlap of (degenerate) mixed states are quantities of reasonable interest, which allow natural extensions of pure state cyclic permutations to mixed states. Purities and overlaps also have a direct relevance to quantum thermalization e.g. from the viewpoint of the eigenstate thermalization hypothesis [14, 15, 52, 71, 82].

## 5.2 Mixed state cyclic permutations for quantum dynamics

In this section, we attempt to formalize the study of  $n$ -element mixed state cyclic permutations, looking for connections to spectral rigidity, prior to the  $n \rightarrow d$  pure state limit (where the connection can be readily made according to the results in Secs. 3 and 4). We find that significant additional structure than what we have assumed here is necessary to investigate spectral rigidity directly for  $n < d$ .

To define an  $n$ -element mixed state cyclic permutation, we partition the energy subspace into  $n$  orthogonal subspaces of roughly equal dimension:

$$\Sigma_d = \bigoplus_{k=0}^{n-1} \Sigma(k), \text{ such that } \dim(\Sigma(n)) \in \left\{ \left\lceil \frac{d}{n} \right\rceil - 1, \left\lceil \frac{d}{n} \right\rceil \right\}, \quad (47)$$

where  $\lceil x \rceil$  denotes the smallest integer larger than  $x$ . The unequal dimensions of the  $\Sigma(k)$  introduces complications in defining a cycling procedure. To avoid tedium, we expand the Hilbert space to  $\bar{\Sigma}_{d_n} = \Sigma_d \oplus \Sigma_{\text{aux}}$  of dimension  $d_n = n \lceil (d/n) \rceil$ , with expanded subspaces  $\bar{\Sigma}(k) \supseteq \Sigma(k)$  of equal dimension  $\lceil (d/n) \rceil = d_n/n$  (i.e. each having at most one added dimension). Correspondingly,  $\hat{U}_H(t)$  is also to be expanded so that it acts as before on  $\Sigma_d$  while each expanded dimension is an eigenstate:  $\hat{U}_H(t)(\bar{\Sigma}(k) \cap \Sigma_{\text{aux}}) = (\bar{\Sigma}(k) \cap \Sigma_{\text{aux}})$ .

Now, we can introduce mixed states  $\hat{\rho}[\bar{\Sigma}(k)]$  that represent normalized (unit trace) projection operators onto  $\bar{\Sigma}(k)$ . We say that  $\mathcal{S} = \{\bar{\Sigma}(k)\}_{k=0}^{n-1}$  forms a mixed state cyclic permutation that approximates  $\hat{U}_H(t_m)$  at some time  $t_m$ , with 1-step persistence probabilities

$$Z_k(1, t_m) = \frac{d_n}{n^2} \text{Tr} \left\{ \hat{U}_H(t_m) \hat{\rho}[\bar{\Sigma}(k)] \hat{U}_H^\dagger(t_m) \hat{\rho}[\bar{\Sigma}(k+1)] \right\}. \quad (48)$$

By the discussion in Sec. 5.1 (specifically, Eq. (46)), these are mixed state analogues of the classical measure of the intersection  $\mu(C_k \cap C_{k+1})$  for an  $n$ -element cyclic permutation. Consequently, the classical error associated with the cyclic permutation is

$$\bar{\epsilon}_C(t_m) = \sum_k (1 - Z_k(1, t_m)). \quad (49)$$

Given this setup, the following statement is proved in Appendix E.

**Theorem 5.1 (Pure state cyclic permutations from mixed states).** *There exists a pure state cyclic permutation  $\mathcal{C}(\mathcal{S})$ , that approximates the modified time evolution operator  $\hat{U}_H(t_m)\hat{U}_\Sigma$  with persistence*

<sup>3</sup>As a simple example of the lack of such a mapping in other bases, classical motion in the coordinate variables (for Hamiltonians quadratic in the momenta) is second order and one cannot define classical cyclic permutations in these variables alone; correspondingly, diagonal mixed states in the coordinate variables would instantly spread [77] over the entire range of positions, which is not close to any other diagonal mixed state in the basis.

amplitudes  $z_k(1, t_m) = \langle C_{k+1} | \hat{U}_H(t_m) \hat{U}_\Sigma | C_k \rangle$  such that

$$\frac{1}{d} \sum_{k=0}^{d-1} z_k(1, t_m) \geq \sum_{j=0}^{n-1} \frac{1}{d} \left( \lfloor d_n Z_j(1, t_m) \rfloor + \sqrt{d_n Z_j(1, t_m) - \lfloor d_n Z_j(1, t_m) \rfloor} \right), \quad (50)$$

for several choices of  $\hat{U}_\Sigma$  each leaving the original partition invariant:  $\hat{U}_\Sigma \Sigma(k) = \Sigma(k)$ . Here  $\lfloor x \rfloor$  represents the greatest integer smaller than  $x$ .

The most significant takeaway from the above statement is that given just the persistence probabilities of Eq. (48), there is no way to further restrict  $\hat{U}_\Sigma$  beyond leaving the  $\Sigma(k)$  invariant, preventing us from making direct statements about the spectral rigidity of  $\hat{U}_H$ . The one exception is the special case  $n = d$  (when we already have a pure state cyclic permutation), for which any choice of  $\hat{U}_\Sigma$  merely amounts to altering the phases of the  $|C_k\rangle$  — practically equivalent to setting  $\hat{U}_\Sigma = \hat{1}$ .

In general, one would have much more information about a system than just a single mixed state cyclic permutation (e.g. a family of such permutations with different values of  $n$ ). We anticipate that such additional information could help narrow down  $\hat{U}_\Sigma \approx \hat{1}$  as an admissible choice (most likely with some error terms, as Eq. (50) requires a rather fine-tuned specification of  $\hat{U}_\Sigma$ ). An alternative is that one would actually need a mixed state cyclic permutation to explicitly go over into its pure state version with precisely  $n = d$  (or with an appropriate accounting of symmetry sectors), for cyclic ergodicity to be reflected in spectral rigidity. This is something that merits further investigation, and is outside the scope of the present work.

For now, we merely note that if there is some reason to set  $\hat{U}_\Sigma \approx \hat{1}$ , then one can heuristically constrain spectral rigidity using Eq. (50) together with a quadratic estimate  $\varepsilon_C(p, t_0) \approx p^2 \varepsilon_C(1, t_0)$  (consistent with both the sinusoidal lower bound of Sec. 3 and the Gaussian estimate of Sec. 4 when  $\varepsilon_C(p, t_0) \ll 1$ ). This requires assuming that  $\mathcal{C}(\mathcal{S})$  is the  $[p = (t_m/t_0)]$ -th power of a pure state cyclic permutation  $\mathcal{C}(t_0)$  defined at  $t_0 = 2\pi\Omega/d$  (the inverse width of some energy shell with density of states  $\Omega$ ). Then, by Eqs. (50) and (49),

$$\varepsilon_C \left( 1, t_0 = \frac{2\pi\Omega}{d} \right) \lesssim \frac{4\pi^2\Omega^2}{t_m^2 d^2} \bar{\varepsilon}_C(t_m). \quad (51)$$

As per Sec. 3.3.2, this restricts the width of the mode fluctuation distribution, leading to more rigid spectra for smaller classical errors  $\varepsilon_C(t_m)$ .

### 5.3 Spectral rigidity of an ergodic flow on a KAM torus

A simple system that can be tuned to show different behaviors is a KAM torus with a *linear* flow, which occur as invariant subsets in the phase space of integrable systems [5, 7, 78]. The Hamiltonian of a 2D KAM torus is given by

$$H = \mathbf{J} \cdot \boldsymbol{\omega} = J_x \omega_x + J_y \omega_y, \quad (52)$$

with angle variables  $\boldsymbol{\theta} = (\theta_x, \theta_y) \in [0, 2\pi)^2$  conjugate to the action variables  $\mathbf{J} = (J_x, J_y)$ . The equation of motion of the linear flow is  $d\boldsymbol{\theta}(t)/dt = \boldsymbol{\omega}$ .

The ergodicity of this system on the 2D phase space  $\mathcal{P}_J = \{(\theta_x, \theta_y)\}$  with fixed  $\mathbf{J}$  is characterized [1, 2] by the ratio  $\alpha = \omega_y/\omega_x$ . When  $\alpha$  is irrational, the dynamics is ergodic on this phase space; but when  $\alpha$  is rational,  $\mathcal{P}_J$  decomposes into an infinite number of invariant ergodic and periodic subsets, which share the same period. In both cases, there is no mixing.

We call the system of Eq. (52) a KAM torus to emphasize its difference from a free particle moving on a torus. The latter is never ergodic in its *phase space*, but possibly (depending on initial conditions) merely visits all points among its position coordinates with conserved momentum. The Hamiltonian of the free particle is quadratic in  $\mathbf{J}$  rather than linear, and its level statistics has been found to be Poissonian [83, 84] (see also Ref. [56] for its mode fluctuations) in accordance with the Berry-Tabor conjecture [22] for integrable systems.

The quantization of the KAM torus of Eq. (52) entails the restriction  $J_x, J_y \in \mathbb{Z}$ . This also leads to an infinite density of energy levels, and we need an additional ultraviolet (UV) restriction of the domain at large  $\mathbf{J}$  to obtain a finite number of levels. It is convenient to choose boundaries along lines parallel and perpendicular to  $\omega$ , i.e.

$$\mathbf{J} \in \mathbb{Z}^2 \cap \{(J_x, J_y) : |J_x \omega_x + J_y \omega_y| < L_1, |J_x \omega_y - J_y \omega_x| < L_2\}. \quad (53)$$

This corresponds to an energy window of width  $\approx 2L_1$ , with mean density of levels  $\Omega \approx 2L_2$ . If there are  $d$  levels in the window and  $L_1 = O(L_2)$ , we have  $\Omega = O(\sqrt{d})$ .

### 5.3.1 Cyclic permutations on the torus

Cyclic permutations that approximate a large class of time evolution operators on the 2D torus, including nonlinear flows, have been studied in great detail [2, 54, 85]. For our purposes, we need a much simpler construction that can be explicitly achieved for the linear flow.

Based on a result in Ref. [86] pertaining to irrational rotations, a classical  $n$ -element cyclic permutation is constructed for the 2D torus in Appendix F.1, with the following error for almost all irrational  $\alpha$ :

$$\bar{\epsilon}_C \left( t_m = O(\omega n^{-1/2}) \right) < O(n^{-3/2}). \quad (54)$$

If we directly set  $n = d$ , we have  $t_m = O(\Omega/d)$  and the right hand side becomes  $O(d^{-3/2})$ . Alternatively, we can identify the cyclic permutation with mixed states diagonal in the  $\theta$  basis<sup>4</sup> (for  $n \ll d$ ) and take the  $n \rightarrow d$  limit in accordance with the estimate of Eq. (51). In both cases, we obtain a pure state cyclic permutation for the torus with

$$\epsilon_C(1, t_0) < O(d^{-3/2}), \quad (55)$$

where  $t_0 = 2\pi\Omega/d$ , corresponding to mode fluctuations. This suggests that the quantized linear flow on the KAM torus has significantly higher spectral rigidity than Poisson statistics (on account of Eq. (39)), for almost all irrational values of  $\alpha$ .

### 5.3.2 Numerical study of level statistics

To observe direct quantum signatures of possible cyclic ergodicity and aperiodicity, we should look at the persistence of a suitably chosen cyclic permutation (as per Eq. (9)) and the SFF (Eq. (11)). Other indicators include the bound of Eq. (23) on the persistence based on the error at  $t_0$ , and the distribution of mode fluctuations  $f(\Delta)$  in Eq. (25). Comparison with random matrix level statistics can be done with the spacing probability distribution  $P(S)$  of neighboring levels, normalized to unit mean level spacing [7, 8]. Numerical results for these quantities are presented in Figs. 7 and 8 for an irrational ( $\alpha = \sqrt{2}$ ) and rational ( $\alpha = 2$ ) ratio respectively, with approximately 2000 levels in

<sup>4</sup>Noting that the linearity of the Hamiltonian Eq. (52) in  $\mathbf{J}$  is crucial to prevent the fast dispersion of narrow wavepackets in the  $\theta$  basis, for heuristically identifying the classical cyclic permutation with mixed states.

each energy subspace. The results are consistent with cyclic ergodicity and quasi-periodicity with  $\varepsilon_C(1, t_0) \sim O(d^{-2})$  (up to small corrections that may only be visible for larger  $d$ ) for the irrational case, and nonergodicity for the rational case.

In fact, Fig. 7e, in particular, indicates that  $\varepsilon_C \approx \pi^2/d^2$  — which is the largest value of the error for which the bound of Eq. (15) guarantees cyclic ergodicity. Additionally, a *slightly* faster decay than the Gaussian estimate is seen at late times in Figs. 7d, 7e compared to Fig. 6 (perhaps most visible in Fig. 7d). But one should be careful not to rule out e.g. slowly changing logarithmic factors, which may become significant only at much larger  $d$ . Some additional visualizations and discussion of the numerical data are presented in Appendix F.2.

A couple of additional remarks are pertinent. The 2D harmonic oscillator is a related system with the restriction  $J_x, J_y > 0$  that has a finite but nonuniform density of levels at any finite energy. Its level statistics has been studied in Ref. [22], which sees level repulsion after unfolding the nonuniform density, but seemingly not in any random matrix universality class — paralleling what we see for the 2D KAM torus. The central conjecture of Ref. [22] is, however, that typical integrable systems have Poisson level statistics. This holds in spite of the rigid spectrum of each invariant torus, as typical integrable systems are collections of several tori with uncorrelated frequencies<sup>5</sup>, whose combination has enhanced spectral fluctuations and low spectral rigidity (analogous to the situation in Refs. [47, 73]).

These results suggest that the criteria based on cyclic ergodicity and aperiodicity of cyclic permutations, may apply more generally as a quantum version of classical ergodicity than a comparison with random matrix level statistics, including in systems such as the 2D KAM torus that have been considered exceptions to the latter [22].

## 6 Discussion

Identifying ergodicity with the persistence of cyclic permutations in Hilbert space — which is strongly suggested by the results of Secs. 3, 4 and 5 — unavoidably leads us to the conclusion that every ergodic energy subspace in an arbitrary quantum system (with unitary time evolution) admits structures resembling motion in a classical phase space. In particular, an ergodic pure state cyclic permutation resembles a discretization of first-order time evolution in an ergodic region of phase space, over (at least) the long Heisenberg time scale  $t_H = 2\pi\Omega(\Sigma_d)$  (we take  $t_0 = 2\pi\Omega(\Sigma_d)/d$  with  $\Sigma_d$  being a shell of consecutive, sorted energy levels throughout this section). Even after the persistence has decayed to the random value  $O(d^{-1/2})$  in some basis, one can transform to a different basis (typically with the same cycling operator e.g. one among the family of DFT bases with different phases in Eq. (19) for optimal cyclic permutations) in which the persistence is again large for a similarly long time.

To determine whether this resemblance between ergodic (quantum) cyclic permutations and ergodic phase space regions can be taken more seriously requires much stronger results on mixed states in the classical limit; however, we have argued in Sec. 5 that tentatively making this identification allows one to make heuristic spectral rigidity arguments that seem consistent with numerical results for linear flows on a KAM torus. Such arguments are made easier by the fact that these tori occur in integrable systems where action-angle variables associated with ergodic sectors are explicitly known, and are likely to be more challenging for genuinely chaotic systems. It also

---

<sup>5</sup>This is related to the nonzero curvature of constant energy surfaces assumed for typical integrable systems in Ref. [22]; the normal vector at each point on the energy surfaces determines the ratio of frequencies of the corresponding torus.

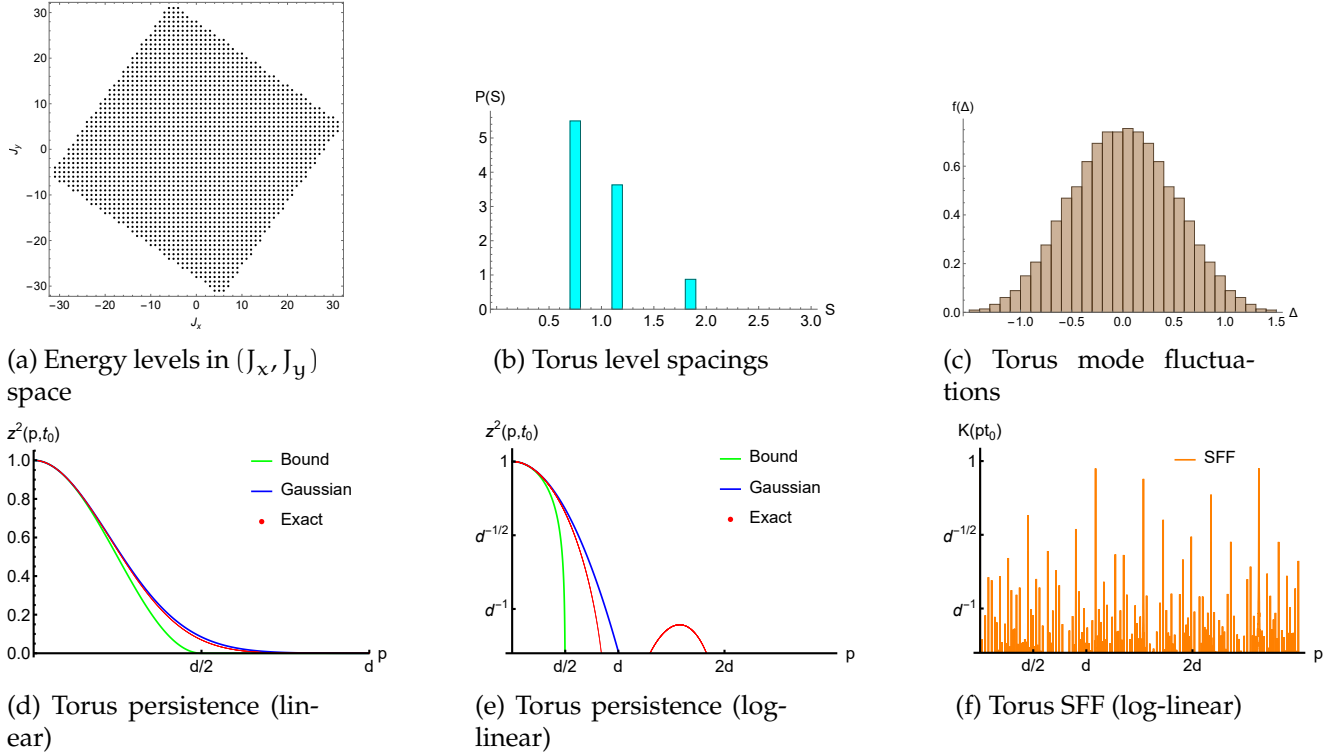


Figure 7: Plots for the 2D KAM torus with irrational  $\alpha = \sqrt{2}$ ;  $\omega_x = 1$ ,  $\omega_y = \sqrt{2}$ ,  $L_1 = L_2 = 40$ ; these correspond to  $d = 2133$ . (b) The neighboring level spacing probability distribution is seen to fall outside the random matrix universality classes (cf. Fig. 6). (c) The width of  $f(\Delta)$  remains close to  $O(1)$  (up to possible corrections at larger  $d$ ). (d,e) The persistence function shows cyclic ergodicity, and is close to the lower bound (Eq. (23)) and the Gaussian estimate (Eq. (35)) at early times; it continues to follow the Gaussian estimate at late times, but appears to deviate a little more than for the Wigner-Dyson ensembles (Fig. 6). (f) The SFF indicates that the system is quasiperiodic (cf. Eq. (21)), ruling out mixing at  $t \sim O(d)$ . These are consistent with the classical system being ergodic and not mixing.

appears likely that it is typically a DFT cyclic permutation that corresponds to an ergodic phase space region; in addition to its optimality, all energy eigenstates in the subspace have a uniform magnitude (ignoring phases) of coefficients in a DFT basis, echoing classical results [3] on the constant magnitude of eigenfunctions of  $U_T$  in an ergodic region (cf. Sec. 2.1).

Given the near-universality (with respect to the Haar measure on the space of time evolution operators) of Wigner-Dyson spectral rigidity [7, 8] and the results of Sec. 4, it follows that almost any randomly chosen quantum system is guaranteed to have this cyclic permutation structure up to a time of at least  $t_H/2$ . However, it is not clear if this structure is easily accessible from physically observable or local bases in which one might traditionally write the Hamiltonian of the system, an ambiguity also present in the statement of ETH [13–15, 87].

Irrespective of this ambiguity, we can ask about the interplay of cyclic ergodicity and aperiodicity on the one hand, and quantum thermalization in the sense of random states (including ETH) on the other, when viewed in an ergodic cyclic permutation basis. These considerations are well-defined for any such basis, but acquire further physical relevance if we assume that one such basis represents the classical phase space (e.g. an ergodic cyclic permutation representing an ergodic subset of the classical phase space). In the remainder of this section, we explore some insights that may be gained from such considerations, which may offer clues to a more rigorous

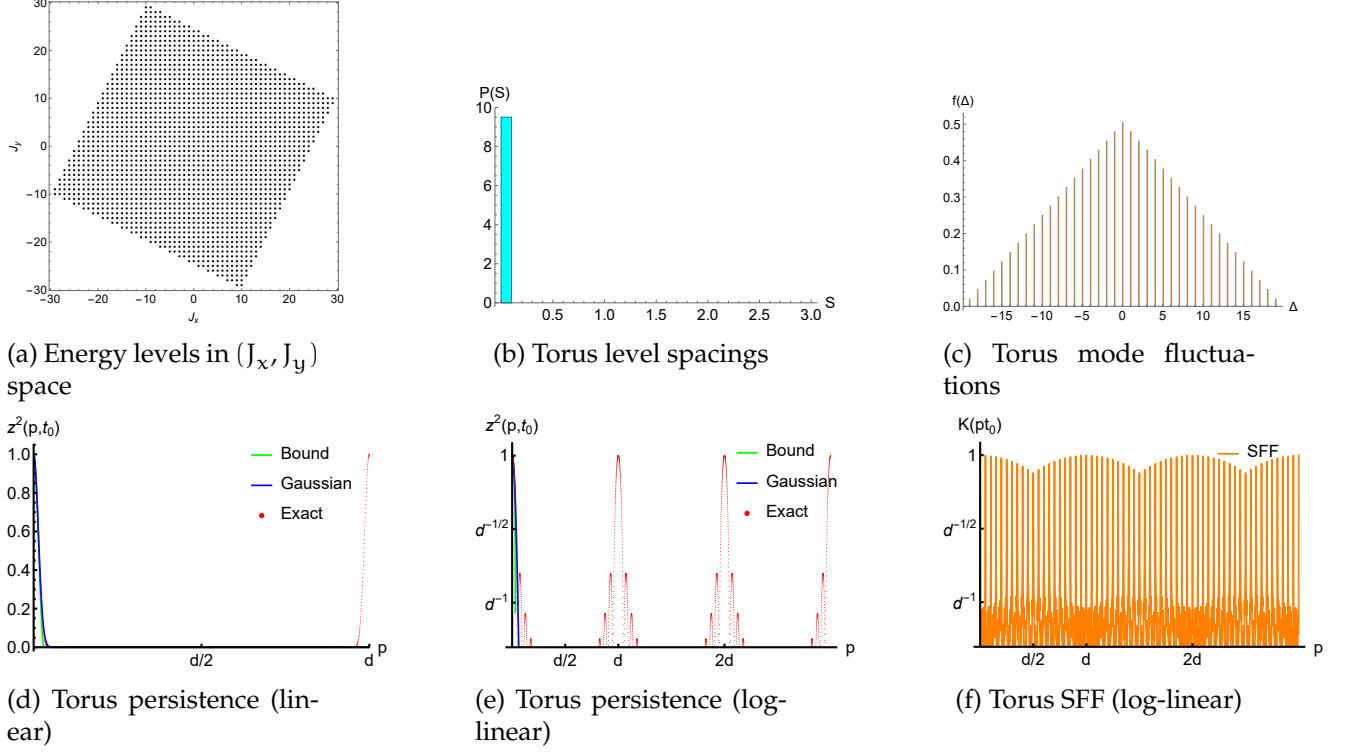


Figure 8: Plots for the 2D KAM torus with rational  $\alpha = 2$ ;  $\omega_x = 1$ ,  $\omega_y = 2$ ,  $L_1 = L_2 = 50$ ; these correspond to  $d = 1961$ . (b) The neighboring level spacings are seen to be equal but with a high degree of degeneracy. (c) The width of  $f(\Delta)$  is  $\gg O(1)$  (as the degeneracy increases with  $L_2$ ). (d,e) The persistence function remains close to the lower bound (Eq. (23)) and Gaussian estimate (Eq. (35)) at early times, and is not ergodic; it also shows periodic revivals. (f) The SFF is periodic. These are consistent with the classical system being non-ergodic and periodic.

study of thermalization.

## 6.1 Thermalization time scales, and a late-time ergodic hierarchy

In general, quantum thermalization depends on both the initial state and the choice of basis in reference to which the randomness of the state is identified [13]. When either is randomly chosen in the Hilbert space of an energy shell (of  $d$  levels and density of states  $\Omega$ ), quantum thermalization occurs extremely fast over the time scale  $t_0 \sim 2\pi\Omega/d$ , irrespective of whether the underlying system is considered chaotic or integrable [88]. To see a difference between systems with different dynamical properties, one would have to choose one of the (relatively rare) physically meaningful bases.

One such basis is what is usually considered the “local” basis [89], in which the Hamiltonian (or Floquet unitary) of the system is easily expressed in terms of a few variables (presumably, with second-order time evolution in some classical or thermodynamic limit). It has been seen in several cases e.g. [36, 38, 48, 90] that correlation functions thermalize rapidly for chaotic systems in such a basis. However, local basis states usually involve superpositions of the entire energy spectrum, due to which all such scrambling [36] phenomena occur prior to the Thouless time ( $\approx t_0$  in our case), while it is only after this time that dynamics within energy shells with a uniform density of states comes into play [36, 50, 73]. In particular, the effect of spectral rigidity (such as Wigner-

Dyson level statistics) and cyclic ergodicity is negligible at these times.

To see the direct impact of spectral rigidity, we consider bases  $\mathcal{C}$  corresponding to cyclic permutations of low error. A basis state for any ergodic cyclic permutation, by definition (Eq. (9)), cannot evolve into a random state until a time  $t_0 d/2 = t_H/2$  (as verified in Figs. 6 and 7). This rules out quantum thermalization in such a basis until the time  $t_H/2$ . Moreover, for non-ergodic permutations, the persistence decays to the random value much faster, allowing a significantly earlier onset of quantum thermalization. Thus, contrary to what one might expect from local basis dynamics prior to  $t_0$ , quantum thermalization in the  $\mathcal{C}$  basis is slower for ergodic (including chaotic) systems and faster for non-ergodic (integrable) systems<sup>6</sup>.

It is also worth noting that over times  $t$  with  $t_0 < t \ll 1/\sqrt{\varepsilon_C(1, t_0)}$  (the latter being  $\sim O(t_H/\sqrt{\ln(t_H/t_0)})$  for Wigner-Dyson statistics), we have  $\hat{U}_H(t_0) \approx \hat{U}_C$ . Consequently, there is negligible inherent randomness in the evolution of an initial basis state up to some long time. Yet, we can characterize a form of randomness over these time scales, with some arguments involving the classical limit. If a phase space region  $A$  corresponds to a degenerate mixed state  $\hat{\rho}(A)$  that is diagonal in this basis, in accordance with Sec. 5.1, we have

$$\hat{\rho}(A) \approx \frac{1}{\mu(A)d} \sum_{k \in C(A)} |C_k\rangle\langle C_k|, \quad (56)$$

where  $C(A) \subseteq \mathbb{Z}_d$  is a set of approximately  $(\mu(A)d)$  indices of the  $|C_k\rangle$ . For some regions  $A$  and  $B$ , using Eq. (46) and approximating  $\hat{U}_H(t_0)$  by  $\hat{U}_C$ , we have

$$\mu(\mathcal{T}^{pt_0}A \cap B) \approx \frac{1}{d} |C(\mathcal{T}^{pt_0}A) \cap C(B)|, \quad (57)$$

with  $|\cdot|$  denoting the cardinality of a finite set. The left hand side can be interpreted in terms of the ergodic hierarchy on the phase space (cf. Sec. 2.1) if  $A$  and  $B$  are chosen from a collection of physical phase space regions (i.e. made up of classically connected regions of nonzero measure) and identified with a “physical” subset of all possible mixed states of the form in Eq. (56); the right hand side is the correlation function of discrete point distributions on a circle ( $\mathbb{Z}_d$ ), corresponding to these mixed states, under a relative shift (of  $\ll d$  steps). This construction can be naturally extended to higher order correlation functions, suggesting that any set of physical point distributions may be assigned a place in the ergodic hierarchy depending on their correlation functions under relative shifts on the circle.

One way to view these arguments is that thermal fluctuations measured by Eq. (57) and (the essentially negligible) quantum fluctuations remain distinct at these times for phase space observables, in contrast to rapidly becoming equivalent for local observables satisfying ETH [11]. Level statistics appears to play no role beyond determining the appropriate time scale for this description (which is directly related to cyclic ergodicity and aperiodicity). These correlation functions instead rely on the more complicated properties of eigenstates (i.e. the representation of energy eigenstates in terms of physical phase space observables). It would be interesting to see if this allows the direct discretization of classical properties beyond ergodicity and aperiodicity through eigenstates e.g. if a mixing behavior of correlation functions of the form of Eq. (57) can be directly connected to the non-existence of non-constant eigenfunctions of the classical unitary  $U_{\mathcal{T}}$  of a

<sup>6</sup>An intuitive explanation for this is as follows. From the level statistics perspective, large spectral fluctuations imply a faster dephasing of the eigenphases of  $\hat{U}_H(t)$ . Alternatively, by appealing to the classical limit (where it exists) and the heuristic arguments of Sec. 5, the ergodic subsets (i.e. tori with largely uncorrelated linear flows) of an integrable system correspond to different ergodic energy subspaces that make up the energy shell, such that a DFT basis state in the shell — which is supported on all tori — is quickly randomized due to the uncorrelated flows of the tori.



mixing system (cf. Sec. 2.1) in the continuum limit [3], via the apparent randomness of the phases of energy eigenstates over the pure states in  $C(A)$ ,  $C(B)$  (see Ref. [58] for a related discussion of “incongruity” of discretized eigenfunctions in the continuum limit).

## 6.2 Poincaré recurrences and eigenstate thermalization

We attempt to identify an analogue of Poincaré recurrence theorem for cyclic permutations within the toy construction of Eq. (56), as an interesting exercise that will reveal a surprising connection to ETH. We recall that quantum recurrences [62] of phases in a subshell occur over times exponentially large in  $d$  [63], and are not directly relevant at earlier times.

We introduce the following ad-hoc definition based on the classical statement (cf. Sec. 2) of the theorem: any subspace  $\Sigma(A) \in \Sigma$  with projector  $\hat{\Pi}(A)$  (and density matrix  $\hat{\rho}(A) \propto \hat{\Pi}(A)$ ) is Poincaré recurrent if for any pure state  $|\psi\rangle \in \Sigma(A)$ , there exists some time  $t$ , with  $t_0 \ll |t| \lesssim O(t_0 d)$  such that the pure state returns to have a larger-than-random overlap with the subspace:

$$\text{Tr} \left[ \hat{\Pi}(A) \hat{U}_H(t) |\psi\rangle \langle \psi| \hat{U}_H^\dagger(t) \right] \gg O(d^{-1}). \quad (58)$$

We note the similarity of the restriction on the range of  $t$  to that in the definition of cyclic aperiodicity (Eq. (11)).

For simplicity, we assume that it is sufficient to consider DFT cyclic permutations as representing any regions in phase space. We also assume that the persistence amplitude is the only greater-than-random component of any state with respect to a DFT basis of interest (in other words, none of the terms  $\varepsilon_C^{1/2}(p, t_0) v_m(p)$  exceed  $O(d^{-1/2})$  in magnitude), as is typically the case for e.g. Wigner-Dyson or Poisson statistics (partly due to Eq. (31)). Let  $t_R(\mathcal{C})$  then represent the randomization time of a DFT cyclic permutation  $\mathcal{C}$  — the smallest time for which  $z(t_R/t_0, t_0) = O(d^{-1/2})$ .

The time  $t_R$  determines the minimum dimension of Poincaré recurrent subspaces that have the diagonal form in Eq. (56). Specifically,

$$\dim \Sigma(A) \geq \frac{t_0 d}{t_R(\mathcal{C})}, \quad (59)$$

if  $\Sigma(A)$  is a Poincaré recurrent subspace spanned by a subset of  $\mathcal{C}$ . Quasi-periodic cyclic permutations have  $t_R(\mathcal{C}) > t_0 d$  and every subspace is recurrent; for ergodic ones,  $t_R(\mathcal{C}) > t_0 d/2$ , and any subspace with  $\dim \Sigma(A) \geq 2$  (in other words, every subspace that is not a pure state) is recurrent.

It follows that the only DFT cyclic permutations that can serve as good candidates for the definition of phase space regions like in Eq. (56) that are also Poincaré recurrent for regions containing more than one pure state ( $\mu(A) > 1/d$ )<sup>7</sup>, are ergodic ones. In other DFT bases, Poincaré recurrence fails for regions  $A$  with some small volume  $1/d < \mu(A) \ll 1$ . Thus, if we want to construct a fictitious phase space for some energy subspace  $\Sigma_d$  that satisfies Poincaré recurrence for arbitrary regions (of greater than the smallest volume  $1/d$ ), there are two possibilities

1.  $\Sigma_d$  is itself ergodic, and the corresponding ergodic (DFT) cyclic permutation  $\mathcal{C}$  allows the definition of mixed states corresponding to Poincaré recurrent phase space regions according to Eq. (56).

---

<sup>7</sup>If we imagine pure states as corresponding to points with negligible ( $= 1/d$ ) phase space measure, they are effectively measure zero sets which are not required to satisfy Poincaré recurrence even classically. More realistically, we should expect recurrence times to increase with decreasing measure

2.  $\Sigma_d$  must be decomposed into  $M$  ergodic subspaces  $\Sigma_{d_1}(1), \dots, \Sigma_{d_M}(M)$ , each spanned by  $d_k$  energy levels (respectively) that add up to  $d$ . Poincaré recurrent phase space regions can then be defined according to Eq. (56) on the combination of their respective ergodic (DFT) cyclic permutations  $\mathcal{C}(1), \dots, \mathcal{C}(M)$ . The previous case corresponds to  $M = 1$ .

In either case, the projectors  $\hat{\Pi}(A)$  can be written as

$$\hat{\Pi}(A) = \sum_{m=1}^M \sum_{k \in C_m(A)} |C_k(m)\rangle \langle C_k(m)| \quad (60)$$

where each  $C_m(A)$  is a set of  $n_m(A) = |C_m(A)|$  indices of elements of  $\mathcal{C}(m)$ , and  $\sum_m n_m(A) = n(A) \approx \mu(A)d$ .

The connection to ETH emerges if one asks for the matrix elements of these projectors in the energy eigenbasis. Let  $\{|E_k(m)\rangle\}_{k=0}^{d_m-1}$  be the energy eigenstates contained in  $\Sigma_{d_m}(m)$ , whose form is explicitly known as DFTs of the  $|C_k(m)\rangle$ . Assuming that (in the generic case) each  $C_m(A)$  is randomly distributed on  $\mathcal{C}(m)$  (so the phases of the DFT can be taken to be random for  $1 \ll n_m \ll d_m$ ), we have

$$\langle E_k(m) | \hat{\Pi}(A) | E_j(m) \rangle = \frac{n_m(A)}{d_m} \delta_{kj} + O\left(\frac{\sqrt{n_m(A)}}{d_m}\right) R_{kj}(m), \quad (61)$$

for some random  $d_m \times d_m$  Hermitian matrix  $R_{kj}(m)$  with  $O(1)$  matrix elements (with weak correlations ensuring  $\hat{\Pi}^2 = \hat{\Pi}$ ). On the other hand, the statement of ETH for an  $n$ -dimensional projector  $\hat{\Pi}$  may be motivated by random matrix arguments (e.g. similar to Refs. [13, 15]; see also Ref. [87] for a discussion of the role of degenerate projectors), giving

$$\langle E_k | \hat{\Pi} | E_j \rangle = \frac{n}{d} \delta_{kj} + O\left(\frac{\sqrt{n}}{d}\right) R_{kj}, \quad (62)$$

in the full energy subspace  $\Sigma_d$ . We see that Eq. (61) and Eq. (62) are guaranteed to agree for  $M = 1$ . For  $M > 1$ , the first (diagonal) terms of Eq. (61) and (62) can only agree through a statistically unlikely coincidence  $n_m/d_m = n/d$ ; even in the rare instance that this holds, the second (fluctuation) term of the former typically has matrix elements of size  $O[(\sqrt{Mn})/d]$  (or zero when  $k, j$  correspond to different  $\Sigma_{d_m}(m)$ ), and ETH can be satisfied only for  $M = O(1)$ .

We have essentially argued, under some simplifications i.e. focusing on DFT bases with typical random parts and diagonal projectors, that generic Poincaré recurrent projectors satisfy ETH only in an energy subspace that admits an ergodic cyclic permutation (and in somewhat less generic cases, up to a small number  $M = O(1)$  of ergodic cyclic permutations).

The above argument could offer hints towards connecting spectral rigidity and ETH, generally seen as distinct manifestations of random matrix behavior [13]. To do so, it would be necessary to determine if there's any link between a Poincaré recurrence requirement for the phase space observables considered here (relevant for  $t > t_0$  dynamics), and the *local* or few-body observables (relevant for  $t < t_0$ ) that are the subject of conventional ETH [9–11, 13–15, 89].

## 7 Conclusions

We have identified a fully quantum notion of ergodicity in the Hilbert space, that can be loosely interpreted as a quantum version of the “visiting (almost) every phase space point” [1, 3] sense of ergodicity. We have shown that energy level statistics determines whether this form of ergodicity

is satisfied by any individual system. Individual systems with Wigner-Dyson level statistics satisfy this property, but so do quantized classically ergodic systems without such statistics as typified by irrational flows on a KAM torus. Random matrix behavior is, therefore, a sufficient condition but not necessary for this form of ergodicity. We also argued that spectral rigidity influences the thermalization of “phase space” observables, potentially admitting a late-time description of thermalization in terms of an ergodic hierarchy, while the connection to local observables is not yet obvious.

We recall that one of our motivations mentioned in Sec. 1 was a semiclassical explanation of spectral rigidity that does not rely on a K-mixing classical limit. Sec. 5 demonstrates that an approach based on cyclic permutations appears to satisfy this criterion even for merely ergodic systems without periodic orbits, and could perhaps even be made mathematically rigorous in some systems if the classical limit is better understood (which has previously been possible only for eigenvectors in a local basis [65, 66]). The fact that it appears to differ significantly from traditional semiclassical periodic orbit arguments [7, 27, 28, 30, 31] warrants some discussion. Approximately periodic structures of any given period can indeed be constructed in an ergodic cyclic permutation basis (e.g. unbiased pure states with regularly spaced support, perhaps excluding a small number of energy levels for divisibility purposes), and may contribute to the calculation of the SFF like a coherent effect of closed Feynman paths in quantum chaotic systems [37, 38, 71] or Haar random unitaries [91, 92]. However, these are not necessarily related to classical periodic *orbits* or trajectories in phase space, and could involve superpositions of actual trajectories. Perhaps a closer connection to the periodic orbit approach would be through periodic structures in the Hilbert space representation of classical mechanics [1–3].

The fact that cyclic ergodicity appears to successfully characterize the spectral rigidity of KAM tori, where the conventional approach based on random matrices does not work, may also allow for a more precise study of the quantum analogue of KAM theory [5] — the study of ergodicity under perturbations to integrable systems. At present, we are far from a detailed understanding of such perturbations [14, 93] in quantum mechanics, particularly for many-particle systems. The development of ergodicity in integrable systems with a large number of particles under vanishingly small perturbations is believed to be essential for the applicability of statistical mechanics [14].

Cyclic permutations may offer other possibilities for transplanting precise ideas from ergodic theory into quantum mechanics. As one example, it would be interesting to explore whether a quantum Kolmogorov-Sinai (KS) entropy can be directly related to level statistics (see e.g. Ref. [94] for candidate definitions) and perhaps obtain a precise characterization of quantum *chaos* as opposed to mere ergodicity beyond intuitive notions; classically, the KS entropy is closely related to Lyapunov exponents that characterize chaotic dynamics [4, 5], and can be accessed through a certain type of cyclic permutations (and generalizations) [2, 54, 58]. In the other direction, it may also be interesting to see if classical cyclic permutations can be optimized in some sense for a given system, as done for quantum cyclic permutations in Sec. 3.3.

## Acknowledgments

This work was supported by the U.S. Department of Energy, Office of Science, Basic Energy Sciences under Award No. DE-SC0001911. We thank Yunxiang Liao, Laura Shou and Michael Winer for useful discussions.

## References

- [1] Y. G. Sinai, *Introduction to ergodic theory*, Vol. 18 (Princeton University Press, 1977), ISBN: 978-0691081823.
- [2] I. P. Cornfield, S. V. Fomin, and Y. G. Sinai, *Ergodic theory* (Springer-Verlag New York, 1982), ISBN: 978-1-4615-6927-5, <https://doi.org/10.1007/978-1-4615-6927-5>.
- [3] P. R. Halmos, *Lectures on ergodic theory* (Dover Publications, 2017), ISBN: 9780486814896.
- [4] R. Frigg, J. Berkovitz, and F. Kronz, “The ergodic hierarchy”, The Stanford Encyclopedia of Philosophy, Fall 2020 Edition, edited by E. N. Zalta, <https://plato.stanford.edu/archives/fall2020/entries/ergodic-hierarchy/>.
- [5] E. Ott, *Chaos in dynamical systems* (Cambridge university press, 2002).
- [6] E. B. Rozenbaum, L. A. Bunimovich, and V. Galitski, “Early-time exponential instabilities in non-chaotic quantum systems”, arXiv preprint arXiv:1902.05466v2 (2019), <https://doi.org/10.48550/arXiv.1902.05466>.
- [7] F. Haake, *Quantum signatures of chaos* (Springer, Berlin, Heidelberg, 2001), <https://doi.org/10.1007/978-3-662-04506-0>.
- [8] M. L. Mehta, *Random matrices* (Elsevier, 2004), ISBN: 978-0-12-088409-4.
- [9] J. M. Deutsch, “Quantum statistical mechanics in a closed system”, Phys. Rev. A **43**, 2046–2049 (1991), <https://link.aps.org/doi/10.1103/PhysRevA.43.2046>.
- [10] M. Srednicki, “Chaos and quantum thermalization”, Phys. Rev. E **50**, 888–901 (1994), <https://link.aps.org/doi/10.1103/PhysRevE.50.888>.
- [11] M. Srednicki, “The approach to thermal equilibrium in quantized chaotic systems”, J. Phys. A **32**, 1163–1175 (1999), <http://dx.doi.org/10.1088/0305-4470/32/7/007>.
- [12] M. Rigol, V. Dunjko, and M. Olshanii, “Thermalization and its mechanism for generic isolated quantum systems”, Nature **452**, 854–858 (2008), <https://doi.org/10.1038/nature06838>.
- [13] L. D’Alessio, Y. Kafri, A. Polkovnikov, and M. Rigol, “From quantum chaos and eigenstate thermalization to statistical mechanics and thermodynamics”, Adv. Phys. **65**, 239–362 (2016), <https://doi.org/10.1080/00018732.2016.1198134>.
- [14] J. M. Deutsch, “Eigenstate thermalization hypothesis”, Rep. Prog. Phys. **81**, 082001 (2018), <http://dx.doi.org/10.1088/1361-6633/aac9f1>.
- [15] A. Dymarsky, N. Lashkari, and H. Liu, “Subsystem eigenstate thermalization hypothesis”, Phys. Rev. E **97**, 012140 (2018), <https://link.aps.org/doi/10.1103/PhysRevE.97.012140>.
- [16] S. Popescu, A. J. Short, and A. Winter, “Entanglement and the foundations of statistical mechanics”, Nat. Phys. **2**, 754–758 (2006), <https://doi.org/10.1038/nphys444>.
- [17] S. Goldstein, J. L. Lebowitz, R. Tumulka, and N. Zanghì, “Canonical typicality”, Phys. Rev. Lett. **96**, 050403 (2006), <https://doi.org/10.1103/PhysRevLett.96.050403>.
- [18] S. Goldstein, J. L. Lebowitz, C. Mastrodonato, R. Tumulka, and N. Zanghì, “Normal typicality and von Neumann’s quantum ergodic theorem”, Proceedings of the Royal Society A: Mathematical, Physical and Engineering Sciences **466**, 3203–3224 (2010), <https://doi.org/10.1098/rspa.2009.0635>.
- [19] P. Reimann, “Foundation of statistical mechanics under experimentally realistic conditions”, Physical Review Letters **101**, 190403 (2008), <https://doi.org/10.1103/PhysRevLett.101.190403>.

- [20] A. J. Short, “Equilibration of quantum systems and subsystems”, *New Journal of Physics* **13**, 053009 (2011), <https://doi.org/10.1088/1367-2630/13/5/053009>.
- [21] D. Zhang, H. T. Quan, and B. Wu, “Ergodicity and mixing in quantum dynamics”, *Physical Review E* **94**, 022150 (2016), <https://doi.org/10.1103/PhysRevE.94.022150>.
- [22] M. V. Berry and M. Tabor, “Level clustering in the regular spectrum”, *Proc. Royal Soc. Lond.* **356**, 375–394 (1977), <https://royalsocietypublishing.org/doi/10.1098/rspa.1977.0140>.
- [23] S. W. McDonald and A. N. Kaufman, “Spectrum and eigenfunctions for a hamiltonian with stochastic trajectories”, *Physical Review Letters* **42**, 1189 (1979), <https://doi.org/10.1103/PhysRevLett.42.1189>.
- [24] G. Casati, F. Valz-Gris, and I. Guarneri, “On the connection between quantization of non-integrable systems and statistical theory of spectra”, *Lettere al Nuovo Cimento* **28**, 279–282 (1980).
- [25] M. V. Berry, “Quantizing a classically ergodic system: Sinai’s billiard and the KKR method”, *Annals of Physics* **131**, 163–216 (1981), [https://doi.org/10.1016/0003-4916\(81\)90189-5](https://doi.org/10.1016/0003-4916(81)90189-5).
- [26] O. Bohigas, M.-J. Giannoni, and C. Schmit, “Characterization of chaotic quantum spectra and universality of level fluctuation laws”, *Physical Review Letters* **52**, 1 (1984), <https://doi.org/10.1103/PhysRevLett.52.1>.
- [27] J. H. Hannay and A. M. Ozorio de Almeida, “Periodic orbits and a correlation function for the semiclassical density of states”, *Journal of Physics A: Mathematical and General* **17**, 3429 (1984), <https://doi.org/10.1088/0305-4470/17/18/013>.
- [28] M. V. Berry, “Semiclassical theory of spectral rigidity”, *Proceedings of the Royal Society of London. A. Mathematical and Physical Sciences* **400**, 229–251 (1985), <https://doi.org/10.1098/rspa.1985.0078>.
- [29] M. Sieber and K. Richter, “Correlations between periodic orbits and their rôle in spectral statistics”, *Physica Scripta* **2001**, 128 (2001), <https://doi.org/10.1238/Physica.Topical.090a00128>.
- [30] S. Müller, S. Heusler, P. Braun, F. Haake, and A. Altland, “Semiclassical foundation of universality in quantum chaos”, *Physical Review Letters* **93**, 014103 (2004), <https://doi.org/10.1103/PhysRevLett.93.014103>.
- [31] S. Müller, S. Heusler, P. Braun, F. Haake, and A. Altland, “Periodic-orbit theory of universality in quantum chaos”, *Physical Review E* **72**, 046207 (2005), <https://doi.org/10.1103/PhysRevE.72.046207>.
- [32] K. Richter, J. D. Urbina, and S. Tomsovic, “Semiclassical roots of universality in many-body quantum chaos”, *arXiv preprint arXiv:2205.02867* (2022), <https://doi.org/10.48550/arXiv.2205.02867>.
- [33] Č. Lozej, G. Casati, and T. Prosen, “Quantum chaos in triangular billiards”, *Physical Review Research* **4**, 013138 (2022), <https://doi.org/10.1103/PhysRevResearch.4.013138>.
- [34] J. Wang, G. Benenti, G. Casati, and W.-g. Wang, “Statistical and dynamical properties of the quantum triangle map”, *arXiv preprint arXiv:2201.05921* (2022), <https://doi.org/10.48550/arXiv.2201.05921>.
- [35] J. S. Cotler, G. Gur-Ari, M. Hanada, J. Polchinski, P. Saad, S. H. Shenker, D. Stanford, A. Streicher, and M. Tezuka, “Black holes and random matrices”, *Journal of High Energy Physics* **2017**, 1–54 (2017), [https://doi.org/10.1007/JHEP05\(2017\)118](https://doi.org/10.1007/JHEP05(2017)118).

- [36] H. Gharibyan, M. Hanada, S. H. Shenker, and M. Tezuka, “Onset of random matrix behavior in scrambling systems”, *Journal of High Energy Physics* **2018**, 1–62 (2018), [https://doi.org/10.1007/JHEP07\(2018\)124](https://doi.org/10.1007/JHEP07(2018)124).
- [37] P. Kos, M. Ljubotina, and T. Prosen, “Many-body quantum chaos: analytic connection to random matrix theory”, *Physical Review X* **8**, 021062 (2018), <https://doi.org/10.1103/PhysRevX.8.021062>.
- [38] A. Chan, A. De Luca, and J. Chalker, “Solution of a minimal model for many-body quantum chaos”, *Physical Review X* **8**, 041019 (2018), <https://doi.org/10.1103/PhysRevX.8.041019>.
- [39] A. Chan, A. De Luca, and J. Chalker, “Spectral statistics in spatially extended chaotic quantum many-body systems”, *Physical Review Letters* **121**, 060601 (2018), <https://doi.org/10.1103/PhysRevLett.121.060601>.
- [40] B. Bertini, P. Kos, and T. Prosen, “Exact spectral form factor in a minimal model of many-body quantum chaos”, *Physical Review Letters* **121**, 264101 (2018), <https://doi.org/10.1103/PhysRevLett.121.264101>.
- [41] P. Saad, S. H. Shenker, and D. Stanford, “A semiclassical ramp in SYK and in gravity”, *arXiv preprint arXiv:1806.06840* (2018), <https://doi.org/10.48550/arXiv.1806.06840>.
- [42] Y. Liao and V. Galitski, “Universal dephasing mechanism of many-body quantum chaos”, *Physical Review Research* **4**, L012037 (2022), <https://doi.org/10.1103/PhysRevResearch.4.L012037>.
- [43] Y. Liao and V. Galitski, “Emergence of many-body quantum chaos via spontaneous breaking of unitarity”, *Physical Review B* **105**, L140202 (2022), <https://doi.org/10.1103/PhysRevB.105.L140202>.
- [44] Y. Liao and V. Galitski, “Effective field theory of random quantum circuits”, *arXiv preprint arXiv:2204.03088* (2022), <https://doi.org/10.48550/arXiv.2204.03088>.
- [45] Y. Liao, A. Vikram, and V. Galitski, “Many-body level statistics of single-particle quantum chaos”, *Physical Review Letters* **125**, 250601 (2020), <https://doi.org/10.1103/PhysRevLett.125.250601>.
- [46] M. Winer, S.-K. Jian, and B. Swingle, “Exponential ramp in the quadratic Sachdev-Ye-Kitaev model”, *Physical Review Letters* **125**, 250602 (2020), <https://doi.org/10.1103/PhysRevLett.125.250602>.
- [47] M. Winer, R. Barney, C. L. Baldwin, V. Galitski, and B. Swingle, “Spectral form factor of a quantum spin glass”, *arXiv preprint arXiv:2203.12753* (2022), <https://doi.org/10.48550/arXiv.2203.12753>.
- [48] B. Bertini, P. Kos, and T. Prosen, “Exact correlation functions for dual-unitary lattice models in 1+ 1 dimensions”, *Physical Review Letters* **123**, 210601 (2019).
- [49] S. Aravinda, S. A. Rather, and A. Lakshminarayan, “From dual-unitary to quantum Bernoulli circuits: Role of the entangling power in constructing a quantum ergodic hierarchy”, *Physical Review Research* **3**, 043034 (2021), <https://doi.org/10.1103/PhysRevResearch.3.043034>.
- [50] M. Schiulaz, E. J. Torres-Herrera, and L. F. Santos, “Thouless and relaxation time scales in many-body quantum systems”, *Physical Review B* **99**, 174313 (2019), <https://doi.org/10.1103/PhysRevB.99.174313>.

- [51] D. V. Vasilyev, A. Grankin, M. A. Baranov, L. M. Sieberer, and P. Zoller, “Monitoring quantum simulators via quantum nondemolition couplings to atomic clock qubits”, *PRX Quantum* **1**, 020302 (2020), <https://doi.org/10.1103/PRXQuantum.1.020302>.
- [52] L. K. Joshi, A. Elben, A. Vikram, B. Vermersch, V. Galitski, and P. Zoller, “Probing many-body quantum chaos with quantum simulators”, *Physical Review X* **12**, 011018 (2022), <https://doi.org/10.1103/PhysRevX.12.011018>.
- [53] A. B. Katok and A. M. Stepin, “Approximation of ergodic dynamic systems by periodic transformations”, in *Dokl. Akad. Nauk SSSR*, Vol. 171, 6 (1966), pp. 1268–1271.
- [54] A. B. Katok and A. M. Stepin, “Approximations in ergodic theory”, *Russian Mathematical Surveys* **22**, 77 (1967).
- [55] R. Aurich, J. Bolte, and F. Steiner, “Universal signatures of quantum chaos”, *Physical Review Letters* **73**, 1356 (1994), <https://doi.org/10.1103/PhysRevLett.73.1356>.
- [56] R. Aurich, A. Bäcker, and F. Steiner, “Mode fluctuations as fingerprints of chaotic and non-chaotic systems”, *International Journal of Modern Physics B* **11**, 805–849 (1997), <https://doi.org/10.1142/S0217979297000459>.
- [57] V. A. Rokhlin, “Lectures on the entropy theory of measure-preserving transformations”, *Russian Mathematical Surveys* **22**, 1 (1967).
- [58] A. B. Katok, Y. G. Sinai, and A. M. Stepin, “Theory of dynamical systems and general transformation groups with invariant measure”, *Journal of Soviet Mathematics* **7**, 974–1065 (1977), <https://doi.org/10.1007/BF01223133>.
- [59] M. G. Nadkarni, *Spectral theory of dynamical systems, 2nd edition* (Springer, Singapore, 2020), ISBN: 978-981-15-6225-9, <https://doi.org/10.1007/978-981-15-6225-9>.
- [60] M. Castagnino and O. Lombardi, “Towards a definition of the quantum ergodic hierarchy: ergodicity and mixing”, *Physica A: Statistical Mechanics and its Applications* **388**, 247–267 (2009), <https://doi.org/10.1016/j.physa.2008.10.019>.
- [61] R. Chacon, “Approximation and spectral multiplicity”, in *Contributions to ergodic theory and probability* (Springer, 1970), pp. 18–27, <https://doi.org/10.1007/BFb0060642>.
- [62] P. Bocchieri and A. Loinger, “Quantum recurrence theorem”, *Physical Review* **107**, 337 (1957), <https://doi.org/10.1103/PhysRev.107.337>.
- [63] A. R. Brown and L. Susskind, “Second law of quantum complexity”, *Physical Review D* **97**, 086015 (2018), <https://doi.org/10.1103/PhysRevD.97.086015>.
- [64] S. Popescu, A. J. Short, and A. Winter, *The foundations of statistical mechanics from entanglement: Individual states vs. averages*, 2005, arXiv:quant-ph/0511225, <https://doi.org/10.48550/arXiv.quant-ph/0511225>.
- [65] S. Zelditch, “Quantum ergodicity and mixing”, arXiv preprint math-ph/0503026 (2005), <https://doi.org/10.48550/arXiv.math-ph/0503026>.
- [66] N. Anantharaman, “Delocalization of Schrödinger eigenfunctions”, in *Proceedings of the International Congress of Mathematicians: Rio de Janeiro 2018* (World Scientific, 2018), pp. 341–375, [https://doi.org/10.1142/9789813272880\\_0016](https://doi.org/10.1142/9789813272880_0016).
- [67] J. French, P. Mello, and A. Pandey, “Statistical properties of many-particle spectra. II. two-point correlations and fluctuations”, *Annals of Physics* **113**, 277–293 (1978), [https://doi.org/10.1016/0003-4916\(78\)90205-1](https://doi.org/10.1016/0003-4916(78)90205-1).

- [68] T. A. Brody, J. Flores, J. B. French, P. Mello, A. Pandey, and S. S. Wong, “Random-matrix physics: spectrum and strength fluctuations”, *Reviews of Modern Physics* **53**, 385 (1981), <https://doi.org/10.1103/RevModPhys.53.385>.
- [69] R. E. Prange, “The spectral form factor is not self-averaging”, *Physical Review Letters* **78**, 2280 (1997), <https://doi.org/10.1103/PhysRevLett.78.2280>.
- [70] M. V. Berry, “Some quantum-to-classical asymptotics”, in *Les houches lecture series LII* (1989), edited by M. J. Giannoni, A. Voros, and J. Zinn-Justin (Elsevier Science Publishers B.V., 1991), pp. 251–304, ISBN: 978-0444892775, <https://michaelberryphysics.files.wordpress.com/2013/07/berry227.pdf>.
- [71] S. J. Garratt and J. T. Chalker, “Local pairing of Feynman histories in many-body Floquet models”, *Physical Review X* **11**, 021051 (2021), <https://doi.org/10.1103/PhysRevX.11.021051>.
- [72] A. J. Friedman, A. Chan, A. De Luca, and J. Chalker, “Spectral statistics and many-body quantum chaos with conserved charge”, *Physical Review Letters* **123**, 210603 (2019), <https://doi.org/10.1103/PhysRevLett.123.210603>.
- [73] M. Winer and B. Swingle, “Hydrodynamic theory of the connected spectral form factor”, *Physical Review X* **12**, 021009 (2022), <https://doi.org/10.1103/PhysRevX.12.021009>.
- [74] O. Costin and J. L. Lebowitz, “Gaussian fluctuation in random matrices”, *Physical Review Letters* **75**, 69 (1995), <https://doi.org/10.1103/PhysRevLett.75.69>.
- [75] F. J. Dyson and M. L. Mehta, “Statistical theory of the energy levels of complex systems. IV”, *Journal of Mathematical Physics* **4**, 701–712 (1963), <https://doi.org/10.1063/1.1704008>.
- [76] A. Polkovnikov, “Phase space representation of quantum dynamics”, *Annals of Physics* **325**, 1790–1852 (2010), <https://doi.org/10.1016/j.aop.2010.02.006>.
- [77] R. Shankar, *Principles of quantum mechanics* (Springer Science & Business Media, 2012), ISBN: 978-1-4757-0576-8, <https://doi.org/10.1007/978-1-4757-0576-8>.
- [78] H. Goldstein, C. Poole, and J. Safko, *Classical mechanics*, 3rd ed. (Pearson, 2002), ISBN: 9780201657029.
- [79] L. D. Landau and E. M. Lifshitz, *Statistical physics*, Vol. 5 (Elsevier, 2013), ISBN: 9780080570464, <https://doi.org/10.1016/C2009-0-24487-4>.
- [80] B. V. Chirikov, F. M. Izrailev, and D. L. Shepelyansky, “Dynamical stochasticity in classical and quantum mechanics”, *Soviet Scientific Reviews 2C* (1981).
- [81] D. Shepelyansky, “Ehrenfest time and chaos”, *Scholarpedia* **15**, 55031 (2020), <https://doi.org/10.4249/scholarpedia.55031>.
- [82] D. A. Abanin, E. Altman, I. Bloch, and M. Serbyn, “Colloquium: Many-body localization, thermalization, and entanglement”, *Reviews of Modern Physics* **91**, 021001 (2019), <https://doi.org/10.1103/RevModPhys.91.021001>.
- [83] Z. Cheng and J. L. Lebowitz, “Statistics of energy levels in integrable quantum systems”, *Physical Review A* **44**, R3399 (1991), <https://doi.org/10.1103/PhysRevA.44.R3399>.
- [84] P. M. Bleher, Z. Cheng, F. J. Dyson, and J. L. Lebowitz, “Distribution of the error term for the number of lattice points inside a shifted circle”, *Communications in Mathematical Physics* **154**, 433–469 (1993), <https://projecteuclid.org/journals/communications-in-mathematical-physics/volume-154/issue-3/Distribution-of-the-error-term-for-the-number-of-lattice/cmp/1104253074.full>.



- [85] A. B. Katok, “Spectral properties of dynamical systems with an integral invariant on the torus”, *Functional Analysis and Its Applications* **1**, 296–305 (1967), <https://doi.org/10.1007/BF01076009>.
- [86] A. Iwanik, “Cyclic approximation of irrational rotations”, *Proceedings of the American Mathematical Society* **121**, 691–695 (1994), <https://doi.org/10.1090/S0002-9939-1994-1221724-X>.
- [87] F. Anza, C. Gogolin, and M. Huber, “Eigenstate thermalization for degenerate observables”, *Physical Review Letters* **120**, 150603 (2018), <https://doi.org/10.1103/PhysRevLett.120.150603>.
- [88] P. Reimann, “Typical fast thermalization processes in closed many-body systems”, *Nat. Comm.* **7**, 10821 (2016), <https://doi.org/10.1038/ncomms10821>.
- [89] R. Nandkishore and D. A. Huse, “Many-body localization and thermalization in quantum statistical mechanics”, *Annu. Rev. Condens. Matter Phys.* **6**, 15–38 (2015), <https://doi.org/10.1146/annurev-conmatphys-031214-014726>.
- [90] X. Mi, P. Roushan, C. Quintana, S. Mandrà, J. Marshall, C. Neill, F. Arute, K. Arya, J. Atalaya, R. Babbush, et al., “Information scrambling in quantum circuits”, *Science* **374**, 1479–1483 (2021), <https://doi.org/10.1126/science.abg5029>.
- [91] B. Collins and P. Śniady, “Integration with respect to the Haar measure on unitary, orthogonal and symplectic group”, *Communications in Mathematical Physics* **264**, 773–795 (2006), <https://doi.org/10.1007/s00220-006-1554-3>.
- [92] G. Köstenberger, “Weingarten calculus”, arXiv preprint arXiv:2101.00921 (2021), <https://doi.org/10.48550/arXiv.2101.00921>.
- [93] G. Brandino, J.-S. Caux, and R. Konik, “Glimmers of a quantum KAM theorem: insights from quantum quenches in one-dimensional Bose gases”, *Physical Review X* **5**, 041043 (2015), <https://doi.org/10.1103/PhysRevX.5.041043>.
- [94] R. Alicki and M. Fannes, *Quantum dynamical systems* (Oxford University Press, 2001), ISBN: 9780198504009, <https://doi.org/10.1093/acprof:oso/9780198504009.001.0001>.
- [95] R. A. Horn and C. R. Johnson, *Matrix analysis* (Cambridge University Press, 2012), ISBN: 9780511810817, <https://doi.org/10.1017/CB09780511810817>.
- [96] I. S. Gradshteyn and I. M. Ryzhik, *Table of integrals, series, and products*, edited by D. Zwillinger and V. Moll (Academic press, 2014), ISBN: 978-0-12-384933-5, <https://doi.org/10.1016/C2010-0-64839-5>.
- [97] R. L. Hudson, “When is the Wigner quasi-probability density non-negative?”, *Reports on Mathematical Physics* **6**, 249–252 (1974), [https://doi.org/10.1016/0034-4877\(74\)90007-X](https://doi.org/10.1016/0034-4877(74)90007-X).
- [98] P. R. Halmos, “Two subspaces”, *Transactions of the American Mathematical Society* **144**, 381–389 (1969), <https://doi.org/10.2307/1995288>.
- [99] A. Böttcher and I. M. Spitkovsky, “A gentle guide to the basics of two projections theory”, *Linear Algebra and its Applications* **432**, 1412–1459 (2010), <https://doi.org/10.1016/j.laa.2009.11.002>.

## Appendix A Classical cyclic permutations (review)

This proof essentially follows Ref. [54]. First, we discuss the bound for cyclic ergodicity. Assume that every element of  $\{\mathcal{P}_j\}_{j=1}^{M_C}$  completely contains at least one element  $C_{p(j)} \subseteq \mathcal{P}_j$  of the decomposition. As  $\mathcal{T}^t C_{p(j)} \in \mathcal{P}_j$  for all  $t$  by definition, we must have  $\mu[(\mathcal{T}^{[p(j+1)-p(j)]t_0} C_{p(j)}) \cap C_{p(j+1)}] = 0$ . An important exception to this behavior is when  $M_C = 1$ , where there is no reason to impose a vanishing intersection. Thus,

$$\frac{1}{2} \sum_{j=1}^{M_C} \mu \left[ (\mathcal{T}^{[p(j+1)-p(j)]t_0} C_{p(j)}) \triangle C_{p(j+1)} \right] = \frac{1}{n} M_C, \text{ for } M_C \geq 2. \quad (63)$$

Now, we need to know how the error in an  $\ell$ -step time evolution  $(\mathcal{T}^{\ell t_0} C_k) \triangle C_{k+\ell}$  is related to the error  $(\mathcal{T}^{t_0} C_m) \triangle C_{m+1}$  made in approximating each step. For this, we note that

$$(\mathcal{T}^{(m+1)t_0} A) - C_{m+1} \subseteq \left[ (\mathcal{T}^{t_0} C_m) - C_{m+1} \right] \cup \mathcal{T}^{t_0} \left[ (\mathcal{T}^{m t_0} A) - C_m \right], \quad \forall A \subseteq \mathcal{P} \quad (64)$$

$$\Rightarrow \mu[(\mathcal{T}^{\ell t_0} C_k) \triangle C_{k+\ell}] \leq \sum_{m=1}^{\ell} \mu[(\mathcal{T} C_{k+m-1}) \triangle C_{k+m}], \quad (65)$$

where the second line follows from recursively applying the first line to  $\mathcal{T}^{(m+1)t_0} C_k \triangle C_{k+q}$  with  $A = C_k$ . Using this in Eq. (63), one obtains  $\bar{\epsilon}_C \geq (M_C/n)$  for  $M_C \geq 2$ .

Cyclic aperiodicity is more straightforward. We have  $\mu[(\mathcal{T}^{n t_0} C_k) \cap C_k] = 0$  (up to possible corrections that vanish as  $n \rightarrow \infty$ ), which implies  $\bar{\epsilon}_C \geq 1/n$  from Eq. (65). More generally, we can relax the requirement of aperiodicity to only after  $r$  returns,  $\mu[(\mathcal{T}^{r n t_0} C_k) \cap C_k] = 0$ , which gives  $\bar{\epsilon}_C \geq 1/(rn)$ .

## Appendix B Quantum cyclic permutations

### B.1 Fastest decay of persistence

Given a cyclic permutation basis  $\mathcal{C} = \{|C_j\rangle\}_{j=0}^{d-1}$ , consider some initial state  $|C_k\rangle$ . After  $p$  steps of time evolution, it evolves into

$$\hat{U}_H(p t_0) |C_k\rangle = z_k(p; t_0) e^{i\phi_k(p; t_0)} |C_{k+p}\rangle + \sqrt{1 - z_k^2(p; t_0)} |v_{k+p}^{(k)}\rangle, \quad (66)$$

where  $|v_{k+p}^{(k)}\rangle$  is some normalized vector orthogonal to  $|C_{k+p}\rangle$ , and  $\phi_k(p; t_0)$  is an unimportant phase. This leads to a recurrence relation for the persistence amplitudes,

$$\begin{aligned} z_k(p+1; t_0) e^{i\phi_k(p+1; t_0)} &= \langle C_{k+p+1} | \hat{U}_H(t_0) \hat{U}_H(p t_0) | C_k \rangle \\ &= z_k(p) e^{i\phi_k(p; t_0)} \langle C_{k+p+1} | \hat{U}_H(t_0) | C_{k+p} \rangle \\ &\quad + \sqrt{1 - z_k^2(p; t_0)} \langle C_{k+p+1} | \hat{U}_H(t_0) | v_{k+p}^{(k)} \rangle. \end{aligned} \quad (67)$$

Using the triangle inequality for the magnitudes of these vectors gives

$$\begin{aligned} &\left| z_k(p; t_0) z_{k+p}(1; t_0) - \sqrt{1 - z_k^2(p; t_0)} \sqrt{1 - z_{k+p}^2(1; t_0)} \right| \\ &\leq z_k(p+1; t_0) \\ &\leq \left\{ z_k(p; t_0) z_{k+p}(1; t_0) + \sqrt{1 - z_k^2(p; t_0)} \sqrt{1 - z_{k+p}^2(1; t_0)} \right\}, \end{aligned} \quad (68)$$

on noting that  $\hat{U}_H(t_0)|v_{k+p}^{(k)}\rangle$  is orthogonal to  $\hat{U}_H(t_0)|C_{k+p}\rangle$ , and consequently the inner product of the former with  $|C_{k+p+1}\rangle$  cannot exceed  $\sqrt{1 - z_{k+p}^2(1; t_0)}$  in magnitude.

The above inequalities can be simplified by defining  $\theta_k(p) = \arccos z_k(p; t_0) \in [0, \pi/2]$ . In terms of these variables, Eq. (68) becomes

$$\min \left\{ \theta_k(p) + \theta_{k+p}(1), \frac{\pi}{2} \right\} \geq \theta_k(p+1) \geq |\theta_k(p) - \theta_{k+p}(1)|. \quad (69)$$

Summing  $\theta_k(p+1) - \theta_k(p)$  from  $p = p_1$  to  $p = p_2$  gives

$$\begin{aligned} & \text{sgn}(p_2) \min \left\{ \theta_{p_2}(p_2), \frac{\pi}{2} \right\} - \text{sgn}(p_1) \min \left\{ \theta_{p_1}(p_1), \frac{\pi}{2} \right\} \\ & \leq (\text{sgn}(p_2) - \text{sgn}(p_1)) \sum_{p=p_1}^{p_2} \theta_{k+p}(1), \end{aligned} \quad (70)$$

which becomes Eq. (13) when expressed in terms of the  $z_k(p; t_0)$ . We see that the bound is saturated when  $\hat{U}_H(t_0)$  at the  $p$ -th step acts like a 2D rotation by the angle  $\theta_{k+p}(1)$  in the same direction as the previous steps.

## B.2 Optimal errors for cyclic permutations

When  $\hat{U}_C$  is a cycling operator,  $\hat{U}_C^p$  is generally a permutation operator on  $\mathcal{C} = \{|C_k\rangle\}_{k=0}^{d-1}$  that can be decomposed into a direct sum of cycling operators, each acting on a separate  $[d/\mathcal{N}(d, p)]$ -sized subset of  $\mathcal{C}$ :

$$\hat{U}_C^p = \bigoplus_{j=1}^{\mathcal{N}(d, p)} \hat{U}_{C, j}(p). \quad (71)$$

The number of cycling operators  $\mathcal{N}(d, p)$  is given by the greatest common divisor of  $p$  and  $d$ ; in particular,  $\mathcal{N}(d, p) = 1$  when  $p$  and  $d$  are coprime, including  $p = 1$ . This is most easily seen in the eigenvalue structure of  $\hat{U}_C^p$ , which consists of  $\mathcal{N}(d, p)$  identical (degenerate) sets of distinct  $[d/\mathcal{N}(d, p)]$ -th roots of unity. It is also convenient to consider *twisted* versions of  $\hat{U}_C^p$ , in which each cycle acquires an additional phase  $\alpha_j(w)$ :

$$w\{\hat{U}_C^p\} \equiv \bigoplus_{j=1}^{\mathcal{N}(d, p)} e^{i\alpha_j(w)} \hat{U}_{C, j}(p). \quad (72)$$

It is worth noting that the twisting functional  $w$  affects only the eigenvalues of  $\hat{U}_C^p$ , lifting the degeneracy for most values of the  $\alpha_j(w)$ , while preserving at least one complete orthonormal set of its eigenvectors. Also, the  $p$ -step persistence amplitudes  $z_k(p; t_0)$  are invariant under the action of  $w$ .

### B.2.1 Optimizing the error via the trace inner product

Due to its non-negativity, the minimum persistence at a given  $p$  is bounded by the mean persistence at that time:

$$\min_{j \in \mathbb{Z}_d} z_j(p; t_0) \leq \frac{1}{d} \sum_{k=0}^{d-1} z_k(p; t_0). \quad (73)$$

We also have the inequality,

$$\left| \frac{1}{d} \text{Tr} \left[ w \{ \hat{U}_C^p \}^\dagger \hat{U}_H(p t_0) \right] \right| \leq \frac{1}{d} \sum_{k=0}^{d-1} \left| \langle C_k | \{ \hat{U}_C^p \}^\dagger \hat{U}_H(p t_0) | C_k \rangle \right|, \quad (74)$$

for any  $w$ , where the right hand side is just the mean persistence at  $p$ , expanded out.

Let us assume that for every  $\mathcal{C}$  and given a  $p$ , there exists a unitary  $\hat{V}_C$  and a twisting functional  $w$  such that

$$\frac{1}{d} \text{Tr} \left[ \hat{V}_C w \{ \hat{U}_C^p \}^\dagger \hat{V}_C^\dagger \hat{U}_H(p t_0) \right] = \frac{1}{d} \sum_{k=0}^{d-1} \left| \langle C_k | w \{ \hat{U}_C^p \}^\dagger \hat{U}_H(p t_0) | C_k \rangle \right|. \quad (75)$$

If this holds, then on account of Eq. (74) and the invariance of the  $z_k(p; t_0)$  under the action of  $w$ ,

$$\max_{\hat{V} \in \mathcal{U}(d)} \left| \frac{1}{d} \text{Tr} \left[ \hat{V} w \{ \hat{U}_C^p \}^\dagger \hat{V}^\dagger \hat{U}_H(p t_0) \right] \right| = \max_{\text{all } e} \frac{1}{d} \sum_{k=0}^{d-1} z_k(p; t_0), \quad (76)$$

where  $w$  is chosen so that Eq. (75) is satisfied for some  $\mathcal{C}$  that maximizes the right hand side of Eq. (76). This follows as  $\hat{V}_C$  becomes a special case of  $\hat{V}$ , and the only freedom to vary the orthonormal basis  $\mathcal{C}$  is through its reorientations in Hilbert space — precisely given by all possible unitary transformations  $\hat{V} \in \mathcal{U}(d)$  acting on the energy subspace  $\Sigma_d$ .

Now, we need to establish that Eq. (75) is indeed valid, and identify  $w$ . It is convenient to consider the two cases of nondegenerate and degenerate  $\hat{U}_C^p$  separately.

1. **Case 1:  $|p|$  and  $d$  are coprime.** In this case,  $\hat{U}_C^p$  is itself a cycling operator. We separate the persistence inner product into an amplitude and phase,

$$\langle C_k | \{ \hat{U}_C^p \}^\dagger \hat{U}_H(p t_0) | C_k \rangle = z_k(p; t_0) e^{i\phi_k(p; t_0)}. \quad (77)$$

Let  $\bar{\phi}(p; t_0) = \sum_{k=0}^{d-1} \phi_k(p; t_0)$ . Define a new cyclic permutation  $\mathcal{C}'$  with basis vectors

$$|C'_k\rangle = e^{i \sum_{j=-1}^{(j+1)p=k} \{ \phi_{jp}(p; t_0) - [\bar{\phi}(p; t_0)/d] \}} |C_k\rangle, \quad (78)$$

where  $\sum_{j=-1}^{(j+1)p=k} \phi_{jp} = \phi_{-p} + \phi_0 + \phi_p + \dots + \phi_{k-p}$  is a sum over the index with steps of size  $p$ , and subtracting  $\bar{\phi}(p; t_0)/d$  from each term ensures the single-valuedness of the phases in the new basis. This induces a unitary transformation  $\hat{U}_C \rightarrow \hat{U}_{C'} = \hat{V}_C \hat{U}_C \hat{V}_C^\dagger$  (where  $\hat{U}_{C'}$  is required to satisfy Eq. (77) with the  $|C_k\rangle$  replaced by  $|C'_k\rangle$ ), such that

$$\langle C_k | \hat{V}_C \{ \hat{U}_C^p \}^\dagger \hat{V}_C^\dagger \hat{U}_H(p t_0) | C_k \rangle = z_k(p; t_0) e^{i\bar{\phi}(p; t_0)/d}. \quad (79)$$

We see that Eq. (75) is then satisfied for a twisting functional  $w$  with  $\alpha_1(w) = -\bar{\phi}(p; t_0)/d$  (however, this phase is inconsequential in this case, being absorbed by the absolute value in Eq. (76)).

2. **Case 2:  $|p|$  and  $d$  have a nontrivial common factor.** For this case, we can ensure that the analogue of Eq. (75) for each  $[d/\mathcal{N}(d, p)]$ -element cycle is satisfied following the procedure leading up to Eq. (79), with the total phase  $\bar{\phi}(p; t_0)$  replaced by that corresponding to the respective cycle,  $\bar{\phi}_j(p; t_0)$ . Then, it follows that Eq. (75) is also satisfied overall for  $\hat{U}_C^p$  with a twisting functional  $w$  given by  $\alpha_j(w) = -\bar{\phi}_j(p; t_0)/d$ .

Thus, from Eq. (76), we can maximize the mean persistence by maximizing the magnitude of the trace

$$f_p(\hat{U}_C) = \left| \text{Tr} \left[ w\{\hat{U}_C^p\}^\dagger \hat{U}_H(pt_0) \right] \right| \quad (80)$$

with respect to reorientations  $\hat{U}_C \rightarrow \hat{V}\hat{U}_C\hat{V}^\dagger$ . In Sec. B.2.2, this maximum is shown to occur for some  $\hat{U}_C$  satisfying

$$\left[ \hat{U}_H(pt_0), w\{\hat{U}_C^p\}^\dagger \right] = 0, \quad (81)$$

as long as  $f_p(\hat{U}_C) \geq \sqrt{d(d-2)}$  at some such point.

If  $\hat{U}_H(pt_0)$  and  $w\{\hat{U}_C^p\}$  both have nondegenerate eigenvalues, each has a unique set of  $d$  eigenvectors corresponding to the respective eigenvectors of  $\hat{U}_H(t_0)$  and  $\hat{U}_C$ . Eq. (81) then implies that both sets of eigenvectors are identical, and  $\hat{U}_C$  must commute with  $\hat{U}_H(t_0)$  to achieve a local extremum of the mean persistence.

When there are degeneracies (in any of  $\hat{U}_H(t_0)$ ,  $\hat{U}_H(pt_0)$  or  $w\{\hat{U}_C^p\}$ ), we can nevertheless reach a similar conclusion by infinitesimally breaking the degeneracies. We can define  $\hat{U}_{H(\delta_u)} = \hat{U}_H(pt_0)e^{i\delta_u\hat{Y}}$  where  $\delta_u \rightarrow 0$  and  $\hat{Y}$  is any finite Hermitian operator (i.e. with finite matrix elements in any orthonormal basis), such that  $\hat{U}_{H(\delta_u)}$  has nondegenerate eigenvalues when  $\delta_u \neq 0$ . Similarly, we define  $w_{(\delta_w)}$  by  $\alpha_j(w_{(\delta_w)}) = \alpha_j(w) + \delta_w\gamma_j$  with  $\delta_w \rightarrow 0$ , with the  $\gamma_j$  chosen so as to ensure the nondegeneracy of the eigenvalues of  $w\{\hat{U}_C^p\}$  (essentially, infinitesimally twisting any degenerate  $e^{i\alpha_j(w)}\hat{U}_{C,j}(p)$ ,  $e^{i\alpha_k(w)}\hat{U}_{C,k}(p)$ , ... relative to each other). Re-expressing Eq. (76) in terms of these variables, gives

$$\max_{\hat{V} \in \mathcal{U}(d)} \left| \frac{1}{d} \text{Tr} \left[ \hat{V} w_{(\delta_w)}\{\hat{U}_C^p\}^\dagger \hat{V}^\dagger \hat{U}_{H(\delta_u)}(pt_0) \right] \right| = \max_{\text{all } \mathcal{C}} \frac{1}{d} \sum_{k=0}^{d-1} z_k(p; t_0) + O(\delta_u, \delta_w), \quad (82)$$

where  $O(\delta_u, \delta_w)$  consists of terms of the form  $(\delta_u)^a(\delta_w)^b y_{ab}$  with  $a, b \geq 1$ . As with Eq. (81), the solution to the maximization on the left hand side must be among its local extrema, given by

$$\left[ \hat{U}_{H(\delta_u)}(pt_0), w_{(\delta_w)}\{\hat{U}_C^p\}^\dagger \right] = 0. \quad (83)$$

Now, each nondegenerate operator  $\hat{U}_{H(\delta_u)}(pt_0)$  and  $w_{(\delta_w)}\{\hat{U}_C^p\}^\dagger$  has a unique set of  $d$  eigenvectors, which the above equation asserts are identical. We can choose  $\hat{Y}$  and  $\gamma_j$  to break the degeneracy of  $\hat{U}_H(pt_0)$  and  $w\{\hat{U}_C^p\}$  in any desired way i.e. to pick any complete orthonormal subset of each set of eigenvectors. By Eq. (82), any such choice is equally good for maximizing the mean persistence in the  $\delta_u, \delta_w \rightarrow 0$  limit. In particular, we can pick  $w_{(\delta_w)}\{\hat{U}_C^p\}^\dagger$  so that its eigenvectors are identical to those of  $\hat{U}_C$ ; similarly, we can choose  $\hat{Y}$  so that the eigenvectors of  $\hat{U}_{H(\delta_u)}(pt_0)$  are identical to any complete orthonormal set of eigenvectors of  $\hat{U}_H(t_0)$ . In other words, any choice of degeneracy breaking in the neighborhood of degenerate operators only infinitesimally affects the local extrema of the left hand side of Eq. (82).

Thus, the right hand side of Eq. (73) attains its global maximum when the eigenvectors of  $\hat{U}_C$  are fixed to be any complete orthonormal set of eigenvectors of  $\hat{U}_H(t_0)$ , with the only freedom remaining in the assignment of the distinct eigenvalues of  $\hat{U}_C$  to these eigenvectors. This can be concisely expressed as follows: the global maximum of the mean persistence occurs among the solutions to

$$\lim_{\delta \rightarrow 0} \left[ \hat{U}_H(t_0)e^{i\delta\hat{Y}}, \hat{U}_C \right] = 0, \quad (84)$$

for any Hermitian  $\hat{Y}$ . For any  $\hat{U}_C$  satisfying this property, all the  $z_j(p; t_0)$  are equal at any given  $p$ . It follows that  $\min_j z_j(p; t_0)$  is also maximized, and the  $p$ -step error minimized, by the same  $\hat{U}_C$  that maximizes the mean persistence. From the requirement  $f_p(\hat{U}_C) \geq \sqrt{d(d-2)}$ , we get the condition  $\varepsilon_C(p, t_0) \leq (2/d)$  on such a minimum of the error.

### B.2.2 Local extrema, and the global maximum for large persistence amplitudes

For simplicity, let  $\hat{U}_1 = w\{\hat{U}_C^p\}$  and  $\hat{U}_2 = \hat{U}_H(pt_0)$ . We seek stationary points of the real valued function (from Eq. (80))

$$\left| \text{Tr} \left( \hat{U}_1^\dagger \hat{U}_2 \right) \right| \quad (85)$$

with respect to small reorientations of  $\hat{U}_1$  by  $\hat{V}$ , to first order. This would yield all the local maxima and minima (as well as saddle and inflection points) of the function except the global minima when the function attains the value 0, where it is not differentiable. We write  $\hat{V} = e^{i\hat{X}}$  with  $\hat{X}$  near 0, and require the phase of the  $O(\hat{X})$  term in  $\text{Tr}[\hat{V}\hat{U}_1^\dagger\hat{V}^\dagger\hat{U}_2]$  to be orthogonal to the phase of the  $O(1)$  term (so that the first variation corresponds only to a change in phase and not in magnitude; alternatively, one could directly extremize the square of Eq. (85)). This gives

$$\text{Tr} \left( \hat{X} \left[ \hat{U}_1^\dagger, \hat{U}_2 \right] \right) = c(\hat{X}) \text{Tr} \left( \hat{U}_1^\dagger \hat{U}_2 \right) \text{ for all Hermitian } \hat{X} \quad (86)$$

with  $c(\hat{X})$  required to be a real-valued function, for the stationary points. As can be verified by imposing this for each independent degree of freedom in the matrix elements of  $\hat{X}$ , this requires

$$\left[ e^{-i\alpha_{12}} \hat{U}_1^\dagger, \hat{U}_2 \right] = \hat{F}, \quad (87)$$

where  $\hat{F}$  is some traceless Hermitian operator, and  $\alpha_{12}$  is the phase of  $\text{Tr}(\hat{U}_1^\dagger \hat{U}_2)$ .

Up to this point, the unitarity of  $\hat{U}_1$  and  $\hat{U}_2$  played no role. Now, we use the fact that their products are unitary, and write

$$e^{-i\alpha_{12}} \hat{U}_1^\dagger \hat{U}_2 = e^{i\hat{A}_{12}}, \text{ and } \hat{U}_2 e^{-i\alpha_{12}} \hat{U}_1^\dagger = e^{i\hat{A}_{21}}, \quad (88)$$

for Hermitian  $\hat{A}_{12}$  and  $\hat{A}_{21}$ . Formally defining sines and cosines of Hermitian operators through their Taylor series (which are also Hermitian), Eq. (87) then gives

$$\cos \hat{A}_{12} - \cos \hat{A}_{21} + i [\sin \hat{A}_{12} - \sin \hat{A}_{21}] = \hat{F}. \quad (89)$$

The Hermiticity of  $\hat{F}$  demands that the anti-Hermitian part of the left hand side vanishes, giving

$$\sin \hat{A}_{12} = \sin \hat{A}_{21}. \quad (90)$$

Let  $\{a(k)\}_{k=0}^{d-1}$  be the eigenvalues of  $\hat{A}_{12}$  and  $\hat{A}_{21}$  (which must have identical eigenvalues up to irrelevant shifts of  $2\pi$ , as products of two unitaries have the same eigenvalues irrespective of the order [95]). As long as it is known that  $a(k) \in [-\pi/2, \pi/2]$ , the sine is invertible<sup>8</sup> and  $\hat{A}_{21} = \hat{A}_{12}$ . Consequently,

$$\left\{ a(k) \in [-\pi/2, \pi/2], \forall k \right\} \implies \left( \left[ e^{-i\alpha_{12}} \hat{U}_1^\dagger, \hat{U}_2 \right] = 0 \right) \quad (91)$$

<sup>8</sup>In fact, one gets  $\hat{A}_{12} = \hat{A}_{21}$  for “generic” values of  $a(k)$  such that the set  $\{a(k), \pi + a(k)\}$  is non-degenerate. But it is not clear if this can be guaranteed for any desired  $\hat{V}$  by imposing simple conditions on  $\hat{U}_2$ .

at a stationary point. The vanishing commutator on the right side of the implication is precisely the condition of Eq. (81).

The question of interest is now if there's a simple way to guarantee the restriction on  $a(k)$  in Eq. (91). To see that there is, we note that  $[e^{-i\alpha_{12}} \text{Tr}(e^{i\hat{A}_{12}})] \in \mathbb{R}$  by the definition of  $\alpha_{12}$ , which implies

$$\sum_k \cos a(k) = e^{-i\alpha_{12}} \text{Tr}(e^{i\hat{A}_{12}}), \quad (92)$$

$$\sum_k \sin a(k) = 0. \quad (93)$$

Let us maximize the multivariable function  $b[a(k)] = \sum_k \cos a(k)$  with *fixed*  $a(0)$  (and free  $a(k \neq 0)$ ) subject to the constraint in Eq. (93) (and implicitly, non-negativity) using e.g. the method of Lagrange multipliers. The stationary points of  $b[a(k)]$  occur at

$$a(k \neq 0) = c + \pi\zeta_k, \text{ with } \zeta_k \in \{0, 1\}, \quad (94)$$

for some constant  $c$ . The global maximum of  $b[a(k)]$  corresponds to  $c \in [-\pi/2, \pi/2]$  and  $\zeta_k = 0 \forall k$ . Imposing Eq. (93) to fix  $c$  in terms of  $a(0)$ , we get

$$\sum_k \cos a(k) \leq b_{\max}[a(0)] \equiv \cos a(0) + (d-1) \sqrt{1 - \frac{\sin^2 a(0)}{(d-1)^2}}. \quad (95)$$

This is a monotonically decreasing function of  $|a(0)|$  in its full domain  $[0, \pi]$  for  $d \geq 2$ . In particular, if  $|a(0)| > \pi/2$ , then it is guaranteed that  $b[a(k)] < b_{\max}[\pi/2] = \sqrt{d(d-2)}$ . Re-expressing  $b[a(k)]$  in terms of the trace of the relevant unitaries, we then have

$$\left\{ \left| \text{Tr}(\hat{U}_1^\dagger \hat{U}_2) \right| \geq \sqrt{d(d-2)} \right\} \implies \left\{ a(k) \in [-\pi/2, \pi/2], \forall k \right\}. \quad (96)$$

Combined with the implication in Eq. (91), it follows that maxima for which the trace is no smaller than  $\sqrt{d(d-2)}$  occur for cycling operators that commute with time evolution, i.e. when  $[\hat{U}_1^\dagger, \hat{U}_2] = 0$ . Such commuting operators remain local extrema of the trace in other cases, but it is unclear in the present analysis if the global maximum is among them.

For comparison with the following subsection, we note that  $a(k) = -2\pi\tau\Delta_k/d$ , where  $\Delta_k$  are the mode fluctuations used elsewhere (see Eq. (25)) in the main text.

### B.3 Decrease of persistence for small permutations of sorted energy levels

When  $\Delta_n \ll d$ , assuming that the energies  $E_n$  have been shifted by some additive constant so that  $\sum_k \Delta_k = 0$ , we have (representing  $d$  times the persistence amplitude as per Eq. (25))

$$\sum_{k=0}^{d-1} e^{-2\pi i \Delta_k/d} = 1 - \frac{2\pi^2}{d^2} \sum_{k=0}^{d-1} \Delta_k^2 + O(\Delta_k^3 d^{-3}). \quad (97)$$

For simplicity, we assume that the levels are already sorted i.e.  $E_n < E_m$  when  $n < m$ . This further implies

$$\Delta_n - \Delta_m > -|n - m|. \quad (98)$$

Any permutation  $q(n)$  can be broken up [8] into a set of cyclic permutations  $q_r(n)$ , each involving a subset of  $N_r$  levels  $\mathcal{E}[q_r] = \{E_{r(k)}\}_{k=0}^{N_r-1}$ . For the rest of the argument, we will require (where the subtraction of  $r$  is on  $\mathbb{Z}$  (linear), and not on  $\mathbb{Z}_d$  (circular or modulo  $d$ ))

$$|r(k) - r(j)| < d/2, \forall k, j \in \mathbb{Z}_{N_r}, \quad (99)$$

for each  $q_r$ ; permutations  $q$  satisfying this are what we refer to as “small” permutations. This will ensure that Eq. (97) remains valid under these permutations without discrete shifts of some of the  $\Delta_k$  by multiples of  $(2\pi)$ .

The new mode fluctuations after permutation are given by

$$\Delta'_{r(k)} = \Delta_{r(k+1)} + [r(k+1) - r(k)], \quad (100)$$

for each cycle  $q_r$ . It follows that the mean is preserved i.e.

$$\sum_{k=0}^{N_r-1} \Delta'_{r(k)} = \sum_{k=0}^{N_r-1} \Delta_{r(k)}. \quad (101)$$

Our goal is to show that the variance of the  $\Delta'_k$  is larger than that of the  $\Delta_k$ , which would translate to a decreased persistence by Eq. (97). We have

$$\sum_{k=0}^{N_r-1} (\Delta'_{r(k)})^2 - \sum_{k=0}^{N_r-1} (\Delta_{r(k)})^2 = 2 \sum_{k=0}^{N_r-1} \Delta_{r(k+1)} [r(k+1) - r(k)] + \sum_{k=0}^{N_r-1} [r(k+1) - r(k)]^2. \quad (102)$$

In general, the  $r(k+1)$  are not in any simple (e.g. ascending or descending) order. We can split each difference  $[r(k+1) - r(k)]$  in the first term on the right hand side into a sum of differences of the  $r(\ell)$  lying between (and inclusive of) them:

$$\Delta_{r(k+1)} [r(k+1) - r(k)] = \sum_{r_j \in [r(k), r(k+1)]} \zeta_k \Delta_{r(k+1)} (r_{j+1} - r_j), \quad (103)$$

where  $\zeta_k = \text{sgn}[r(k+1) - r(k)]$ , and the  $r_j$  are chosen to be sorted according to  $j$ . On including terms with different values of  $k$ , each interval  $(r_{j+1} - r_j)$  occurs in an equal number of terms with positive  $\zeta_k = +1$  ( $r(k+1) \geq r_{j+1}$ ) and negative  $\zeta_k = -1$  ( $r(k+1) \leq r_j$ ). We can arbitrarily pair each positive term  $r_+$  with a negative term  $r_-$ , and use Eq. (98) for the difference  $\Delta_{r_+} - \Delta_{r_-}$  noting that  $r_+ > r_-$ . This amounts to replacing the equality with  $\geq$ , and each  $\Delta_{r(k+1)}$  with  $-r(k+1)$ , in Eq. (102). We therefore obtain

$$\begin{aligned} \sum_{k=0}^{N_r-1} (\Delta'_{r(k)})^2 - \sum_{k=0}^{N_r-1} (\Delta_{r(k)})^2 &\geq \left\{ -2 \sum_{k=0}^{N_r-1} r(k+1) [r(k+1) - r(k)] \right\} + \sum_{k=0}^{N_r-1} [r(k+1) - r(k)]^2 \\ \implies \sum_{k=0}^{N_r-1} (\Delta'_{r(k)})^2 &\geq \sum_{k=0}^{N_r-1} (\Delta_{r(k)})^2. \end{aligned} \quad (104)$$

The second line follows from simplifying the first. Adding all such equations from each  $q_r$  together, we get

$$\sum_{k=0}^{d-1} e^{-2\pi i \Delta'_k / d} \leq \sum_{k=0}^{d-1} e^{-2\pi i \Delta_k / d} + O(\Delta^3 d^{-3}). \quad (105)$$



This shows that sorting the energy levels corresponds to the maximum persistence at  $p = 1$  for a given  $t_0$  and small  $\Delta_k$ , at least among other possibilities that can be obtained as small permutations of the sorted levels. This is more like a discrete version of a local extremum. It would be interesting to check if “larger” permutations not subject to Eq. (99) would lead to significantly better maxima; this is unlikely to be the case without some non-intuitive conspiracy between distant energy levels.

## Appendix C Time dependence of persistence amplitudes

### C.1 Error coefficient pairing in discrete sum over paths

We rewrite Eq. (28) for  $p = 1$  as

$$\hat{U}_\Delta e^{-i\phi_\Delta(1)} = (1 - \varepsilon_1)^{1/2} \left[ \hat{1} + g_1 \sum_{m=1}^{d-1} v_m(1) \hat{U}_C^m \right], \quad (106)$$

where  $\varepsilon_p \equiv \varepsilon_C(p, t_0)$  and  $g_1 = \sqrt{\varepsilon_1/(1 - \varepsilon_1)}$ . We note that  $g_1$  is also the coefficient that occurs on the right hand side of Eq. (30). The  $p$ -th power of the error unitary is

$$\begin{aligned} \hat{U}_\Delta^p e^{-ip\phi_\Delta(1)} &= (1 - \varepsilon_1)^{p/2} \sum_{s=0}^p \binom{p}{s} g_1^s \sum_{m_1, \dots, m_s} v_{m_1}(1) \dots v_{m_s}(1) \hat{U}_C^{m_1 + \dots + m_s}, \\ &= (1 - \varepsilon_1)^{p/2} \sum_{r=0}^{d-1} \left( \sum_{s=0}^p \Gamma_r^{(s)} \right) \hat{U}_C^r \end{aligned} \quad (107)$$

where  $\binom{p}{s} = p!/(s!(p-s)!)$  is the binomial coefficient, and we recall that the sums are modulo  $d$ . We have also defined

$$\Gamma_r^{(s)} = \binom{p}{s} g_1^s \sum_{m_1, \dots, m_s} v_{m_1}(1) \dots v_{m_s}(1) \bar{\Theta}(m_1 + \dots + m_s = r), \quad (108)$$

with  $\bar{\Theta}(x) = 1$  if  $x$  is true and 0 otherwise. Each term with fixed  $r$  in (107) represents a sum over paths for the transition amplitude from any  $|C_k\rangle$  to  $|C_{k+r}\rangle$ .

Now, we apply the assumption of error coefficient pairing, by considering only terms where  $s$  is even in Eq. (108), restricting to such pairings necessarily implies that  $m_1 + \dots + m_s = 0$ . For odd  $s$ , it is not possible to pair all error coefficients and a free error coefficient remains, whose index must necessarily be  $r$  if the remaining coefficients are paired. Schematically (in the sense that we avoid explicitly enumerating the possible pairings), for non-negative integer  $u$ ,

$$\Gamma_r^{(2u)} \approx \delta_{r0} \left\{ \binom{p}{2u} g_1^{2u} \sum_{\text{pairings}} [v_{m_1}(1) v_{-m_1}(1)] \dots [v_{m_u}(1) v_{-m_u}(1)] \right\}, \quad (109)$$

$$\Gamma_r^{(2u+1)} \approx g_1 v_r(p-2u) \left\{ \binom{p}{2u} g_1^{2u} \sum_{\text{pairings}} [v_{m_1}(1) v_{-m_1}(1)] \dots [v_{m_u}(1) v_{-m_u}(1)] \right\}. \quad (110)$$

In the second line, we have accounted for  $s = 2u + 1$  different ways of choosing the unpaired coefficient, and used  $s \binom{p}{s} = (p+1-s) \binom{p}{s-1}$ .

For a given  $u$ , the sum over pairings and coefficients within the braces in Eqs. (109) and (110) are identical, irrespective of the value of  $r$ . Treating  $g_1$  as a formally independent parameter that

we can take partial derivatives with respect to, we can further replace  $(p - 2u)$  with  $(p - g_1 \vec{\partial}/\partial g_1)$  acting on its right in Eq. (110), which moves all the  $u$  dependence to inside the braces. For even  $p$ , this means that each sum over  $s$  in Eq. (107) — which is naturally restricted to even  $s$  for  $r = 0$  and odd  $s$  for  $r \neq 0$  after pairing — produces coefficients for all  $r$  that are identical except for the operators outside the braces in Eqs. (109) and (110). If the time dependence is sufficiently slow, the result for odd  $p$  can be extrapolated (to a good approximation) in any convenient way between those for  $p \pm 1$ . Thus, we have the approximate form

$$\hat{U}_\Delta^p e^{-ip\Phi_\Delta(1)} \approx (1 - \varepsilon_1)^{p/2} \left[ \hat{1} + g_1 \sum_{r=1}^{d-1} \nu_r(1) \hat{U}_C^r \left( p - g_1 \frac{\vec{\partial}}{\partial g_1} \right) \right] h(p, g_1). \quad (111)$$

The function  $h(p, g_1)$  originates in the sum over pairings within the braces of Eqs. (109) and (110); from the above expression, it is formally related to the persistence amplitude at  $p$  by

$$z(p, t_0) = (1 - \varepsilon_1)^{p/2} h \left( p, \sqrt{\frac{\varepsilon_1}{1 - \varepsilon_1}} \right). \quad (112)$$

## C.2 Gaussian estimate

The persistence amplitude at  $p + 1$  can be expressed in terms of the coefficients in  $\hat{U}_\Delta^p$  and  $\hat{U}_\Delta^1$  as follows:

$$\begin{aligned} z(p + 1, t_0) &= \left| \frac{1}{d} \text{Tr} [\hat{U}_\Delta^1 \hat{U}_\Delta^p] \right| \\ &= \left| \sqrt{1 - \varepsilon_1} \sqrt{1 - \varepsilon_p} + \sqrt{\varepsilon_1 \varepsilon_p} \sum_{r=1}^{d-1} \nu_r(1) \nu_{-r}(p) \right|. \end{aligned} \quad (113)$$

Substituting the appropriate expressions for  $\varepsilon_p$  and  $\nu_p$  from Eq. (111), we get

$$z(p + 1, t_0) \approx (1 - \varepsilon_1)^{1/2} \left| z(p, t_0) + (1 - \varepsilon_1)^{(p)/2} g_1^2 \sum_{r=1}^{d-1} \nu_r(1) \nu_{-r}(1) \left( p - g_1 \frac{\vec{\partial}}{\partial g_1} \right) h(p, g_1) \right| \quad (114)$$

Now, we assume that the second term within the absolute value is smaller than the first, and  $ph \gg g_1 \partial h / \partial g_1$ ; both will be justified retroactively. Further defining

$$\nu_C = - \sum_{r=1}^{d-1} \nu_r(1) \nu_{-r}(1), \quad (115)$$

which happens to measure the goodness of the approximation in Eq. (33), we are led to

$$z(p + 1, t_0) \approx (1 - \varepsilon_1)^{1/2} \left[ 1 - g_1^2 p \nu_C \right] z(p, t_0). \quad (116)$$

It is now straightforward to multiply over values of  $p$  from some given  $\bar{p}$  through to 1. For  $\varepsilon_1 \ll 1$  and setting  $\nu_C \approx 1$  as per Eq. (33), we get

$$z(\bar{p}, t_0) \approx \exp \left[ -\frac{\varepsilon_1}{2} |\bar{p}| - \frac{g_1^2}{2} \bar{p}^2 \right]. \quad (117)$$

We see that the smallness of the second term in Eq. (114) and  $ph \gg g_1 \partial h / \partial g_1$  are both satisfied when  $p \ll 1/g_1$ , i.e. when the persistence amplitude is still close to 1.

### C.3 Minimum error constraints from the SFF

Substituting the form  $K(t) = \lambda t^\gamma$  in Eq. (37) and dropping subleading terms in  $\varepsilon_1 = \varepsilon_C(1, t_0)$  gives

$$2\lambda t_0^\gamma \sum_{p=1}^{1/(M\sqrt{\varepsilon_1})} p^{\gamma-2} \lesssim \varepsilon_1. \quad (118)$$

For  $\gamma \in [0, 1)$ , the left hand side is dominated by small  $p$  and is independent of  $M$ . Replacing  $1/(M\sqrt{\varepsilon_1}) \rightarrow \infty$ , we obtain

$$\varepsilon_1 \gtrsim 2\lambda t_0^\gamma \zeta(2-\gamma), \quad (119)$$

where  $\zeta(x)$  is the Riemann zeta function. In particular, for  $\gamma = 0$  and  $\lambda = 1/d$  (Poisson statistics), we have  $\varepsilon \gtrsim \pi^2/(3d) = O(1/d)$ . For  $\gamma > 1$ , it is instead the terms with larger  $p$  that dominate. Using the leading term in Faulhaber's formula for the sum (formula (0.121) in Ref. [96]; equivalent to replacing the sum with an integral), we have

$$2\lambda t_0^\gamma \frac{[1/(M\sqrt{\varepsilon_1})]^{\gamma-1}}{\gamma-1} \lesssim \varepsilon_1. \quad (120)$$

The presence of  $M = O(1) \geq 1$  in this expression allows us to make only order of magnitude statements. We get

$$\varepsilon_1^{(1+\gamma)/2} \gtrsim 2\lambda t_0^\gamma \frac{(\gamma-1)}{M^{\gamma-1}}, \quad (121)$$

which implies  $\varepsilon_1 \geq O(d^{-4/(\gamma+1)})$  when  $\lambda = O(d^{-2})$  and  $t_0 = O(1)$ , for any  $\gamma = O(1) > 1$ . The most generic case (i.e. typical for Haar random [7, 8] systems),  $\gamma = 1$ , is a bit more subtle. Here, it is again the large- $p$  terms that dominate, so we take the  $\gamma \rightarrow 1$  limit of Eq. (120), which gives

$$\frac{\varepsilon_1}{\ln\left(\frac{1}{M\sqrt{\varepsilon_1}}\right)} \gtrsim 2\lambda t_0. \quad (122)$$

This is a transcendental equation for  $\varepsilon_1$ , but we can nevertheless invert it to leading order in  $\lambda^{-1}$  (i.e. substituting  $\varepsilon_1 = \mu(\lambda)\lambda$  and solving for  $\mu$ , neglecting  $\ln(\ln \lambda)$ ), obtaining

$$\varepsilon_1 \gtrsim \lambda t_0 \ln \frac{1}{\lambda}. \quad (123)$$

For Wigner-Dyson statistics,  $\lambda = O(d^{-2})$  and  $t_0 = O(1)$  gives  $\varepsilon \geq O(d^{-2} \ln d)$ .

### C.4 Numerical evidence for error coefficient pairing

To provide numerical evidence for the pairing of error coefficients, we test the prediction of Eq. (111) when  $g_1 \partial h / \partial g_1$  is negligible i.e. Eq. (34) in the main text. More directly, we define

$$\tilde{v}_m(p) = \frac{1}{pz(p, t_0)} v_m(p). \quad (124)$$

Eqs. (111), (34) then imply that  $\tilde{v}_m(p) = \tilde{v}_m(1)$  for any  $p \ll 1/\sqrt{\varepsilon_C(1, t_0)}$ . This is verified in Fig. 9 for the ( $\beta = 2$ ,  $d = 2048$ ) CUE dataset of Fig. 6, for which  $1/\sqrt{\varepsilon_C(1, t_0)} \approx 525$ .

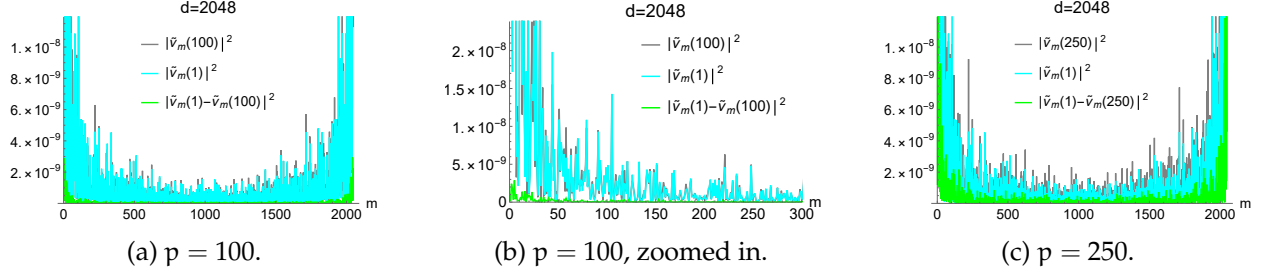


Figure 9: Comparison of  $\tilde{v}_m(p)$  with  $\tilde{v}_m(1)$ , using magnitudes  $|\tilde{v}_m(p)|^2$ ,  $|\tilde{v}_m(1)|^2$  and residuals  $|\tilde{v}_m(1) - \tilde{v}_m(p)|^2$  for  $d = 2048$ . The residuals are predicted to be negligible compared to the magnitudes at the same  $m$  for  $p \ll 525$ , which these plots are in good agreement with even when  $p$  is a considerable fraction of 525.

## Appendix D The classical limit

### D.1 Wigner quasiprobabilities and mixed states

We consider the special problem of a particle with position coordinates  $\mathbf{x} \in \mathbb{R}^N$ , allowing the definition of the real-valued Wigner quasiprobability functions  $W$  (following the conventions adopted in Ref. [76]) in an effective Hamiltonian phase space  $\mathcal{P} = \{(\mathbf{x}, \mathbf{p})\} = \mathbb{R}^{2N}$ . For a general (i.e. mixed state) density matrix  $\hat{\rho}$  (in units where the reduced Planck's constant  $\hbar = 1$ ),

$$W(\mathbf{x}, \mathbf{p}) = \int_{\mathbf{L}} d\mathbf{y} \langle \mathbf{x} - \frac{1}{2}\mathbf{y} | \hat{\rho} | \mathbf{x} + \frac{1}{2}\mathbf{y} \rangle e^{i\mathbf{p} \cdot \mathbf{y}}, \quad (125)$$

where  $W$  is normalized according to  $\int d\mathbf{x} d\mathbf{p} W(\mathbf{x}, \mathbf{p}) = (2\pi)^N$ . The overlap of the density matrices is directly given by the overlap of these quasiprobabilities,

$$\text{Tr}(\hat{\rho}_1 \hat{\rho}_2) = \frac{1}{(2\pi)^N} \int d\mathbf{x} \int d\mathbf{p} W_1(\mathbf{x}, \mathbf{p}) W_2(\mathbf{x}, \mathbf{p}). \quad (126)$$

When  $W_A(\mathbf{x}, \mathbf{p})$  is a uniform distribution over some region  $A$  in the phase space (at least at some level of approximation;  $W$  is in general not non-negative everywhere [97]), we have  $W_A[(\mathbf{x}, \mathbf{p}) \in A] = [(2\pi)^N / \tilde{\mu}(A)]$ , with its value being (approximately) 0 elsewhere. Here,  $\tilde{\mu}(A) = \int_A d\mathbf{x} d\mathbf{p}$ . Using this expression in Eq. (126), we get for any two regions  $A$  and  $B$  and the density matrices  $\hat{\rho}_A$  and  $\hat{\rho}_B$  corresponding to such uniform Wigner functions,

$$\frac{1}{(2\pi)^N} \text{Tr}(\hat{\rho}_A^2) = \frac{1}{\tilde{\mu}(A)}, \quad (127)$$

$$\frac{1}{(2\pi)^N} \text{Tr}(\hat{\rho}_A \hat{\rho}_B) = \frac{\tilde{\mu}(A \cap B)}{\tilde{\mu}(A)\tilde{\mu}(B)}. \quad (128)$$

These are equivalent to Eqs. (45) and (46) in the main text, subject to the normalization of the measure  $\tilde{\mu}$ . The expressions in the main text assume that  $\mu(\mathcal{P}) = 1$ , but the system considered in this Appendix has an infinite phase space with  $\tilde{\mu}(\mathcal{P}) = \infty$ , as well as an infinite dimensional Hilbert space with  $d = \infty$ . By requiring that the maximally mixed state  $\hat{\rho} = \hat{1}/d$  corresponds to a uniform distribution over the full phase space  $\mathcal{P}$  (e.g. any projective measurement onto an orthonormal basis has equal probabilities for every outcome in the former, and the latter is equally distributed over any foliation of the phase space into surfaces of constant position coordinates e.g.  $\mathbf{x}$ ), we heuristically obtain  $\tilde{\mu}(\mathcal{P}) = (2\pi)^N d$ , fixing the normalization of  $\mu$  and directly giving

Eqs. (45) and (46). We expect this reasoning to go through without dealing with infinities, if one can suitably define analogues of the Wigner functions restricted to energy shells of finite measure.

## D.2 Cyclic permutations for a harmonic oscillator

Here, we consider the example of the 1D harmonic oscillator, mainly to illustrate the relationship between ergodicity and cyclic ergodicity. The classical Hamiltonian  $H = p^2/(2m) + m\omega^2 x^2/2$  can be rewritten in terms of action-angle [5, 78] variables  $(J, \theta)$  as  $H = J\omega$ , where the equation of motion is  $\theta = \omega t$ . The action variable  $J > 0$  is a conserved quantity, and the phase space  $\mathcal{P}$  decomposes into subsets  $\mathcal{P}_J$  with fixed  $J = J_0$  and measure induced by  $d\theta$  on  $\theta \in [0, 2\pi)$ , each of which is ergodic and periodic.

We can construct  $n$ -element cyclic permutations of zero error in an energy window with arbitrary base  $E_0 = J_0\omega$  and arbitrary width  $\delta E = \omega\delta J$ , by choosing the sets

$$C_k = \left\{ (J, \theta) : J \in [J_0, J_0 + \delta J], \theta \in \left[ \frac{2\pi k}{n}, \frac{2\pi(k+1)}{n} \right] \right\} \quad (129)$$

and  $t_0 = 2\pi/(\omega n)$ . That the error is zero requires that none of the  $C_k$  are completely contained in any  $\mathcal{P}_n$ , which is indeed the case. At the same time, if we take  $\delta J \rightarrow 0$ , the  $C_k$  are all contained in  $\mathcal{P}_{J_0}$ ; zero error now implies ergodicity and periodicity within  $\mathcal{P}_{J_0}$ .

The quantized oscillator has  $J \in \mathbb{N}_0$  with energy eigenstates  $|J\rangle$  and eigenvalues  $J\omega$ , and the DFT basis states

$$|\theta \in \mathbb{Z}_{\delta J}\rangle = \frac{1}{\sqrt{\delta J}} \sum_{k=0}^{\delta J-1} e^{-2\pi i k \theta / \delta J} |J_0 + k\rangle \quad (130)$$

provide a zero error cyclic permutation for time evolution (with  $t_0 = 2\pi/(\omega\delta J)$ ) in the energy subspace spanned by  $\{|J_0\rangle, \dots, |J_0 + \delta J\rangle\}$  (implying quantum cyclic ergodicity and periodicity). In the classical limit ( $J_0 \gg 1$ ,  $\delta J \gg 1$ ), the  $|\theta\rangle$  have the same equations of motion as localized points in  $\theta$ , and identifying the two leads to the identification of the  $C_k$  with diagonal mixed states supported on  $\delta J/n$  contiguous  $|\theta\rangle$  states.

## Appendix E Mixed state cyclic permutations

Let  $\hat{\Pi}_k = (d_n/n)\hat{\rho}[\bar{\Sigma}(k)]$  be the projection operators onto the subspaces  $\bar{\Sigma}(k)$ . Focus on the two subspaces with projectors  $\hat{\Pi}_k(t_m) \equiv \hat{U}_H(t_m)\hat{\Pi}_k\hat{U}_H^\dagger(t_m)$  and  $\hat{\Pi}_{k+1}$  for a given  $k$ . The expanded energy subspace  $\bar{\Sigma}_{d_n}$  can be expressed using Halmos' decomposition [98, 99] relative to the two projectors:

$$\bar{\Sigma} = (\mathcal{H}_{00} \oplus \mathcal{H}_{01} \oplus \mathcal{H}_{10} \oplus \mathcal{H}_{11}) \oplus [\mathcal{H}_1 \oplus \mathcal{H}_0] \quad (131)$$

where  $\dim(\mathcal{H}_1) = \dim(\mathcal{H}_0)$  always, and  $\dim(\mathcal{H}_{01}) = \dim(\mathcal{H}_{10})$  in our case as  $\text{Tr } \hat{\Pi}_k(t_m) = \text{Tr } \hat{\Pi}_{k+1}$ . These subspaces are such that  $\hat{\Pi}_k(t_m)$  and  $\hat{\Pi}_{k+1}$  take the following forms (in the same order of subspaces):

$$\hat{\Pi}_k(t_m) = (0 \oplus 0 \oplus \hat{1} \oplus \hat{1}) \oplus \begin{bmatrix} \hat{1} & 0 \\ 0 & 0 \end{bmatrix}, \quad (132)$$

$$\hat{\Pi}_{k+1} = (0 \oplus \hat{1} \oplus 0 \oplus \hat{1}) \oplus \begin{bmatrix} \hat{\Lambda}^2 & \hat{\Lambda}\hat{K}\hat{V}^\dagger \\ \hat{V}\hat{\Lambda}\hat{K} & \hat{V}\hat{K}^2\hat{V}^\dagger \end{bmatrix}, \quad (133)$$

with Hermitian  $0 < \hat{\Lambda} < \hat{1}$  and  $0 < \hat{K} < \hat{1}$  satisfying  $\hat{\Lambda}^2 + \hat{K}^2 = \hat{1}$  (both acting on  $\mathcal{H}_1$ ), and some unitary  $\hat{V} : \mathcal{H}_1 \rightarrow \mathcal{H}_0$ . The only subspace in which both projectors have nonzero matrix elements is  $\mathcal{H}_{11} \oplus \mathcal{H}_1$ . Further,  $\mathcal{H}_{11} = [\hat{U}_H(t_m)\bar{\Sigma}(k)] \cap \bar{\Sigma}(k+1)$  is the intersection of the subspaces, while  $\mathcal{H}_{11} \oplus \mathcal{H}_1$  is completely contained within the first subspace  $[\hat{U}_H(t_m)\bar{\Sigma}(k)]$ . Additionally,  $\hat{\Lambda}$  and  $\hat{K}$  necessarily commute, and have a shared eigenbasis (due to the non-negativity of their eigenvalues).

Let  $\lambda_j \in (0, 1)$  be the eigenvalues of  $\hat{\Lambda}$ , and  $\kappa_j \in (0, 1)$  those of  $\hat{K}$ . It is instructive to write the matrix in Eq. (133) in terms of the shared eigenbasis  $|\xi_j\rangle$  of  $\hat{\Lambda}, \hat{K}$ :

$$\begin{bmatrix} \hat{\Lambda}^2 & \hat{\Lambda}\hat{K}\hat{V}^\dagger \\ \hat{V}\hat{\Lambda}\hat{K} & \hat{V}\hat{K}^2\hat{V}^\dagger \end{bmatrix} = \sum_{j=0}^{\dim(\mathcal{H}_1)-1} (\lambda_j|\xi_j\rangle + \kappa_j\hat{V}|\xi_j\rangle) (\lambda_j|\xi_j\rangle + \kappa_j\hat{V}|\xi_j\rangle)^\dagger, \quad (134)$$

from which we see that the orthonormal set of vectors

$$|\eta_j\rangle \equiv \lambda_j|\xi_j\rangle + \kappa_j\hat{V}|\xi_j\rangle \quad (135)$$

are completely contained in  $\bar{\Sigma}(k+1)$ . We can use this fact to identify a convenient orthonormal basis in each subspace. Namely, with  $\mathcal{B}_{uv} = \{|\mathcal{B}_{uv}; j\rangle\}_{j=0}^{\dim(\mathcal{H}_{uv})-1}$  representing some orthonormal basis in  $\mathcal{H}_{uv}$ , we define the following orthonormal bases in  $\hat{\Pi}_k(t_m)$  and  $\hat{\Pi}_{k+1}$ :

$$\mathcal{B}_k(t_m) = \mathcal{B}_{10} \oplus \mathcal{B}_{11} \oplus \{|\xi_j\rangle\}_{j=0}^{\dim(\mathcal{H}_1)-1}, \quad (136)$$

$$\mathcal{B}_{k+1} = \mathcal{B}_{01} \oplus \mathcal{B}_{11} \oplus \{|\eta_j\rangle\}_{j=0}^{\dim(\mathcal{H}_1)-1}, \quad (137)$$

It is important to note that the auxiliary directions in  $\Sigma_{aux}$ , introduced in the main text to make  $d_n$  a multiple of  $n$ , are in  $\mathcal{H}_{10}$  or  $\mathcal{H}_{01}$  if present in  $\bar{\Sigma}(k)$ ,  $\bar{\Sigma}(k+1)$ , as  $\hat{U}_H(t_m)\Sigma_{aux} = \Sigma_{aux}$  by definition. We will require the auxiliary dimension  $\bar{\Sigma}(k) \cap \Sigma_{aux}$  of each subspace to be an element of the corresponding  $\mathcal{B}_{01}$  or  $\mathcal{B}_{10}$ . We will also require the indices  $j$  in  $|\mathcal{B}_k(t_m); j\rangle$  and  $|\mathcal{B}_{k+1}; j\rangle$  to be such that elements in  $\mathcal{B}_{11}$  have the same index, as do  $|\xi_\ell\rangle$  and  $|\eta_\ell\rangle$  for a given  $\ell$ .

The overlap of the projectors is

$$P_k(1, t_m) \equiv \text{Tr} [\hat{\Pi}_k(t_m)\hat{\Pi}_{k+1}] = \dim(\mathcal{H}_{11}) + \sum_j \lambda_j^2. \quad (138)$$

Similarly, the total magnitude of overlap amplitudes between the corresponding elements of the two orthonormal bases is

$$\begin{aligned} R_k(1, t_m) &\equiv \sum_{j=0}^{\dim(\mathcal{H}_{11})-1} |\langle \mathcal{B}_{11}; j | \mathcal{B}_{11}; j \rangle| + \sum_{j=0}^{\dim(\mathcal{H}_1)-1} |\langle \eta_j | \xi_j \rangle| \\ &= \dim(\mathcal{H}_{11}) + \sum_j \lambda_j. \end{aligned} \quad (139)$$

We want to find a lower bound for  $R_k(1, t_m)$  from the overlap. The free variables at our disposal are  $\dim(\mathcal{H}_{10})$ ,  $\dim(\mathcal{H}_{11})$ ,  $\dim(\mathcal{H}_1)$  and all of the  $\lambda_j$ , constrained by  $\lambda_j \in (0, 1)$ , Eq. (138) and

$$\frac{d_n}{n} = \dim(\mathcal{H}_{10}) + \dim(\mathcal{H}_{11}) + \dim(\mathcal{H}_1), \quad (140)$$

from  $\text{Tr} \hat{\Pi}_k(t_m) = \text{Tr} \hat{\Pi}_{k+1} = (d_n/n)$ . This is conveniently done by introducing  $\bar{\lambda}_j \in (0, 1]$  representing the eigenvalues of  $\hat{\Pi}_{k+1}$  in  $\mathcal{H}_{11} \oplus \mathcal{H}_1$  (which reduce to 1 in  $\mathcal{H}_{11}$  and the  $\lambda_j$  in  $\mathcal{H}_1$ ), so

that  $R_k(1, t_m)$  is the sum of these eigenvalues and  $P_k(1, t_m)$  the sum of their squares. Using the method of Lagrange multipliers immediately shows that the sum of a set of non-negative variables, with a fixed sum of squares, has no local minima with respect to first order variations (but a local maximum when they are equal). The true minimum is then to be found somewhere on the boundary of the (constrained) domain of the  $\bar{\lambda}_j$  (i.e. setting as many  $\bar{\lambda}_j$ s to 1 as possible to minimize the excess of the variables over their squares), which gives

$$R_k(1, t_m) \geq \lfloor P_k(1, t_m) \rfloor + \sqrt{P_k(1, t_m) - \lfloor P_k(1, t_m) \rfloor} \equiv \tilde{P}_k(1, t_m). \quad (141)$$

Here  $\lfloor x \rfloor$  denotes the greatest integer smaller than  $x$ , so the right hand side is between  $P_k(1, t_m)$  and  $P_k(1, t_m) + 1$ . Thus,  $\dim(\mathcal{H}_{11}) = \lfloor P_k(1, t_m) \rfloor$ , and  $\dim(\mathcal{H}_1) \in \{0, 1\}$  (depending on the fractional part) minimizes  $R_k(1, t_m)$ , which achieves a larger value in every other situation.

Now, let  $\hat{U}_\Sigma$  be a unitary that satisfies

$$\hat{U}_\Sigma |\mathcal{B}_k; j\rangle = \begin{cases} \hat{U}_H^\dagger(t_m) |\mathcal{B}_k(t_m); j\rangle, & \text{for } 0 \leq k < n-1, \\ \hat{U}_H^\dagger(t_m) |\mathcal{B}_k(t_m); j+1\rangle, & \text{for } k = n-1, \end{cases} \quad (142)$$

for any fixed labeling of the basis elements of the  $\mathcal{B}_k$  with the addition  $j+1$  being modulo  $d_n$ . As  $\hat{U}_H(t_m)$  acts trivially (i.e. as identity) on  $\Sigma_{\text{aux}}$ , we have

$$\hat{U}_\Sigma \Sigma(k) = \Sigma(k), \quad (143)$$

$$\hat{U}_\Sigma \Sigma_{\text{aux}} = \Sigma_{\text{aux}}, \quad (144)$$

which follows from a complete orthonormal set of vectors in  $\Sigma_{\text{aux}}$  being chosen to be elements of  $\mathcal{B}_{10}$  and  $\mathcal{B}_{01}$  for the respective subspaces.

For any such unitary, the cycling operator of the basis  $\bar{\mathcal{C}} = \{|\bar{\mathcal{C}}_\ell\rangle\}_{\ell=0}^{(d_n)-1}$  formed by

$$|\bar{\mathcal{C}}_{j_n+k}\rangle = |\mathcal{B}_k; j\rangle, \quad (145)$$

is a pure state cyclic permutation, which approximates  $\hat{U}_H(t_m)\hat{U}_\Sigma$  with mean persistence

$$\frac{1}{d_n} \sum_{\ell=0}^{d_n-1} |\langle \bar{\mathcal{C}}_{\ell+1} | \hat{U}_H(t_m) \hat{U}_\Sigma | \bar{\mathcal{C}}_\ell \rangle| \geq \frac{1}{d_n} \sum_{k=0}^{n-1} \tilde{P}_k(1, t_m), \quad (146)$$

from Eq. (141). However, there are  $(d_n - d)$  invariant states in this basis under the action of  $\hat{U}_H(t_m)$  — a consequence of artificially expanding the Hilbert space by  $\Sigma_{\text{aux}}$  to define mixed state cyclic permutations — and any persistence amplitude involving these states is zero. We can then construct a restricted basis  $\mathcal{C} \subseteq \bar{\mathcal{C}}$  of  $d$  elements that inherits the ordering of  $\bar{\mathcal{C}}$  but drops any members of the latter in  $\Sigma_{\text{aux}}$ :

$$\mathcal{C} = \left\{ |C_k\rangle \in \bar{\mathcal{C}} \cap \Sigma : \left[ |C_k\rangle = |\bar{\mathcal{C}}_{j_k}\rangle \implies (|\bar{\mathcal{C}}_j\rangle \in \Sigma_{\text{aux}} \forall j \in (j_k, j_{k+1})) \forall k \in \mathbb{Z}_d \right] \right\}. \quad (147)$$

The condition in square brackets formally states the ordering requirement, that consecutive elements of  $\mathcal{C}$  can only be separated by elements of  $\Sigma_{\text{aux}}$  in  $\bar{\mathcal{C}}$ . The mean persistence of  $\mathcal{C}$  is

$$\frac{1}{d} \sum_{\ell=0}^{d-1} |\langle C_{\ell+1} | \hat{U}_H(t_m) \hat{U}_\Sigma | C_\ell \rangle| \geq \frac{1}{d} \sum_{k=0}^{n-1} \tilde{P}_k(1, t_m) \quad (148)$$

Rewriting Eq. (148) using  $P_k(1, t_m) = d_n Z_k(1, t_m)$  gives Eq. (50) in the main text.

In summary, we have constructed a pure state cyclic permutation for  $\hat{U}_H(t_m)\hat{U}_\Sigma$  with  $\hat{U}_\Sigma$  leaving each subspace  $\Sigma(k)$  of the mixed state cyclic permutation invariant, whose mean persistence is determined by the mixed state overlaps  $P_k(1, t_m)$ .

## Appendix F Cyclic permutations for linear flows on a 2D torus

### F.1 Classical cyclic permutations for the 2D torus

We are interested in the flow  $\mathcal{T}^t$ , defined by  $\theta_x = \omega_x t$ ,  $\theta_y = \omega_y t$  (modulo  $2\pi$ ) with  $\theta_x \in [0, 2\pi)_x$ ,  $\theta_y \in [0, 2\pi)_y$  (subscripts introduced for convenience) for irrational  $\alpha = \omega_y/\omega_x$ . Singling out the  $x$  direction, the period of the flow along  $\theta_x$  is  $T_x = 2\pi/\omega_x$ .

While leaving  $\theta_x$  invariant,  $\mathcal{T}^{pT_x}$  acts as  $p$  steps of an irrational rotation of  $\theta_y$  by the angle  $\vartheta = 2\pi\alpha$ . In Ref. [86], it is shown that if  $\vartheta$  has a rational approximation of speed  $f_\vartheta(q)$ , i.e. if there exists a sequence of co-prime integers  $p, q$  such that

$$\left| \vartheta - \frac{p}{q} \right| < f_\vartheta(q) \quad (149)$$

as  $q \rightarrow \infty$ , then the irrational rotation of  $\theta_y$  by  $\vartheta$  can be approximated by an  $n_y$ -element cyclic permutation  $\mathcal{C}(y) = \{C_k(y)\}_{k=0}^{n_y-1}$  in  $[0, 2\pi)_y$  with error

$$\bar{\epsilon}_C(T_x) < O(f_\vartheta(n_y)), \quad (150)$$

as  $n_y \rightarrow \infty$ .

Divide  $[0, 2\pi)_x$  into any  $n_x$  equal segments  $\mathcal{N}_x(r) = [2\pi r/n_x, 2\pi(r+1)/n_x]$  for  $r \in \mathbb{Z}_{n_x}$ . With  $t_m = T_x/n_x$ , we have

$$\mathcal{T}^{t_m} \mathcal{N}_x(r) = \mathcal{N}_x(r+1), \quad \forall r \in \mathbb{Z}_{n_x}. \quad (151)$$

Now, define the  $(n = n_x n_y)$ -element cyclic permutation  $\mathcal{C} = \{C_k\}_{k=0}^{n-1}$

$$C_{kn_x+j} = \mathcal{T}^{jt_m} [\mathcal{N}_x(0) \times C_k(y)], \quad \text{for } j \in \mathbb{Z}_{n_x}, j \in \mathbb{Z}_{n_y}. \quad (152)$$

To obtain the error for approximating  $\mathcal{T}^{t_m}$  by  $\mathcal{T}_C$  (the cycling operator for  $\mathcal{C}$ ), we note that

$$\mu \left( (\mathcal{T}^{t_m} C_{kn_x+j}) \cap C_{kn_x+j+1} \right) = \begin{cases} 1, & \text{for } 0 \leq j < n_x - 1, \\ \frac{1}{n_x} \mu \left( (\mathcal{T}^{T_x} C_k(t)) \cap C_{k+1}(y) \right), & \text{for } j = n_x - 1. \end{cases} \quad (153)$$

This immediately gives

$$\bar{\epsilon}_C(t_m) < \frac{1}{n_x} O(f_\vartheta(n_y)). \quad (154)$$

As an aside, we note the qualitative similarity of Eqs. (152) and (153) to Eqs. (145) and (142).

For almost all irrational  $\vartheta$  (and therefore, almost all  $\alpha = \vartheta/(2\pi)$ ),  $f_\vartheta(q) < O(q^{-2})$ , as discussed in Ref. [86]. Taking  $n_x \sim O(n_y)$  for the  $n \rightarrow \infty$  limit, it follows that  $t_m \sim O(\omega n^{-1/2})$  and  $\bar{\epsilon}_C(t_m) < O(n^{-3/2})$ , giving Eq. (54) in the main text. It is possible for cyclic permutations with lower error to exist (and perhaps likely, as suggested by the numerical results of Sec. 5.3.2), but their construction is not obvious using the present method.

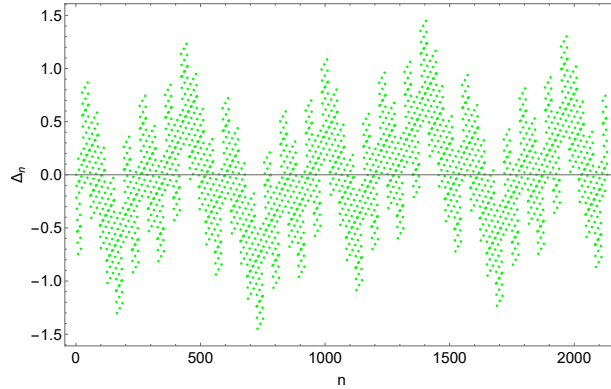
### F.2 Additional data and discussion for quantized torus

Some additional insight into the nature of the spectrum for the irrational ( $\alpha = \sqrt{2}$ ) and rational ( $\alpha = 2$ ) torus is provided by a plot of the mode fluctuations themselves i.e.  $\Delta_n$  vs.  $n$ , as in Fig. 10. In particular, the choice of  $t_0 = 2\pi\Omega/d$  seems to be (close to) optimal for the irrational case, with

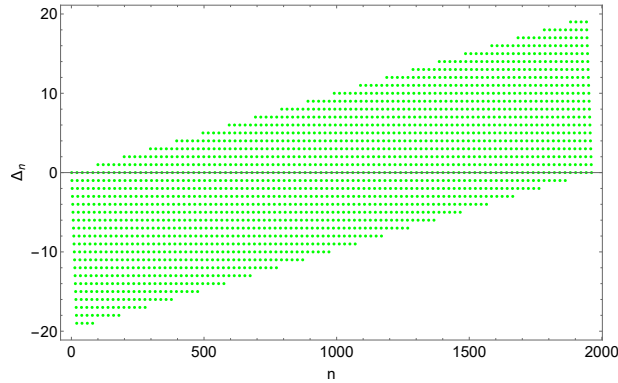


e.g. the fluctuations appearing to be centered around 0 (cf. Refs. [33, 56]). However, there is an additional linear trend for the rational case, likely due to the multiplicity of eigenvalues differing near the edge of the spectrum for the chosen  $L_1, L_2$ . This indicates a more optimal  $t_0$  could have been chosen for the rational case to minimize the error further (without affecting the order of magnitude), but the present choice of  $t_0$  clearly illustrates the periodicity (in Figs. 8d, 8e) expected from the classical decomposition into periodic subsets.

To conclude this Appendix, we mention an alternate quantization of the torus, for which the choice of  $t_0$  is more nontrivial. Instead of the UV cutoff in Eq. (53), one could have imposed  $|J_x| < L_x, |J_y| < L_y$  to obtain an alternate quantization, where the energy levels in Fig. 7a or 8a would be bounded along a rectangle whose sides are parallel to the axes. In that case, the density of states is not uniform but generally has 3 parts: a linear increase, a constant part, and a linear decrease that mirrors the increase. But one should not hastily conclude from the nonuniform density of states that the system is non-ergodic. When the eigenphases of  $\hat{U}_H(t)$  corresponding to these energy eigenvalues are wrapped around a circle with increasing  $t$ , there will eventually come a time  $t_0$  where the linear increase and decrease overlap precisely and produce an effective uniform density of eigenphases. The spectrum can in fact be rearranged in the  $J_x, J_y$  plane to look like Figs. 7a, 8a without affecting the “wrapped” eigenphases at  $t_0$ , resulting in the same *eigenphase* statistics. In this special instance, ergodicity is preserved in spite of a varying density of states due to the wrapping of the spectrum, suggesting that this property is not significantly sensitive to the choice of UV cutoff.



(a) Irrational case:  $\alpha = \sqrt{2}$ ,  $d = 2133$ .



(b) Rational case:  $\alpha = 2$ ,  $d = 1961$ .

Figure 10: Mode fluctuations  $\Delta_n$  plotted against  $n$  for the rational and irrational datasets in Figs. 7 and 8.